TECHNISCHE UNIVERSITÄT MÜNCHEN

Lehrstuhl für Technische Chemie II

New supports and catalytic materials based on silicon polymers

Sabine Scholz

Vollständiger Abdruck der von der Fakultät für Chemie der Technischen Universität München zur Erlangung des akademischen Grades eines

Doktors der Naturwissenschaften (Dr. rer. nat.)

genehmigten Dissertation.

Vorsitzender:		Univ.-Prof. Dr. K.-O. Hinrichsen
Prüfer der Dissertation:	1.	Univ.-Prof. Dr. J. A. Lercher
	2.	Univ.-Prof. Dr. M. Tromp

Die Dissertation wurde am 28.10.2010 bei der Technischen Universität München eingereicht und durch die Fakultät der Chemie am 13.12.2010 angenommen.

Curiosity is the essence of the scientific mind

Bill Watterson

Die vorliegende Arbeit entstand in der Zeit von April 2007 bis Oktober 2010 unter Leitung von Prof. Dr. Johannes A. Lercher am Wacker-Institut für Siliciumchemie und Catalysis Research Center der Technischen Universität München.

First of all I want to thank Prof. Dr. Johannes A. Lercher for the possibility to work on this interesting topic and to join so many conferences and scientific workshops, for his trust and advice, the scientific freedom and the interesting discussions. Johannes, thank you for the possibility to organize the Ski-Seminar in Kühtai and the Ferienakademie, for the chance to meet your *'Doppelgänger'* and for the interesting time in TC II.

Furthermore I want to thank:

The Wacker Chemie AG for the financial support and Dr. Jürgen Stohrer as well as Dr. Alexander Zipp for the helpful discussions within the Wacker-Institut für Siliciumchemie.

Prof. Wilhelm Schwieger for inviting me to present my results at the FAU Erlangen-Nürnberg, for many interesting and helpful discussions and for a really nice time with the TUM-FAU student group in the Ferienakademie.

Dipl.-Ing. Martin Neukamm for the endless hours in front of the scanning electron microscope and for AAS measurements as well as Dipl.-Ing. Xaver Hecht for measuring N_2 physisorption and Hg porosimetry and both for being good friends and helping me whenever I had problems with analytical measurements or with my setup.

Dipl.-Ing. Matthias Lesti for measuring Hg porosimetry, especially for my last-minute samples.

Dr. Marianne Hanzlik for introducing me to transmission electron microscopy, for her interest in my research and for the nice discussions.

Hans Bongard of the MPI in Mülheim an der Ruhr for taking time to analyze a few of my samples with SEM.

Georgeta Krutsch and Aleksandra Jonovich for NMR and TGA measurements.

Stefanie Maier, Helen Lemmermöhle and Katharina Thies for all the administrative organization and Andreas Marx for keeping my computer running.

The students B. Sc. Timon Geppert, Dipl.-Chem. Annemarie Frey, Dipl.-Chem. Konrad Hindelang, M. Sc. Stefan Meier, Jiaqi Li, Dipl.-Ing. Beatriz Blas Molinos, B. Sc. Philipp Burmann, B. Sc. Daniela Köhler, Marie-Mathilde Millet and B. Sc. Eva Schachtl, who did a great job and spent a lot of time in my laboratory during their practical work, semester, bachelor, master or diploma thesis.

My present and former colleagues Dipl.-Ing. Florian Schüßler, Dipl.-Chem. Anna Lubinus, Dipl.-Ing. Oliver Gobin, Dipl.-Chem. Matteo Branzi, Dipl.-Chem. Sarah Maier, Dipl.-Chem. Claudia Schneider, Dipl.-Ing. Ana Hrabar, Dipl.-Chem. Sonja Wyrzgol, Dipl.-Chem. Daniela Hartmann, Dipl.-Chem. Tobias Förster, Dipl.-Chem. Frederik Naraschewski, Dipl.-Chem. Linus Schulz, Dipl.-Ing. Stefanie Reiner, M. Sc. Baoxiang Peng, Dr. Despina Tzoulaki, Dr. Michael Salzinger, Dr. Stephan Reitmeier, PD Dr. Andreas Jentys and all the other members of TC II for the nice and friendly working atmosphere, the countless funny moments and the scientific discussions. Thanks for the nice time.

All the people, who made my everyday life at university enjoyable by diverting coffee breaks and words of encouragement – special thanks to Dr. Markus Gretz and Dipl.-Chem. Elke Otto.

And with my favorite SEM image of one of my samples I want to express my very special thanks to my parents Karin and Manfred Scholz for supporting me all the time and calm me down when I was stressed out, since without them I wouldn't have the chance to do my doctoral thesis. Also I want to thank my sister Susanne and my brothers Florian, Dominik and Manuel for their support beyond chemistry, whereas I want to point out Florians' great help, because sometimes my computer seems to have a life of its own.

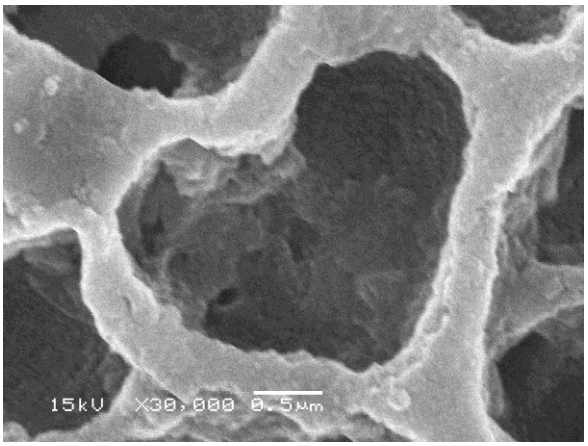

With all my heart I want to thank Dr. Patrick Wilhelm for proofreading my thesis, for the motivation and the encouragement, his patience and for all his love.

Sabine

October, 2010

AAMS	[3-(2-Aminoethylamino)propyl]trimethoxysilane, N-[3-(Trimethoxysilyl)propyl]-ethylenediamine
AAS	Atomic absorption spectroscopy
acac	Acetylacetonate
BET	Brunauer – Emmett – Teller
BJH	Barrett – Joyner – Halenda
Brij 76	$C_{18}H_{37}(EO)_{10}$
cmc	Critical micelle concentration
CTAB	Cetyltrimethylammonium bromide
EO	Ethylene oxide
Geniosil® GF92	N-Cyclohexyl-3-aminopropyltrimethoxysilane
Geniosil® XL924	N-Cyclohexylaminomethylmethyldiethoxysilane
Geniosil® XL926	N-Cyclohexylaminomethyltriethoxysilane
Geniosil® XL973	N-Phenylaminomethyltrimethoxysilane
IUPAC	International Union of Pure and Applied Chemistry
MALDI-TOF	Matrix-assisted laser desorption ionization – Time-of-flight
MCM	Mobil composition of matter
MCP	Methylcyclopentane
MOF	Metal Organic Framework
MP	methylpentane
NMR	Nuclear magnetic resonance
o/w	Oil-in-water
ORMOSIL	Organically Modified Silicates
PDI	Polydispersity index
PEO	Poly(ethylene oxide)
Pluronic® 25R4	$(PO)_{18}(EO)_{45}(PO)_{18}$
Pluronic® P123	$(EO)_{20}(PO)_{70}(EO)_{20}$
Pluronic® PE 6100	$(EO)_3(PO)_{31}(EO)_3$

Pluronic® RPE 1720	$(PO)_{13}(EO)_{16}(PO)_{13}$
Pluronic® RPE 1740	$(PO)_{11}(EO)_{27}(PO)_{11}$
Pluronic® RPE 2520	$(PO)_{18}(EO)_{14}(PO)_{18}$
Pluronic® RPE 3110	$(PO)_{27}(EO)_{6}(PO)_{27}$
PO	Propylene oxide
PPO	Poly(propylene oxide)
PTMS	Phenyltrimethoxysilane
PVP	Poly(vinylpyrrolidone)
SBA	Santa Barbara
SDS	Sodium dodecyl sulfate
SEM	Scanning electron microscopy
Span 80	Octadecanoic acid [2-[3,4-dihydroxy-2-tetrahydrofuranyl]-2-hydroxyethyl]
TBOS	Tetrabutyl orthosilicate
TCD	Thermal conductivity detector
TEM	Transmission electron microscopy
TEOS	Tetraethoxysilane (tetraethyl orthosilicate)
TES	Tetraethyl orthosilicate
TGA	Thermogravimetric analysis
TOF	Turnover frequency
TPAOH	Tetrapropylammonium hydroxide
TTAB	Tetradecyltrimethylammonium bromide
Tween 20	Polyoxyethylene (20) sorbitan monolaurate
UV	Ultraviolet
w/o	Water-in-oil
wt.	weight
XRD	X-ray diffraction
ZSM	Zeolite Socony Mobil

Chapter 1

General Introduction

1.1 Challenges in material science

Silica based materials play a major role in several everyday products such as plastics or cosmetics and in many fields of technical applications such as catalysis,[1] chromatographic or adsorption techniques,[2] electronics,[3] targeted drug delivery[4] and biotechnology[5]. In each case, the material requirements are completely different regarding the morphology (colloids, powder, thin film, monolith), the structure (porosity, pore size, pore arrangement), the composition (crystallinity, functionality) and the physical properties (thermal and mechanical stability, biocompatibility). The versatility and the technical, economical and environmental advances challenge the continuous improvement and development of tailor-made materials for specific applications. Thereby, the relationship between synthesis, composition, structure and properties of different (functional) materials represents the crucial point in modern material science, which is the interface between chemistry, physics and engineering.[6]

The preparation of hierarchical porous materials, i.e. the multidimensional structural control over several length scales from the molecular to the macroscopic level and the synthesis of composite materials including inorganic and organic functionalities is still a challenge in materials chemistry.[7] Obviously, hierarchically structured materials with macroscopic shapes and controlled micro-, meso- and macroporosity are advantageous for sorption and diffusion processes, e.g. as membranes and as catalyst support to prevent mass transport limitations.[8] Composite materials, which include inorganic and organic building blocks, can be used to adsorb metal ions or to immobilize complexes or organic molecules, such as enzymes. Hence, composite materials consisting of an inorganic support and anchored active species fill the gap between homogeneous and heterogeneous catalysis.

A special group of composite materials is ordered mesoporous silica, like SBA-15 or MCM-41, since the intermediate state before calcination or extraction consists of organic template molecules embedded in the silica matrix.[9] Such materials are commonly prepared by sol-gel processes, a controlled acid or base catalyzed hydrolysis and condensation reaction.

1.2 Scope of the thesis

The focus of this thesis was the design of new hierarchically structured materials with a macroscopic spherical shape and controlled porosity. The investigations tend to unravel the relationship between synthesis, chemical composition, structure, properties and performance for the prepared materials, since this is the key to tailor-made products.[6] The most favored method to synthesize such materials is the sol-gel process, which represents a highly variable preparation method for diverse morphologies, various porous systems, inorganic-organic composites and hierarchical structures (see chapter 2).

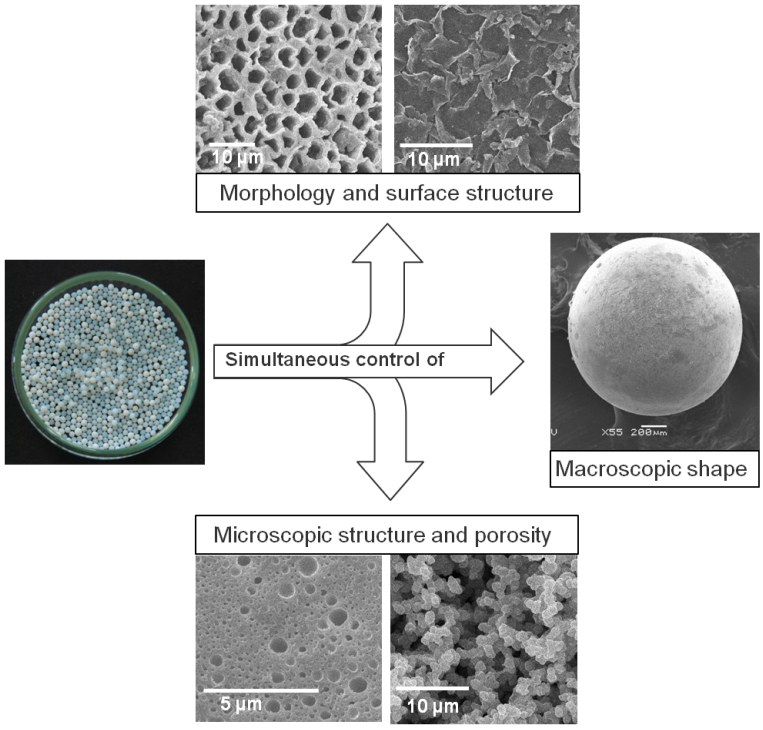

Figure 1.1. Synthesis strategy for hierarchically structured macroscopic silica spheres.

The formation of the macroscopically shaped silica composite spheres was achieved using an emulsion based sol-gel reaction with water as continuous phase. This process was carried out in a continuously operated reactor column with a recycling heated water flow, which is described in the appendix. This method allows highly reproducible preparation of macroscopic silica composite spheres with a narrow size distribution. The applied precursor solution contained different silanes, a surfactant, a solvent and optionally also further functional compounds, such as transition metal complexes.

The relationship between the composition of the precursor mixture and the porosity, structure and properties of the resulting silica composite spheres was extensively studied. The influence of the surfactant on the morphology and the chemical and physical properties of the silica spheres is described in chapter 3. It is shown that the crucial step for the formation of mechanically stable macroscopic silica spheres is the balance between the stabilization of the oil-water interface and the efficiency of water diffusion inside the precursor droplet. Besides this aspect, also the hierarchical structure, the mesopore diameter and the specific surface area is controlled by the hydrophobicity of the surfactant.

In chapter 4 the role of each precursor component and their interactions is pointed out by variation of the silane mixture, the solvent and the surfactant concentration. This allowed fine tuning of the properties including the ratio of micro-, meso- and macropores and the morphology of the spheres. In this context, the impact of the condensation rate as well as the possibility to achieve organo-functionalized silica spheres was investigated.

Based on these results, macroscopic silica spheres functionalized with platinum nanoparticles were prepared in a one-step synthesis by coordination of platinum via the aminosilane or the surfactant of the precursor solution (see chapter 5). The size and concentration of the supported platinum nanoparticles was controlled by the platinum compound, the kind of surfactant and the preparation method. The catalytic activity of these materials was determined using methylcyclopentane ring opening as probe reaction.

1.3 References

[1] A. Corma, *Chemical Reviews* **1997**, *97*, 2373.

[2] M. Grün, A. A. Kurganov, S. Schacht, F. Schüth, K. K. Unger, *Journal of Chromatography A* **1996**, *740*, 1.

[3] Q. R. Huang, W. Volksen, E. Huang, M. Toney, C. W. Frank, R. D. Miller, *Chemistry of Materials* **2002**, *14*, 3676.

[4] C. Y. Lai, B. G. Trewyn, D. M. Jeftinija, K. Jeftinija, S. Xu, S. Jeftinija, V. S. Y. Lin, *Journal of the American Chemical Society* **2003**, *125*, 4451.

[5] T. Buranda, J. Huang, G. V. Ramarao, L. K. Ista, R. S. Larson, T. L. Ward, L. A. Sklar, G. P. Lopez, *Langmuir* **2003**, *19*, 1654.

[6] U. Schubert, N. Hüsing, *Synthesis of Inorganic Materials*, 2 ed., Wiley VCH, Weinheim, **2005**.

[7] N. Hüsing, in *Sol-Gel Methods for Materials Processing* (Eds.: P. Innocenzi, Y. L. Zub, V. G. Kessler), Springer, Dordrecht, **2008**.

[8] C. Yacou, A. Ayral, A. Giroir-Fendler, M. L. Fontaine, A. Julbe, *Microporous and Mesoporous Materials* **2009**, *126*, 222.

[9] S. Polarz, in *Handbook of Organic-Inorganic Hybrid Materials and Nanocomposites, Vol. 1* (Ed.: H. S. Nalwa), American Scientific Publishers, Stevenson Ranch/California, **2003**.

Chapter 2

Fundamentals of siliceous porous materials

2.1 Porous silica

The deliberate control of porosity is a fundamental issue for industrial applications such as design of catalysts, membranes or adsorbents. Porous materials are usually distinguished by the pore size and pore size distribution. The pore structure (inter-, intraparticle pores), the arrangement (random, periodic) as well as the connectivity and shape of the pores are also important characteristics. The classification of porous solids by the IUPAC distinguishes between three pore size regimes: micropores (< 2 nm), mesopores (2 – 50 nm) and macropores (> 50 nm).[1] Typical inorganic representatives for the different classes are shown in Figure 2.1. Among these, zeolites are the most prominent example, since they are widely-used in common products (detergents,[2, 3] cosmetics,[4] water purification[5, 6]) and industrial applications, e.g. as catalyst in petrochemistry.[7, 8] Due to the small pore diameter the application of zeolites is restricted to processes involving small molecules mainly in gas phase.

The groundbreaking development to achieve materials with larger ordered pores was the synthesis of MCM-41 by the Mobil Oil Company in 1992. In recent years, the effort in materials research is focused on hierarchical and hybrid structures with the objective of designing tailor-made materials for different applications.[9] This scientific field, which is often called nanoscience, includes the multidimensional control from molecular building blocks to the macroscopic particle morphology and the combination of inorganic and organic functionalities.[10, 11] A suitable synthesis method to merge all these material requirements is the sol-gel process, which is highly versatile including organo-functionalized silanes, additives such as templating molecules and different morphologies due to controlled hydrolysis and condensation reactions.

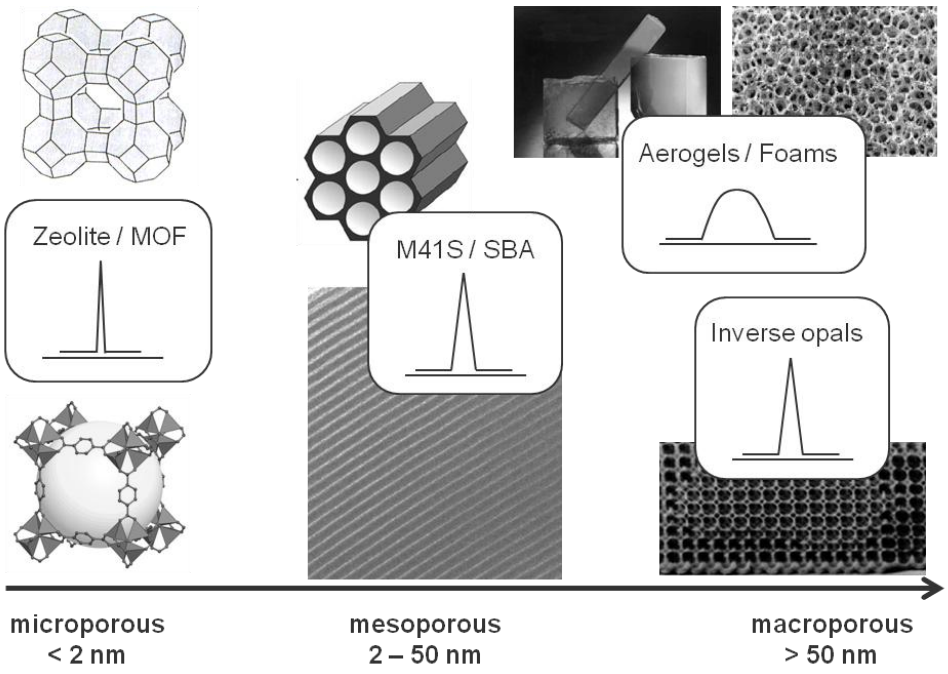

Figure 2.1. Typical porous materials classified according to their pore size and pore size distribution (adapted from [12]).

2.1.1 Sol-gel processing of silica materials

Sol-gel chemistry describes the formation of three-dimensional inorganic polymers via hydrolysis and condensation reactions. In the case of siloxane polymers the common precursors are aqueous solutions of sodium silicates (water glass) or silicon alkoxides. The mechanism of the sol-gel reaction depends on the catalyst, which is usually an acid or base.[13] Both pathways include pentacoordinated transition states, but under acidic conditions the silanol or alkoxy group is primarily protonated resulting in a good leaving group and a higher electrophilicity of the silicon atom (Scheme 2.1).[14] This facilitates the next step, which is either the attack by water leading to the hydrolyzed species or by a silanol group representing the condensation reaction by the formation of a siloxane bond.

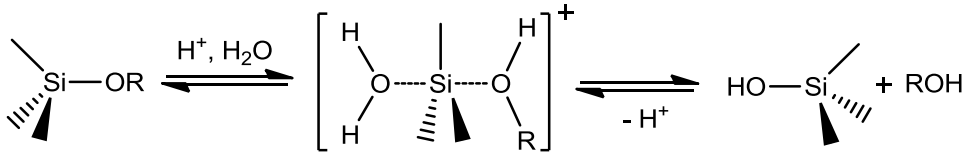

Scheme 2.1. Mechanism of acid catalyzed hydrolysis of silicon alkoxides.

In basic conditions the transition state originates from the S_N2-type addition of a hydroxide anion, which subsequently replaces the alkoxide group (Scheme 2.2).[14] The condensation reaction takes place after deprotonation of the silanol and the nucleophilic attack of neutral silicate species by the silanolate anion followed by hydroxy- or alkoxy-elimination. In both cases – acid or base catalysis - the condensation reaction to form Si-O-Si bonds leads to a release of water or alcohol.[15]

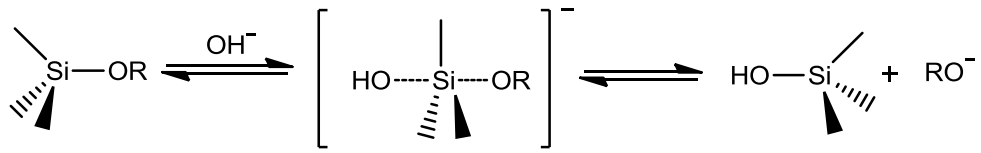

Scheme 2.2. Mechanism of base catalyzed hydrolysis of silicon alkoxides.

It should be noticed that the hydrolysis and condensation usually occur in parallel and that the relative reaction rate determines the primary product composition, which contains linear, cyclic or three-dimensional connected silicate species. If the hydrolysis is favored, as it is the case at low pH values, a chain-like network and fine-grained silica is obtained. In contrast, basic catalysis leads to a highly branched network and a coarser, particle-like morphology, since the condensation is faster than the hydrolysis. The influence of the pH on the structural development during sol-gel formation is schematically shown in Figure 2.2. The first step is the formation of small oligomeric particles, which may either grow or agglomerate at a certain size. The agglomeration of the colloidal silica particles (sol) takes place via the reaction of surface silanol groups, whereas at high pH stable sols can be formed due to the repulsion between negatively charged particles.[15]

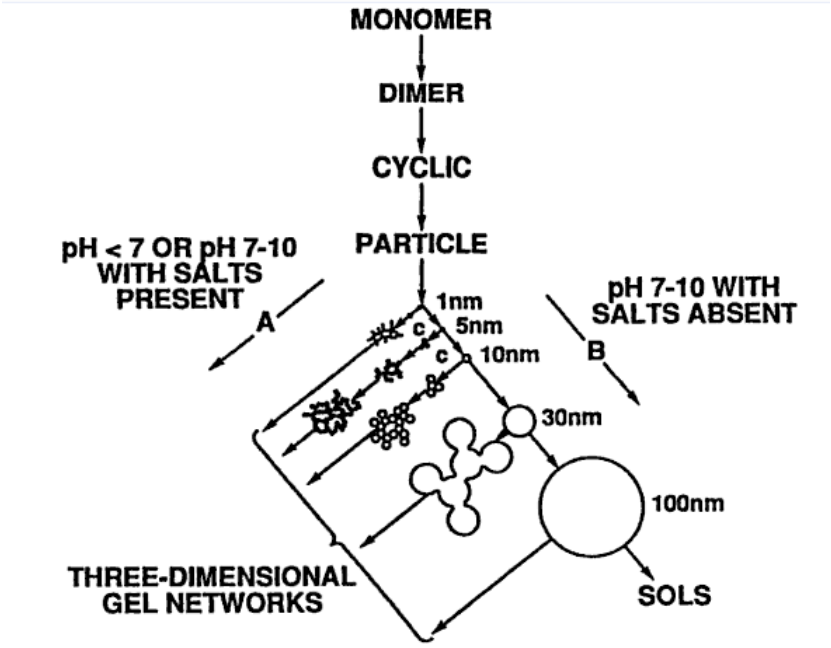

Figure 2.2. Polymerization behavior and structural development of silica in dependency of the pH.[13]

Besides the influence of the catalyst and the pH, there are several parameters which affect the chemical and physical properties of the final material. The hydrolysis and condensation rate of the reaction mixture depends also on the precursors, the solvent, the amount of water as well as the ratio and concentration of these components. The reactivity of the alkoxysilane is defined by steric and inductive effects caused by different substituents attached to the Si atom. Since the solvent interacts with the silica species, the polarity and protic or non-protic character impact the reaction rate and stability of the sol.[13]

The high variability distinguishes the sol-gel reaction as ideal method to design tailor made materials for various applications. The properties of the product are not only determined by the composition of the reaction mixture, but also by the parameters during the sol-gel process such as temperature, gelation time as well as the ageing and drying conditions. The colloidal particles of the sol agglomerate under certain conditions to form a three-dimensional continuous network inside the liquid phase – the gel. The drying procedure leads either to xerogels by shrinkage of the gel due to evaporation of the liquid or to aerogels by supercritical solvent extraction.[16] As it is shown in Figure 2.3, various materials like powders, monoliths, ceramics, films or fibres can be obtained, depending on the sol and gel treatment.

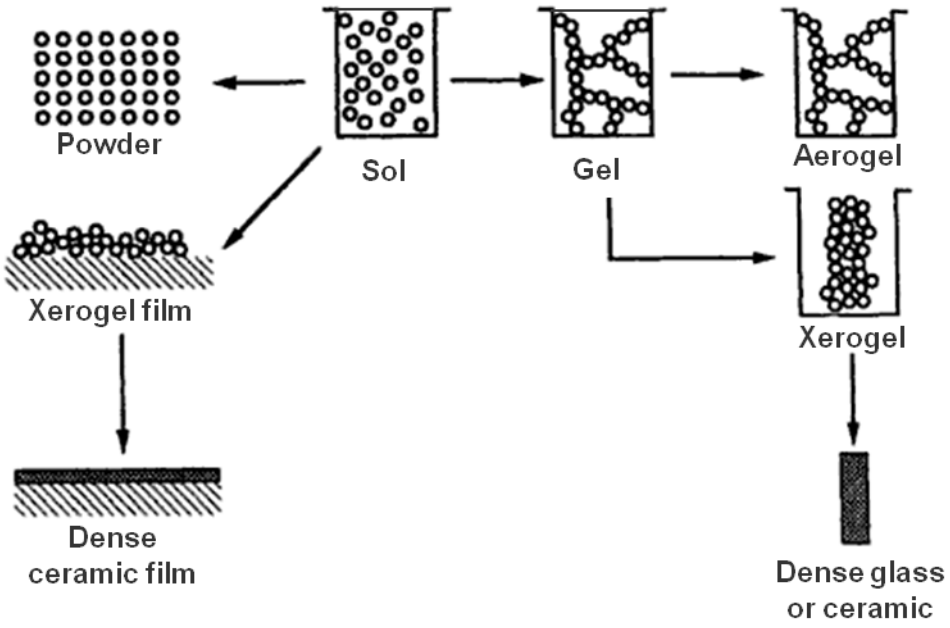

Figure 2.3. Overview about the product morphologies as a result of sol-gel processing.[16]

2.1.2 Hybrid silica materials

Sol-gel chemistry allows not only the synthesis of various inorganic solids, but also, due to the mild processing conditions the combination of inorganic and organic components forming a hybrid material. The possibilities of composition and structure of such materials is nearly unlimited including covalently linked units, embedded building blocks (e.g. complexes, biomolecules or particles) or interpenetrating networks of organic and inorganic polymers.[17] Thereby, the term hybrid materials define the combination of different molecular building blocks, whereas (nano)composite materials consist of larger structural units (1 – 100 nm) which exhibit an interface. However, the classification provides no clear borderline, because large molecular building blocks like inorganic clusters or polymers are already in the nanometer size range and weak interactions between molecular building blocks can also induce phase separation inside the material. This led to a more precise definition, restricting the term hybrid material to structures with covalently connected organic and inorganic components.[11, 15] This definition is also used within this thesis.

The advantage for the preparation of hybrid silica materials is the hydrolytic stability of the Si-C bond, which opened, in combination with the versatility of sol-gel chemistry a wide field in material science.[18, 19] The substitution of one or two alkoxy groups of silicon alkoxide precursors by organic ligands allows the synthesis of organically modified silicates

(ORMOSILs). This approach intends to combine the thermal and mechanical stability of SiO_2 with the high variability of organic chemistry by mixing $RSi(OR')_3$ or $R_2Si(OR')_2$ with tetraalkoxysilane as network building compound in order to create new materials with tailored properties. Thus phenyl or alkyl groups increase the hydrophobicity and reactive groups such as amino, thio, epoxy or vinyl provide basicity, acidity or the possibility for further functionalizations, e.g. the immobilization of catalytic active compounds. However, for the co-condensation of precursor mixtures with organo-functionalized silanes the different reactivities of the compounds have to be considered, since it directly affects the structure of the material.[15]

Besides the co-condensation, parent silica can also be functionalized by post-synthetic modification (Figure 2.4). The grafting method exclusively changes the surface of the silica, whereas the co-condensation influences the connectivity of the complete siloxane network. Functionalization of the silica framework can be achieved with bridging organic units.

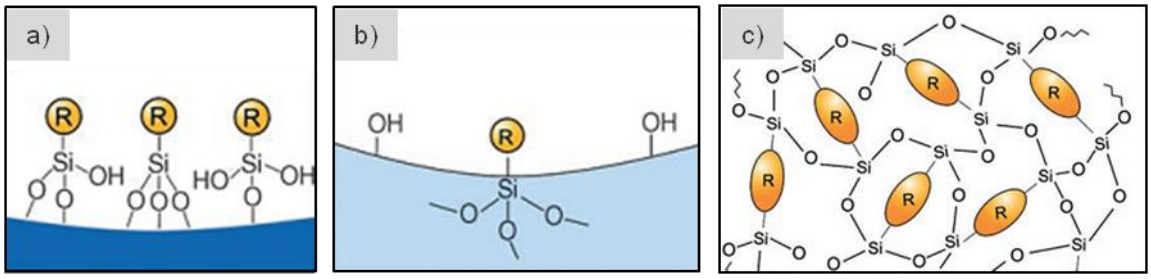

Figure 2.4. Schematic presentation of organofunctionalized silica prepared with grafting (a), co-condensation (b) and bissilylated organic bridging units (c).[11]

2.1.3 Ordered mesoporous silica

The template based method for mesoporous silica was already invented in 1969, but the remarkable properties were not recognized at that time.[20, 21] In 1992 the development of MCM-41 by the Mobil Oil Company gave the starting signal for the synthesis of various ordered mesoporous materials.[22-25] In contrast to zeolites, these molecular sieves are not prepared with single molecules as templates, but with supramolecular assemblies in order to create pores larger than 2 nm. This templating approach is based on the ability of amphiphilic molecules to form micelles and, with increasing concentration, dense packed micelles (e.g. cubic) as well as lyotropic liquid crystalline mesophases (hexagonal, bicontinuous

cubic/gyroid or lamellar).[26] Typical self-assembled geometric structures of the M41S series are shown in Figure 2.5.

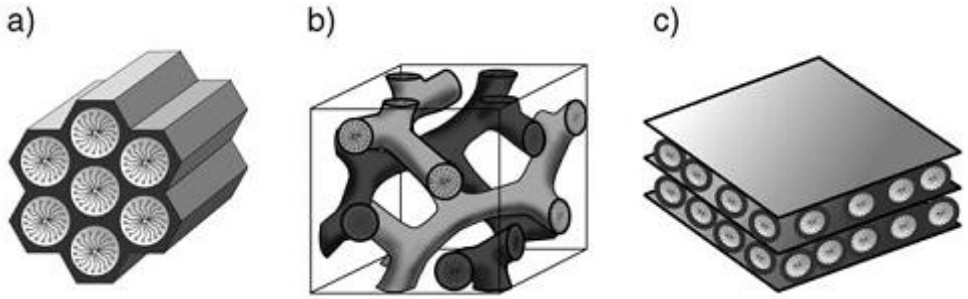

Figure 2.5. Schematic presentation of the geometric structures of M41S silica-surfactant composites: a) hexagonal MCM-41, b) bicontinuous cubic MCM-48 and c) lamellar MCM-50.[11]

The silica-surfactant composite can be either generated via a true liquid crystalline mechanism with a preformed mesophase or via cooperative formation of the liquid crystal in presence of the inorganic precursor (Figure 2.6). In both cases, the mesophase directs the growth of the inorganic matrix through attractive interaction between the surfactant (S) and the inorganic species (I). Since the surfactants are categorized by their hydrophilic head group in cationic (S^+, e.g. cetyl trimethylammonium bromide/CTAB), anionic (S^-, e.g. sodium dodecyl sulfate/SDS) and nonionic (S^0, e.g. triblock copolymer Pluronic® P123) structure directing agents and the silica species are negatively (I^-), neutral (I^0) or positively charged (I^+) in dependency of the pH, various interactions are possible.[11, 27]

- Direct electrostatic interaction: S^+I^-, S^-I^+
- Counterion mediated electrostatic interaction: $S^+X^-I^+$, $S^-M^+I^-$
- Hydrogen bond interaction: S^0I^0

The inorganic mesoporous materials, which provides variable pore diameters and high surface areas are obtained after crosslinking of the precursor usually by acidic or basic sol-gel processing followed by removal of the surfactant by calcination,[28] extraction,[29, 30] UV/ plasma treatment[31, 32] or chemical oxidation[33].

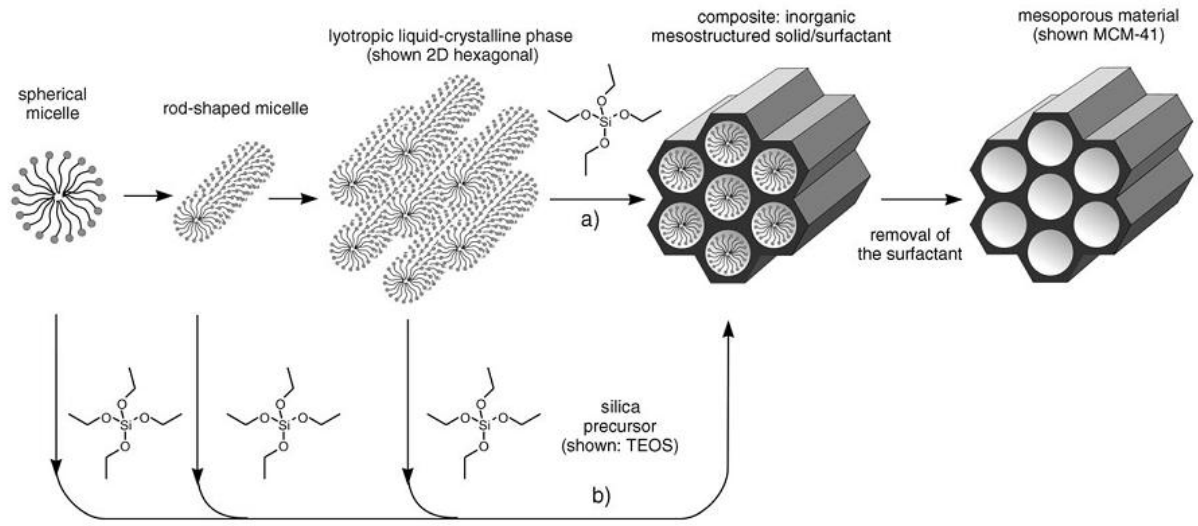

Figure 2.6. Mechanism for the formation of mesoporous silica by structure directing agents: a) true liquid-crystal mechanism, b) cooperative liquid-crystal mechanism.[11]

Meanwhile, more than 10 years after the development by the group of Stucky,[34] SBA-15 is established as prototype for mesoporous silica materials in various research fields from heterogenous catalysis[35] to medical and biological applications[36]. This is reasonable not only due to the outstanding material properties[1], but also due to the biocompatibility and relatively low cost of the commercially available poloxamers (Pluronic® triblock copolymers), which is required for potential industrial applications.[29, 35]

The current focus of material science concerning the templating approach is shifted to non-siliceous mesoporous metal oxides, such as catalytically active titania or zirconia and mesoporous organic-inorganic hybrid materials as adsorbents, chromatographic solid phases, low-k materials or catalysts.[11, 37-39] Further, the simultaneous control of micro-, meso- and macroporosity as well as the macroscopic shape is an important issue related to the tailor-made design of materials for special applications.

2.2 Hierarchically porous materials

The concept of hierarchy in material science describes the combination of structural elements over several length scales. In nature, hierarchical structures are ubiquitous in order to facilitate transport and diffusion processes or to provide exceptional mechanical properties like stability, flexibility and low density.[40] Typical examples are the water and nutrients transport

[1] adjustable pore diameter between 6 – 15 nm, 3 – 7 nm thick microporous walls and hydrothermal stability.

in trees or the blood circulation system as well as biological materials such as nacre, bone or wood. Especially the enormous number of fascinating microorganisms originating from biomineralization (formation of inorganic complex structures via biological processes) generated a great input to material scientists (Figure 2.7).

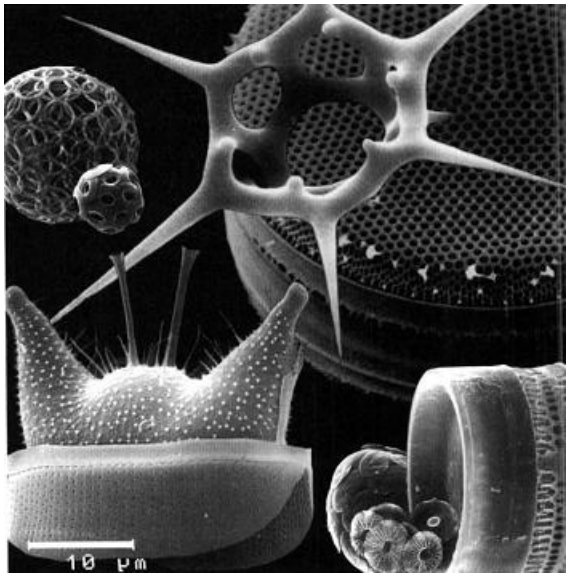

Figure 2.7. SEM image of the shell of marine microorganisms to get an impression about the structural diversity.[41]

In this regard, learning from nature means to construct materials from the molecular to the macroscopic level including the chemical composition, porosity, interfaces and morphology, which is often called structural engineering.[42] This field of research encompasses not only the combination of inorganic and organic building blocks in hybrid or composite materials (see chapter 2.1.2) and the usage of self-assembling polymers as templates for mesopores (see chapter 2.1.3) but also the multiscale control of porosity and morphology.[26]

Adjusting the pore size, distribution and connectivity is the crucial point to optimize the diffusion and confinement regimes in the design of catalysts and separation media.[40] Thus, successful developments in this area can tremendously enhance the effectiveness of industrial processes.

In principle, hierarchically structured porous materials can be classified according to their pore size combination, e.g. into micro-mesoporous or meso-macroporous architectures or according to the applied synthesis pathways. Thereby, the top-down approach describes the

post-synthetic treatment of preformed porous materials mainly via physical methods, whereas the bottom-up approach is based on the chemical interaction between different inorganic and organic building blocks to combine them to complex assemblies.[43]

2.2.1 Top-down approach

Besides lithography[44] and anodic oxidation[45], the most important top-down strategy to hierarchically structured porous materials is the generation of mesopores inside the zeolite framework. The great efforts are owed to the wide application of zeolites in chemical industry, wherein the application as catalysts in oil refinery has to be emphasized.[46] The benefit of zeolite catalysts are their unique properties, such as the ordered microporous structure, crystalline framework, strong acidity and hydrothermal stability, which allows high activity and selectivity.[47, 48] However, the micropore diameter, which is required for shape selective processes, restricts the applicability of zeolites to small molecules due to steric constraints and severe mass transfer limitations.[35] The endeavor to optimize the accessibility of active sites and thus the catalytic effectiveness are focused on three different attempts: i) increasing the zeolite pore size, ii) decreasing the zeolite crystal size and iii) introducing a second (meso)porous system. In particular the last approach was emphasized during the last years due to increasing industrial interest in hierarchically structured zeolites.[49, 50] The most frequently employed methods are dealumination or desilication of the zeolite framework via steaming or leaching techniques.

Steaming, i.e. hydrothermal treatment of the zeolite leads to hydrolysis of Al-O-Si bonds and removal of aluminum from the framework resulting in a vacancy (hydroxyl nest) or amorphous regions. Due to the partial amorphization mobile silica species are caused, which can repair some of the vacancies, whereas other parts grow to mesopores.[51, 52] Disadvantageous some of the pores are subsequently blocked by amorphous residues. Therefore, dealumination via steaming is often followed by mild acid treatment to dissolve extra-framework material (Figure 2.8).[53]

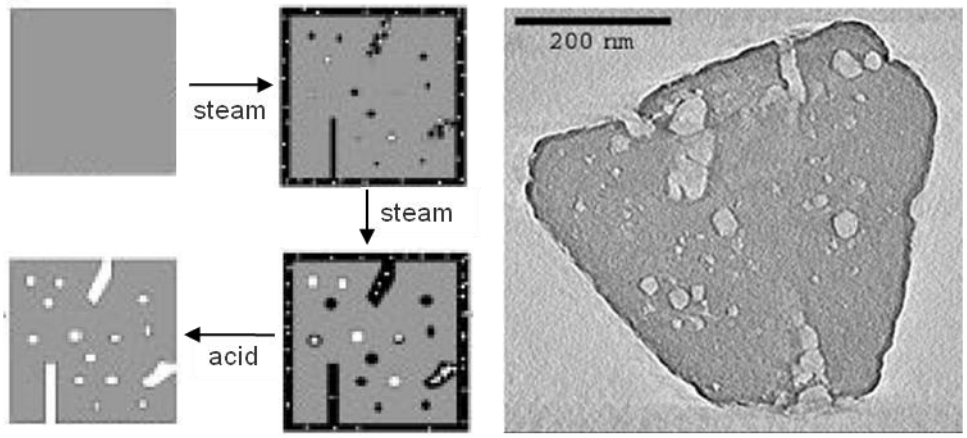

Figure 2.8. Schematic drawing (left) and TEM image (right) of the mesopore formation in a zeolite framework via dealumination.[50, 53]

Otherwise, acid leaching can also be used for direct creation of mesopores inside the zeolite framework, especially in the case of mordenite.[54] The treatment with strong acids like HCl or HNO_3 removes aluminum from the framework, which results in mesopores and therefore in a higher accessibility of the acid sites. At the same time the removal of aluminum represents a major problem because of the loss of active sites by the changed Si/Al ratio of the framework.

Another method to generate mesopores and mostly maintain the crystallinity and acidity is the extraction of silicon by basic leaching of zeolites, viz. desilication. This treatment is usually performed with ZSM-5 leading to uniform mesopores controllable by the leaching time, concentration and type of base.[55, 56] A further improvement of this technique can be achieved by a subsequently acid washing step to remove silicate debris deposited during the alkali treatment.[57]

Despite of the enhanced properties of mesoporous zeolite, especially in catalysis, it has to be kept in mind that the top-down approach is a ‘destructive’ method, which is often difficult to control and requires a series of synthesis steps including the composition of a complex structure and the following partial decomposition to finally achieve the hierarchical structured material.

2.2.2 Bottom-up approach

In contrast to the top-down approach, hierarchically porous materials can also be formed via a 'constructive' pathway, i.e. the hierarchical architecture is designed by the combination of molecular or nanometer sized building blocks. These processes are typically based on sol-gel chemistry with different templates, which allows usually a better control over the pore diameter and distribution. Possible templating agents for the formation of macropores are polymer or silica spheres, biological materials or emulsion systems, which are assigned to the following preparation processes (Figure 2.9).[10, 40, 58]

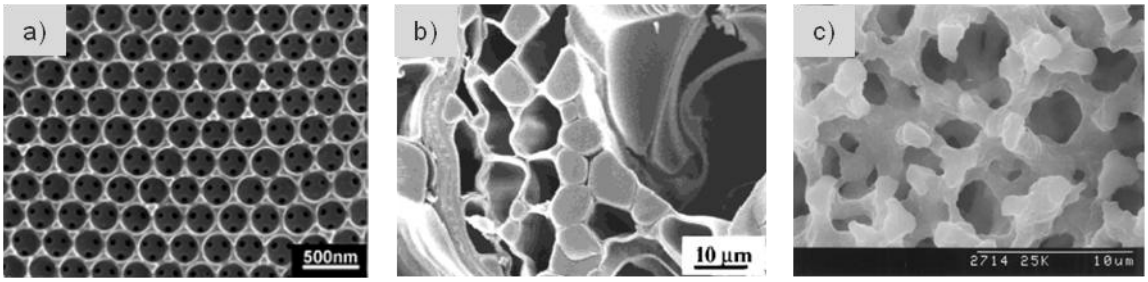

Figure 2.9. SEM images of porous materials made via micromolding with silica spheres[59] (a), biotemplating with wood[60] (b) and phase separation[61] (c).

Micromolding

The method combines the synthesis of macro- and meso- or microporous materials via the usage of 'hard' macrotemplates coupled with surfactants as structure directing agents for meso- or micropore formation. This allows an individual control of the hierarchical levels and ordered pore arrangements can be easily achieved. The most prominent example for micromolding is the condensation of a solution containing a silica precursor (e.g. TEOS) and a self-assembled surfactant in the interstitial spaces between colloidal latex particles.[62, 63] After calcination, a bimodal porous material remains with ordered macropores caused by colloids surrounded by pore walls of mesoporous silica. A similar reaction system can be used for the preparation of macroporous zeolite by filling the voids of an ordered polystyrene sphere array with a solution of TEOS and tetrapropylammonium hydroxide (TPAOH), which results in zeolitic macropore walls after removing the polymeric macrotemplate.[64] Another way to introduce mesopores into a zeolite crystal is the addition of carbon templates, e.g. particles, nanofibres or nanotubes to the zeolite precursor mixture.[49, 65, 66]

Biotemplating

In order to find novel hierarchical porous composites, which provide a low-cost and environmental friendly synthesis the usage of biological templates already is an established branch in material research.[67, 68] Therefore different kinds of bio-templates are suitable for the synthesis of macro-mesoporous morphologies including natural chemicals (e.g. starch, polysaccharides, chitin),[69] plants (e.g. wood, pollen)[60, 70] or bacteria[71]. The preparation of the inorganic replica is similar to the micromolding technique, meaning the infiltration of a silica or silica-surfactant solution in the porous biological structure.

Phase separation

Various morphologies and macro- as well as mesoporous structures can be obtained by inducing phase separation parallel to the sol-gel reaction.[72] Regarding the kind and effect of phase separation it is distinguished between the formation of mesopores via silica-surfactant assemblies, which is termed microphase separation (see Chapter 2.1.3) and the polymerization induced macroscopic ordering by the arrangement of larger surfactant-solvent domains.[73] Thereby, the macropore size is determined by the sol-gel transition relative to the onset and development of phase separation. The process can be seen as a freezing of the transient phase separation structure through the competitive formation of the (silica) gel network. The ratio and size of macro- and mesopores during the synthesis of hierarchical porous oxides can be controlled by the reaction conditions, such as pH and temperature and by the combination of different solvents and micelle-forming surfactants to cause simultaneous micro- and macrophase separation.[61, 74] After drying and calcination the hierarchical porous product is usually obtained as a meso-cellular foam-like structure.[75]

2.2.3 Macroscopic shaping

The last step to complete the whole size range from nanometer sized particles or pores to the millimeter sized morphology of hierarchical porous materials is macroscopic shaping, which is required for technical usage.[13] The dimensions and shape of the macroscopic body are determined by the type of application, e.g. materials as separation membrane, catalyst support, biomimetic tissue or drug delivery system.

The most frequently applied method is pelleting or extruding of pulverized material with the help of binders.[76, 77] Instead, silica or other sol-gel derived materials can be formed without any additives by casting the precursor solution or sol into the desired mold for subsequent gel formation. This methods results usually in metal oxide monoliths, whereas the drying and calcination procedure has to be performed very carefully since such structures easily collapse into powder.[78, 79] The risk for cracking can be minimized due to controlled shrinkage of the precursor, solvent exchange, slow solvent evaporation and hierarchical porous structures to target lower capillary tension during the crucial step of drying.[80] Thus crack-free thin metal oxide films can be prepared by dip coating of a sol on glass or silicon wafers as support.[81] An overview about typical shaping processes based on metal alkoxide sols is shown in Figure 2.3.

Additionally, the formation of monodisperse spherical metal oxide particles from the nanometer to the millimeter dimension with a dense or porous structure is extensively studied since the development of the Stöber silica particles in 1968.[82] This method is based on the controlled hydrolysis and condensation of silicon alkoxides, which was, 30 years later, adapted for the synthesis of mesoporous silica spheres.[83] Nowadays methods utilizing biphasic systems, such as spray-drying[84, 85] and emulsion processing[86, 87] are well established in the synthesis of porous spherical silica particles. In particular, the versatility of sol-gel transformations combined with emulsion chemistry is a precious tool for the design of tailor-made hierarchical architectures including marble-like millimeter-sized silica spheres,[88] hollow spheres,[89] capsules,[73] microballoons[90] and colloidal particles[86]. The reactions are performed either in oil-in-water (o/w) or in water-in-oil (w/o) emulsions, whereas the crucial point in each case is the stabilization of the interface between the dispersed and the continuous phase to prevent coalescence of the dispersed droplets. A typical method to increase the kinetic stability of emulsions is the addition of surfactants, which reduce the surface or interfacial tension by interaction with both phases via hydrophobic and hydrophilic groups.

2.3 Supported platinum nanoparticles

The initial idea to reduce the size of metal particles for industrial catalysts was the increase of the surface area, and thus the optimization of the accessible active sites. This means especially in the case of precious metals to minimize the specific cost per catalytically active site.[91, 92] From practical point of view, metal nanoparticles are supported on oxidic materials, like SiO_2

or Al_2O_3, which allow easier handling due to the possibility of macroscopic shaping. However, the catalytic activity can be strongly influenced by the type and structure of the support. The chemical composition of the support affects the stability of the metal nanoparticles concerning sintering processes on the one hand and the activity due to the intimate interconnection between the substrate and the catalytic active species on the other hand. In terms of diffusion of reactants and products and the transport of energy, the structural properties on the meso- and macroscopic scale are decisive.[91] Due to the increasing importance of bulky reactant molecules, the development of support materials is focused on materials with larger pore diameters and multiscale hierarchical pore structures (see Chapter 2.2).[93]

Depending on the kind of support material different procedures for the immobilization of metal nanoparticles are established. The most prominent methods are impregnation and ion exchange with dissolved metal salts and subsequent thermal and H_2 treatment to obtain metal particles.[94]

2.3.1 Impregnation and encapsulation

Usually, impregnation is carried out with metal salts to achieve well dispersed and small platinum particles. In the case of mesoporous supports impregnation can also be conducted with preformed poly(vinylpyrrolidone) (PVP) stabilized Pt nanoparticles, which are incorporated into the mesopore channels of SBA-15 via low-power ultrasonication.[95] The confinement inside the pores prevents particle growth and agglomeration during calcination and reduction of the catalyst and provides an excellent thermal stability of the catalyst.

The inverse method of the described impregnation is the encapsulation of metal particles by in situ hydrothermal growth of the mesoporous support. Therefore mesoporous SBA-15 is formed in the presence of PVP-capped Pt nanoparticles, whereas the high dispersion is explained by encapsulation of the particles in the core of the tribock copolymer micelles.[94]

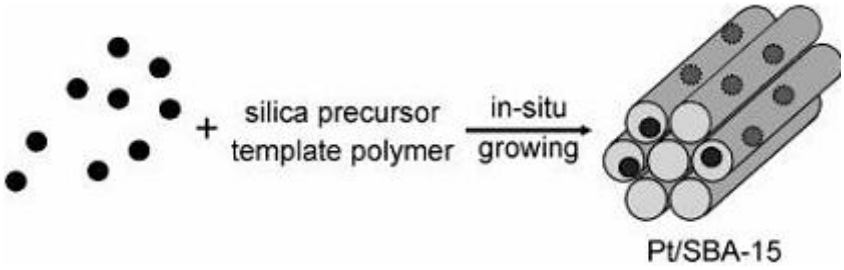

Figure 2.10. Schematic representation of the encapsulation method.[94]

Another possibility for the preparation of thermally stable Pt particles was recently developed by the group of Somorjai.[96] They prepared core-shell particles with platinum core surrounded by a mesoporous silica shell by the simultaneously usage of tetradecyltrimethylammonium bromide (TTAB) as stabilizing agent for the Pt-nanoparticles and as template for the synthesis of mesoporous silica.

The advantage of the application of preformed metal particles for impregnation or encapsulation is the well controlled size and shape of the particles, since they are prepared in a separated step.

2.3.2 Ion-exchange

The common way to introduce platinum into zeolite is the exchange of Na^+ or H^+ ions with the platinum complex $[Pt(NH_3)_4]^{2+}$ resulting in small catalytically active Pt clusters.[97-99] Similar to this method, Ryoo et al.[100] immobilized Pt cluster in the mesopores of AlMCM-41.

The functionalization of silica materials with platinum nanoparticles via ion-exchange requires a pH above the point of zero charge. Under this condition the silica surface is negatively charged and can interact with cationic platinum complexes via the formation of $(\equiv SiO)_2[Pt(NH_3)_4]$.[101] In this procedure drying is determined as crucial step to observe small nanoparticles, which should therefore be done in vacuum.

2.3.3 Immobilization via complexation

Supporting metal atoms at inorganic materials via anchoring metal complexes for catalytic applications represents the intersection between homogeneous and heterogeneous catalysis. The confinement of metal complexes in regular mesopore systems can even control the selectivity of the catalyzed reaction comparable to enzyme catalysis.[102, 103]

However, for the synthesis of Pt-functionalized silica the covalent linkage of metal complexes at the silica surface is usually applied as intermediate product to achieve homogenous platinum distribution and small Pt-particles after calcination and reduction. Extensive work on the coordination of Pt by different amino-functionalized silanes in order to anchor the complex via siloxane bonds in the silica network was done by the group of Schubert.[104-108] The effective complexation of Pt by amino donor ligands was also used to tether platinum in the ordered mesopores of MCM-41 or SBA-15.[109, 110] Therefore, aminosilanes were grafted at the pore walls and loaded with Pt by dispersion of the solid support in aqueous H_2PtCl_6. Besides amino ligands platinum can also be coordinated by the electron donating thiol group of 3-mercaptopropyltrimethoxysilane.[111] This interaction was used in combination with the block copolymer assembly and the network building compound TEOS to immobilize Pt nanoparticles in the mesochannels of SBA-15.

2.4 References

[1] K. S. W. Sing, D. H. Everett, R. A. W. Haul, L. Moscou, R. A. Pierotti, J. Rouquerol, T. Siemieniewska, *Pure and Applied Chemistry* **1985**, *57*, 603.

[2] C. Fruijtier-Pölloth, *Archives of Toxicology* **2009**, *83*, 23.

[3] P. Berth, G. Jakobi, E. Schmadel, M. J. Schwuger, C. H. Krauch, *Angewandte Chemie-International Edition in English* **1975**, *14*, 94.

[4] T. Nakane, H. Gomyo, I. Sasaki, Y. Kimoto, N. Hanzawa, Y. Teshima, T. Namba, *International Journal of Cosmetic Science* **2006**, *28*, 299.

[5] F. Schwochow, L. Puppe, *Angewandte Chemie-International Edition in English* **1975**, *14*, 620.

[6] A. Metes, D. Kovacevic, D. Vujevic, S. Papic, *Water Research* **2004**, *38*, 3373.

[7] T. F. Degnan, *Topics in Catalysis* **2000**, *13*, 349.

[8] C. R. Marcilly, *Topics in Catalysis* **2000**, *13*, 357.

[9] N. Hüsing, in *Sol-Gel Methods for Materials Processing* (Eds.: P. Innocenzi, Y. L. Zub, V. G. Kessler), Springer, Dordrecht, **2008**.

[10] G. J. D. Soler-illia, C. Sanchez, B. Lebeau, J. Patarin, *Chemical Reviews* **2002**, *102*, 4093.

[11] F. Hoffmann, M. Cornelius, J. Morell, M. Fröba, *Angewandte Chemie-International Edition* **2006**, *45*, 3216.

[12] N. Hüsing, in *Hybrid Materials* (Ed.: G. Kickelbick), Wiley-VCH, Weinheim, **2007**.

[13] R. K. Iler, *The Chemistry of Silica*, John Wiley & Sons, New York, **1979**.

[14] R. J. P. Corriu, D. Leclercq, *Angewandte Chemie-International Edition in English* **1996**, *35*, 1420.

[15] U. Schubert, N. Hüsing, *Synthesis of Inorganic Materials*, 2 ed., Wiley VCH, Weinheim, **2005**.

[16] C. J. Brinker, G. W. Scherer, *Sol-Gel Science: the Physics and Chemistry of Sol-Gel Processing*, Academic Press Ltd. Elsevier, London, **1990**.

[17] G. Kickelbick, in *Hybrid Materials* (Ed.: G. Kickelbick), Wiley VCH, Weinheim, **2007**.

[18] F. Schwertfeger, N. Hüsing, U. Schubert, *Journal of Sol-Gel Science and Technology* **1994**, *2*, 103.

[19] U. Schubert, N. Hüsing, A. Lorenz, *Chemistry of Materials* **1995**, *7*, 2010.

[20] V. Chiola, J. E. Ritsko, C. D. Vanderpool, US patent No. 3 556 725, Sylvania Electric Products Inc., Delaware, **1971**.

[21] F. Di Renzo, H. Cambon, R. Dutartre, *Microporous Materials* **1997**, *10*, 283.

[22] C. T. Kresge, M. E. Leonowicz, W. J. Roth, J. C. Vartuli, J. S. Beck, *Nature* **1992**, *359*, 710.

[23] J. S. Beck, J. C. Vartuli, W. J. Roth, M. E. Leonowicz, C. T. Kresge, K. D. Schmitt, C. T. W. Chu, D. H. Olson, E. W. Sheppard, S. B. Mccullen, J. B. Higgins, J. L. Schlenker, *Journal of the American Chemical Society* **1992**, *114*, 10834.

[24] S. A. Bagshaw, E. Prouzet, T. J. Pinnavaia, *Science* **1995**, *269*, 1242.

[25] S. S. Kim, T. R. Pauly, T. J. Pinnavaia, *Chemical Communications* **2000**, 835.

[26] S. Polarz, in *Handbook of Organic-Inorganic Hybrid Materials and Nanocomposites, Vol. 1* (Ed.: H. S. Nalwa), American Scientific Publishers, Stevenson Ranch/California, **2003**.

[27] Q. S. Huo, D. I. Margolese, U. Ciesla, D. G. Demuth, P. Y. Feng, T. E. Gier, P. Sieger, A. Firouzi, B. F. Chmelka, F. Schuth, G. D. Stucky, *Chemistry of Materials* **1994**, *6*, 1176.

[28] F. Kleitz, W. Schmidt, F. Schüth, *Microporous and Mesoporous Materials* **2003**, *65*, 1.

[29] D. Y. Zhao, J. L. Feng, Q. S. Huo, N. Melosh, G. H. Fredrickson, B. F. Chmelka, G. D. Stucky, *Science* **1998**, *279*, 548.

[30] X. Zhuang, X. F. Qian, J. H. Lv, Y. Wan, *Applied Surface Science* **2010**, *256*, 5343.

[31] A. Palaniappan, J. Zhang, X. D. Su, F. E. H. Tay, *Chemical Physics Letters* **2004**, *395*, 70.

[32] L. P. Xiao, J. Y. Li, H. X. Jin, R. R. Xu, *Microporous and Mesoporous Materials* **2006**, *96*, 413.

[33] H. Q. Cai, D. Y. Zhao, *Microporous and Mesoporous Materials* **2009**, *118*, 513.

[34] D. Y. Zhao, Q. S. Huo, J. L. Feng, B. F. Chmelka, G. D. Stucky, *Journal of the American Chemical Society* **1998**, *120*, 6024.

[35] A. Taguchi, F. Schüth, *Microporous and Mesoporous Materials* **2005**, *77*, 1.

[36] H. Yu, Q. Z. Zhai, *Microporous and Mesoporous Materials* **2009**, *123*, 298.

[37] A. Stein, *Advanced Materials* **2003**, *15*, 763.

[38] C. Sanchez, B. Julián, P. Belleville, M. Popall, *Journal of Materials Chemistry* **2005**, *15*, 3559.

[39] P. C. A. Alberius, K. L. Frindell, R. C. Hayward, E. J. Kramer, G. D. Stucky, B. F. Chmelka, *Chemistry of Materials* **2002**, *14*, 3284.

[40] A. Léonard, A. Vantomme, B.-L. Su, in *Annual Review of Nano Research, Vol. 2* (Eds.: G. Cao, C. J. Brinker), World Scientific Publishing Co. Pte. Ltd., Singapur, **2008**.

[41] D. Volkmer, *Chemie in Unserer Zeit* **1999**, *33*, 6.

[42] R. Lakes, *Nature* **1993**, *361*, 511.

[43] J. C. Groen, J. Pèrez-Ramírez, in *Novel Concepts in Catalysis and Chemical Reactors* (Eds.: A. Cybulski, J. A. Moulijn, A. Stankiewicz), Wiley VCH, Weinheim, **2010**.

[44] J. Grunes, J. Zhu, E. A. Anderson, G. A. Somorjai, *Journal of Physical Chemistry B* **2002**, *106*, 11463.

[45] S. Z. Chu, K. Wada, S. Inoue, M. Isogai, A. Yasumori, *Advanced Materials* **2005**, *17*, 2115.

[46] A. Corma, *Chemical Reviews* **1995**, *95*, 559.

[47] R. Chal, T. Cacciaguerra, S. van Donk, C. Gérardin, *Chemical Communications* **2010**, DOI: 10.1039/c0cc02073g.

[48] L. Puppe, *Chemie in Unserer Zeit* **1986**, *20*, 117.

[49] I. Schmidt, A. Boisen, E. Gustavsson, K. Stahl, S. Pehrson, S. Dahl, A. Carlsson, C. J. H. Jacobsen, *Chemistry of Materials* **2001**, *13*, 4416.

[50] S. van Donk, A. H. Janssen, J. H. Bitter, K. P. de Jong, *Catalysis Reviews* **2003**, *45*, 297.

[51] C. Choi-Feng, J. B. Hall, B. J. Huggins, R. A. Beyerlein, *Journal of Catalysis* **1993**, *140*, 395.

[52] C. R. Marcilly, *Petrole et Techniques* **1986**, *328*, 12.

[53] A. H. Janssen, A. J. Koster, K. P. de Jong, *Angewandte Chemie-International Edition* **2001**, *40*, 1102.

[54] M. Tromp, J. A. van Bokhoven, M. T. G. Oostenbrink, J. H. Bitter, K. P. de Jong, D. C. Koningsberger, *Journal of Catalysis* **2000**, *190*, 209.

[55] J. C. Groen, J. A. Moulijn, J. Pérez-Ramírez, *Journal of Materials Chemistry* **2006**, *16*, 2121.

[56] M. Ogura, S. Y. Shinomiya, J. Tateno, Y. Nara, M. Nomura, E. Kikuchi, M. Matsukata, *Applied Catalysis a-General* **2001**, *219*, 33.

[57] R. Caicedo-Realpe, J. Pérez-Ramírez, *Microporous and Mesoporous Materials* **2010**, *128*, 91.

[58] S. Mann, S. L. Burkett, S. A. Davis, C. E. Fowler, N. H. Mendelson, S. D. Sims, D. Walsh, N. T. Whilton, *Chemistry of Materials* **1997**, *9*, 2300.

[59] W. S. Chae, P. V. Braun, *Chemistry of Materials* **2007**, *19*, 5593.

[60] Y. S. Shin, J. Liu, J. H. Chang, Z. M. Nie, G. Exarhos, *Advanced Materials* **2001**, *13*, 728.

[61] K. Nakanishi, R. Takahashi, T. Nagakane, K. Kitayama, N. Koheiya, H. Shikata, N. Soga, *Journal of Sol-Gel Science and Technology* **2000**, *17*, 191.

[62] M. Antonietti, B. Berton, C. Göltner, H. P. Hentze, *Advanced Materials* **1998**, *10*, 154.

[63] P. D. Yang, T. Deng, D. Y. Zhao, P. Y. Feng, D. Pine, B. F. Chmelka, G. M. Whitesides, G. D. Stucky, *Science* **1998**, *282*, 2244.

[64] B. T. Holland, L. Abrams, A. Stein, *Journal of the American Chemical Society* **1999**, *121*, 4308.

[65] K. Egeblad, C. H. Christensen, M. Kustova, C. H. Christensen, *Chemistry of Materials* **2008**, *20*, 946.

[66] C. J. H. Jacobsen, C. Madsen, J. Houzvicka, I. Schmidt, A. Carlsson, *Journal of the American Chemical Society* **2000**, *122*, 7116.

[67] F. Y. Qu, H. M. Lin, X. Wu, X. F. Li, S. L. Qiu, G. S. Zhu, *Solid State Sciences* **2010**, *12*, 851.

[68] S. Mann, G. A. Ozin, *Nature* **1996**, *382*, 313.

[69] W. Ogasawara, W. Shenton, S. A. Davis, S. Mann, *Chemistry of Materials* **2000**, *12*, 2835.

[70] S. R. Hall, H. Bolger, S. Mann, *Chemical Communications* **2003**, 2784.

[71] S. A. Davis, S. L. Burkett, N. H. Mendelson, S. Mann, *Nature* **1997**, *385*, 420.

[72] K. Nakanishi, *Journal of Porous Materials* **1997**, *4*, 67.

[73] R. Schiller, C. K. Weiss, J. Geserick, N. Hüsing, K. Landfester, *Chemistry of Materials* **2009**, *21*, 5088.

[74] S. D. Sims, D. Walsh, S. Mann, *Advanced Materials* **2005**, *10*, 151.

[75] T. Sen, G. J. T. Tiddy, J. L. Casci, M. W. Anderson, *Microporous and Mesoporous Materials* **2005**, *78*, 255.

[76] F. Schüth, in *Handbook of Porous Solids, Vol. 1* (Eds.: F. Schüth, K. S. W. Sing, J. Weitkamp), Wiley-VCH, Weinheim, **2002**.

[77] J. F. Le Page, in *Handbook of Heterogeneous Catalysis, Vol. 1* (Eds.: G. Ertl, H. Knözinger, J. Weitkamp), Wiley-VCH, Weinheim, **1997**.

[78] J. H. Smatt, S. Schunk, M. Linden, *Chemistry of Materials* **2003**, *15*, 2354.

[79] K. Nakanishi, T. Amatani, S. Yano, T. Kodaira, *Chemistry of Materials* **2008**, *20*, 1108.

[80] X. D. Ma, H. W. Sun, P. Yu, *Journal of Materials Science* **2008**, *43*, 887.

[81] M. C. Fuertes, G. J. A. A. Soler-Illia, *Chemistry of Materials* **2006**, *18*, 2109.

[82] W. Stöber, A. Fink, E. Bohn, *Journal of Colloid and Interface Science* **1968**, *26*, 62.

[83] M. Grün, I. Lauer, K. K. Unger, *Advanced Materials* **1997**, *9*, 254.

[84] B. Alonso, A. Douy, E. Veron, J. Perez, M. N. Rager, D. Massiot, *Journal of Materials Chemistry* **2004**, *14*, 2006.

[85] I. V. Melnyk, Y. L. Zub, E. Veron, D. Massiot, T. Cacciaguerra, B. Alonso, *Journal of Materials Chemistry* **2008**, *18*, 1368.

[86] K. Landfester, *Annual Review of Materials Research* **2006**, *36*, 231.

[87] H. F. Zhang, A. I. Cooper, *Soft Matter* **2005**, *1*, 107.

[88] Q. S. Huo, J. L. Feng, F. Schüth, G. D. Stucky, *Chemistry of Materials* **1997**, *9*, 14.

[89] S. Schacht, Q. Huo, I. G. Voigt-Martin, G. D. Stucky, F. Schüth, *Science* **1996**, *273*, 768.

[90] C. I. Zoldesi, A. Imhof, *Advanced Materials* **2005**, *17*, 924.

[91] R. Schlögl, S. B. Abd Hamid, *Angewandte Chemie-International Edition* **2004**, *43*, 1628.

[92] M. Che, C. O. Bennett, *Advances in Catalysis* **1989**, *36*, 55.

[93] C. Yacou, A. Ayral, A. Giroir-Fendler, M. L. Fontaine, A. Julbe, *Microporous and Mesoporous Materials* **2009**, *126*, 222.

[94] H. Song, R. M. Rioux, J. D. Hoefelmeyer, R. Komor, K. Niesz, M. Grass, P. Yang, G. A. Somorjai, *Journal of the American Chemical Society* **2006**, *128*, 3027.

[95] R. M. Rioux, H. Song, J. D. Hoefelmeyer, P. Yang, G. A. Somorjai, *The Journal of Physical Chemistry B* **2004**, *109*, 2192.

[96] S. H. Joo, J. Y. Park, C.-K. Tsung, Y. Yamada, P. Yang, G. A. Somorjai, *Nat Mater* **2009**, *8*, 126.

[97] J. de Graaf, A. J. van Dillen, K. P. de Jong, D. C. Koningsberger, *Journal of Catalysis* **2001**, *203*, 307.

[98] A. C. M. van den Broek, J. van Grondelle, R. A. van Santen, *Journal of Catalysis* **1997**, *167*, 417.

[99] R. Ryoo, S. J. Cho, C. Pak, J. Y. Lee, *Catalysis Letters* **1993**, *20*, 107.

[100] R. Ryoo, C. H. Ko, J. M. Kim, R. Howe, *Catalysis Letters* **1996**, *37*, 29.

[101] A. Goguet, M. Aouine, F. J. Cadete Santos Aires, A. De Mallmann, D. Schweich, J. P. Candy, *Journal of Catalysis* **2002**, *209*, 135.

[102] D. M. Ford, E. E. Simanek, D. F. Shantz, *Nanotechnology* **2005**, *16*, S458.

[103] K. Moller, T. Bein, *Chemistry of Materials* **1998**, *10*, 2950.

[104] M. Malenovska, S. Martinez, M. A. Neouze, U. Schubert, *European Journal of Inorganic Chemistry* **2007**, 2609.

[105] C. Lembacher, U. Schubert, *New Journal of Chemistry* **1998**, *22*, 721.

[106] B. Breitscheidel, J. Zieder, U. Schubert, *Chemistry of Materials* **1991**, *3*, 559.

[107] U. Schubert, *Advanced Engineering Materials* **2004**, *6*, 173.

[108] U. Schubert, *Polymer International* **2009**, *58*, 317.

[109] S. S. Park, Y. K. Park, S. J. Choe, D. H. Park, *Journal of Sol-Gel Science and Technology* **2007**, *42*, 35.

[110] T. Huang, W. Tu, *Applied Surface Science* **2009**, *255*, 7672.

[111] A. Chen, W. Zhang, X. Li, D. Tan, X. Han, X. Bao, *Catalysis Letters* **2007**, *119*, 6.

Chapter 3

Synthesis of hierarchically structured macroscopic silica spheres

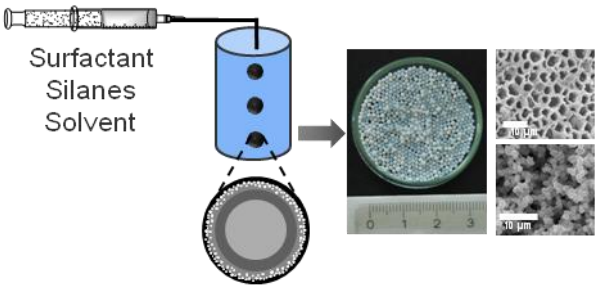

Novel hierarchically structured macroscopic silica spheres have been synthesized using a biphasic oil-in-water system. The spheres are prepared in a one-step process by injection of the precursor solution into water. This leads to controlled hydrolysis and condensation of the silanes. The precursor solution contained three different silanes, a block co-polymer acting as surfactant and a solvent. To remove the surfactants the obtained composite spheres were dried and calcined. The spheres have a hierarchically layered morphology, high mechanical stability, specific surface areas up to 700 m^2/g with mesopores in the range of 9 – 22 nm. The synthesis of such materials with a simultaneous control of the macroscopic and microscopic structure allows facile implementation in separation and catalysis.

3.1 Introduction

Technical applications of porous materials require macroscopic physical shapes including extrudates of porous materials (using binders), monoliths or spherical shapes depending on the particular application. These processes require extensive pre- and post-processing and are cost intensive. In addition, the physicochemical properties of the materials may change during forming. It is, therefore, desirable to combine the synthesis of porous material with the forming procedure.

Realizing the formation of a macroscopic body with a meso- and microscopic structure requires that structures form on several length scales simultaneously. The best results are achieved by separating and partitioning the synthesized material with the help of binders and additives. Typical methods are spray-drying of sol droplets,[1] dropping sol-gel derived particles into an oil phase[2] or extrusion. While it may occur that the final material is only formed in this last step, the methods do not constitute an integrated preparation procedure. Conceptually, the kinetics of the formation of pores on a nanometer level requires sufficient time in the formation process of the macroscopic body. This eliminates spray drying and extrusion processes for practical use. Thus, the partitioning of matter would preferentially occur in biphasic immiscible liquid media (water in oil or oil in water dispersions). An example for this would be to drop a water insoluble precursor mixture into water to induce hydrolysis and condensation.[3]

Having achieved such macroscopically shaped materials, the next step on the way to towards hierarchical structuring is the control of the texture, i.e., the distribution of macro-, meso- and micropores. Macropores are typically formed via phase separation or the application of templates parallel to the sol-gel transition. Biphasic air-liquid[4] or oil-water[5] systems results in solid foams, whereas polymeric templates such as polystyrene spheres[6] can be used to prepare foam like or ordered macropores. However, for the construction of mesopores the templates are usually polymers, which can agglomerate to micelles or a liquid crystal phase. The most prominent examples synthesized according to this approach are the M41S[7] and the SBA[8] materials. Amongst all porous materials the microporous zeolite structures are the most frequently applied materials in industry. The ordered crystalline structures of zeolites are controlled via templating molecules such as tetramethylammonium hydroxide.

Hence, the most versatile approach to prepare materials structured on several length scales is the combination of (templated) sol-gel processing with the emulsion technique. The key step

of this method is the confined reaction environment, which is given by homogeneous dispersed droplets. As described by Schiller et al.[9] each droplet represents an independent nanoreactor resulting in versatile tunable properties of the final particles via changing the size and chemical composition of the droplet. This method results usually in nanosized particles. However, as already suggested by Grün et al.[10] it is advantageous to generate larger, mechanically stable spheres with highly tunable porosity, which can be used directly as catalyst support or sorbent. The first synthesis of transparent mesoporous silica spheres in the millimeter size range was published by Schüth and the group of Stucky,[11] but the pore diameters of these spheres are limited to 5 nm due to the application of the cationic template cetyltrimethylammonium bromide (CTAB).

The paper addresses the preparation of macroscopic hierarchically structured silica spheres with controlled porosity in the macro-, meso- and micropore region. The synthesis was realized by combining the emulsion technique with the sol-gel chemistry of surfactant containing precursor solutions in a continuous operated reactor column.[12] This novel synthesis route allows the preparation of millimeter-sized mesoporous silica spheres with tunable morphology and porosity.

To design the structural properties of the final silica spheres on a knowledge basis, the different stages of synthesis from the initial contact of the precursor solution with water to the solidification of the core have been explored individually, i.e., the precursor solution was optimized for the emulsion based sol-gel processing and the hydrophobicity and molecular weight of the surfactant molecules were tailored with respect to the targeted morphology and porosity of the final spheres.

3.2 Experimental

3.2.1 Materials

Tetraethylorthosilicate (TES40) from Wacker Chemie AG; [3-(2-aminoethylamino)propyl]trimethoxysilane (AAMS, 97%), phenyltrimethoxysilane (PTMS, 97%) and aniline (99%) from Sigma Aldrich, the surfactants Pluronic® 25R4, Pluronic® RPE2520, Pluronic® RPE1740, Pluronic® RPE1720, Pluronic® RPE3110 and Pluronic® PE6100 from BASF were used in the described synthesis. All chemicals were processed without further purification and the reactions were carried out with deionized water.

3.2.2 Water solubility measurements

The copolymers were dissolved in aniline to prepare 3.5 g solution, each containing 20 wt. % copolymer. Water was titrated to these solutions in increments of 10 µl at 25°C. After each step of water addition the emulsion was homogenized for 30 s using a vortex mixer and left equilibrating for at least 30 min. When the mixture became homogeneous and transparent more water was added. The change of the sample appearance to a hazy or milky mixture indicated the maximum concentration of soluble water. The reversibility of the phase separation was demonstrated by back-titration with 20 wt. % copolymer-aniline solution.

3.2.3 Synthesis of silica spheres

The precursor solution was prepared by dissolving the copolymer (14.0 g) in 15 mL aniline under stirring and addition of the silanes TES40 (15.50 g), PTMS (11.16 g) and AAMS (8.63 g). The various used surfactants are listed in Table 3.1.

Table 3.1. Properties of the block copolymers used in this study.

Surfactant	Chemical formula*	Molecular mass M_n / gmol^{-1}	Molecular mass M_w / gmol^{-1}	PDI
Pluronic 25R4	$(PO)_{18}(EO)_{45}(PO)_{18}$	4046	4074	1.01
Pluronic RPE 1740	$(PO)_{11}(EO)_{27}(PO)_{11}$	2476	2503	1.01
Pluronic RPE 1720	$(PO)_{13}(EO)_{16}(PO)_{13}$	2270	2297	1.01
Pluronic RPE 2520	$(PO)_{18}(EO)_{14}(PO)_{18}$	2667	2699	1.01
Pluronic RPE 3110	$(PO)_{27}(EO)_{6}(PO)_{27}$	3437	3459	1.01
Pluronic PE 6100	$(EO)_{3}(PO)_{31}(EO)_{3}$	2046	2077	1.02

* Chemical formula is determined via ^{1}H-NMR (monomer ratio) and MALDI-TOF mass spectrometry (molecular mass).

The precursor solution was injected via a syringe pump with ca. 15 mL/h into the recycling water flow (heated to 65°C) of the reactor column, which is shown in Figure 3.1. The size of the droplets and thus the size of the resulting spheres were controlled via the injection rate and the bypass flow. The reaction parameters (injection and recycling flow) and the diameter of the injection cannula were set in order to produce spheres with a diameter of approximately

1 mm, usually in a size range of 1.1 – 1.3 mm in the as-synthesized status. The solid silica spheres were collected in the product vessel at the bottom of the column, recovered by decantation, washed three times with water and dried under ambient conditions. The samples were calcined in air at 600°C for 3h with a heating rate of 1 K/min to remove the surfactant and organic moieties.

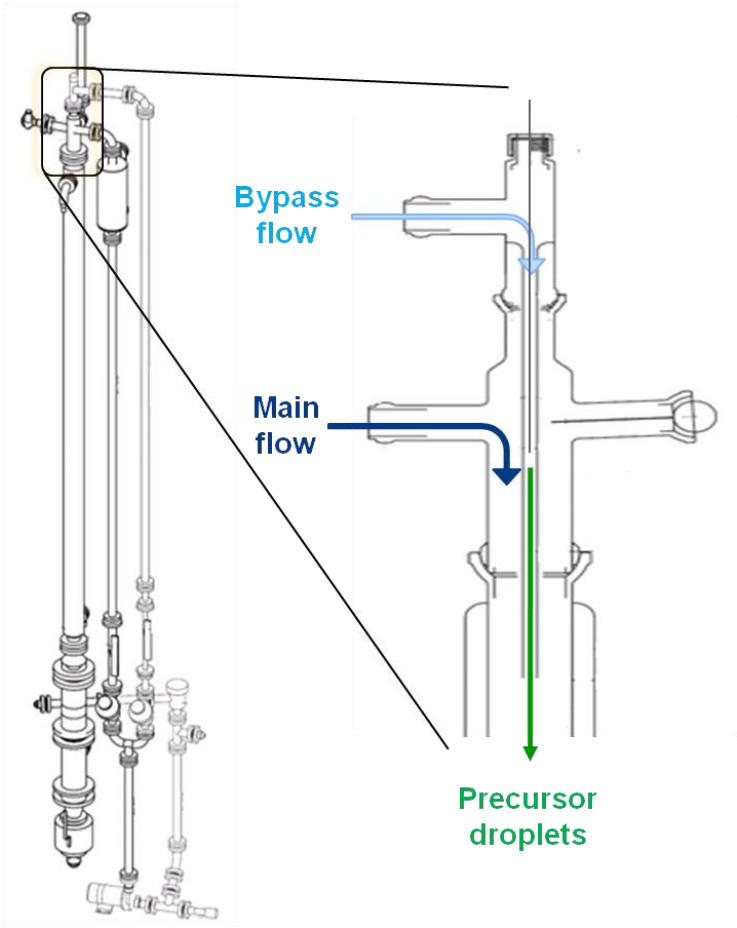

Figure 3.1. Set-up of the reactor column (left) with a magnification of the injection unit showing the principle for the preparation of macroscopic silica spheres.

3.2.4 Characterization

The block copolymers were characterized via ^{1}H-NMR spectroscopy (Bruker, Advance DPX 400) and MALDI-TOF mass spectrometry (Bruker Daltonics Ultraflex TOF/TOF). The particle size distribution was determined using a laser particle size analyzer (Markus Klotz, Analytische Messtechnik). The number of particles was at least 100 at a measurement time of 2 min. The mechanical stability was analyzed by measuring the maximum applied force to break the spheres (crash test). The thermogravimetric analyses of the samples were performed

on a Netzsch STA 409PC Luxx instrument. The measurements for the as-synthesized samples were carried out in air with a heating rate of 5°C/min. The morphology of the samples was studied by investigating the polished cross-section of the spheres with optical microscopy (Leica DM 2500M) and scanning electron microscopy (SEM) (JEOL JSM-5900LV, Hitachi S3500N). SEM images of the Au-sputtered samples (whole spheres and cross-section) were taken at acceleration voltages between 10 and 25 kV. The condensation behavior was visualized via high speed real-time microscopy (Qimaging, MicroPublisher 3.3 RTV). The porosity of the products was investigated using nitrogen physisorption (Thermo Finnigan, Sorptomatic 1990 series) and mercury porosimetry (PMI Europe, Porous Materials Inc.). Prior to the measurements the samples were degassed at 250°C for 2 h. The specific surface area was calculated according to the BET methodology and the mesopores were analyzed according to the BJH method.

3.3 Results and discussion

To form hierarchically structured macroscopic silica spheres the structure of the spheres was designed stepwise by combining the variability of sol-gel chemistry with different interactions of amphiphilic block copolymers in an emulsion based reaction system. This allowed the simultaneous control of the macroscopic shape and the microscopic structure including the morphology and porosity of the sample. In this strategy the macroscopic shape of the material is defined via the droplet size of the oil-in-water emulsion, while the formation of the sphere occurs from the precursor solution in the hydrophobic phase. The morphology of the spheres is so controlled by the cooperation of surfactant molecules, water and silanes at the phase boundaries within several length scales. The core structure depends on the reaction rate of the silane hydrolysis and condensation, while the (meso)porosity is determined by the self-assembling of the surfactant molecules.

3.3.1 Precursor solutions in an emulsion based reaction system

The precursor solution consists of different silanes, a block copolymer as surface active compound and a structure directing agent as well as a hydrophobic solvent.

The crucial point with respect to the macroscopic shape is the stabilization of the interface between the dispersed oil and continuous water phase to prevent coalescence of the droplets.

Thus, as a first priority a significant, but balanced hydrophobicity of the reacting mixture and a rapid formation of a non-reactive interface to the aqueous phase are required.

The inner structure of the sphere is determined by the nature of the surfactant and the reactivity of the siloxane precursor. "Reverse" Pluronic® triblock copolymers with the general molecular formula $(PO)_x(EO)_y(PO)_x$ were chosen as primary templating agents because of their hydrophobicity and their ability to order in a wide variety of structures. In contrast, regular triblock copolymers, such as Pluronic® P123, which are normally applied in the synthesis of ordered mesoporous materials, cannot be utilized due to the high ethylene oxide content and thus high hydrophilicity, therefore the stability of the precursor droplets is too low.

However, while it is necessary that the templating agent is hardly soluble in water, it must allow and support the diffusion of water into the precursor to react in the solid forming sol-gel process. Thus, the ability of "reverse" Pluronic® block copolymers to absorb water was examined by stepwise addition of water to a surfactant-aniline solution containing 20 wt. % of surfactant. The absorption of water can be explained by the insertion of water into micelles within the hydrophobic phase formed by the "reverse" triblock copolymers. The maximum uptake of water is determined by the amount of water which can be dissolved in the organic solution. The correlation of the water uptake of the analyzed "reverse" Pluronic® polymers is shown in Figure 3.2. Increasing M(PO)/M(EO) ratio of the surfactants correlates with the decreasing water uptake, since only the ethylene oxide block of the polymer interacts with water. Due to the identical value for Pluronic® 25R4 and RPE 1740 an influence of the molecular mass of the polymer can be excluded.

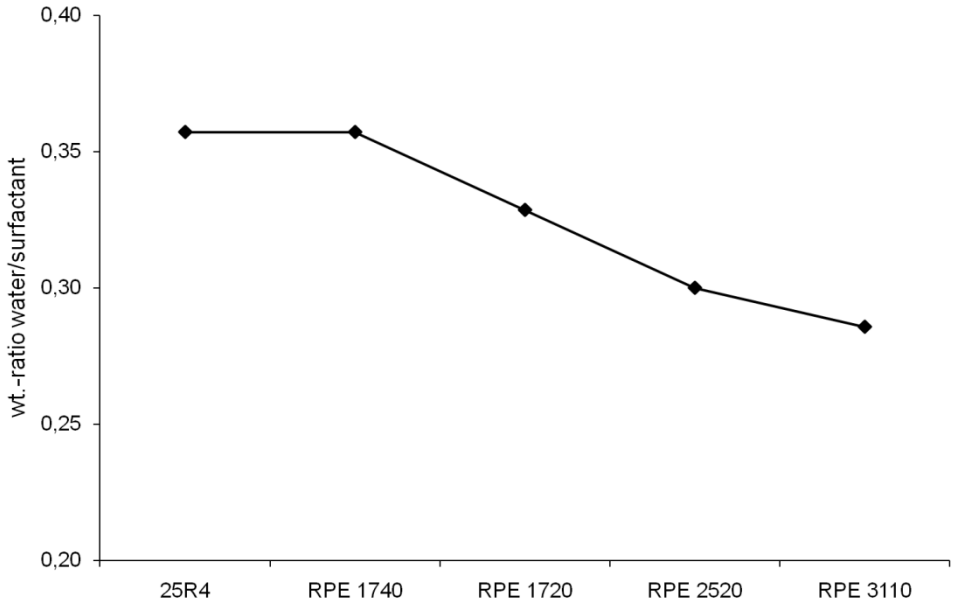

Figure 3.2. Water solubility in surfactant-aniline solutions containing 20 wt. % surfactant.

Alternatively copolymers with a PEO-PPO-PEO structure can also be used if the PO/EO ratio is high enough and the polymers exhibit sufficient water uptake. The employed Pluronic® PE 6100 ($EO_3PO_{31}EO_3$) shows a water uptake of 0.30 g water per gram surfactant which is identical to the "reverse" Pluronic® RPE 2520.

The most critical step for the successful preparation of the spheres is the balance between the stabilization of the oil-water interface and the efficiency of water diffusion into and inside the precursor droplet, which is largely controlled by the combination of surfactants/templating agents.

The challenge is the formation of a stable three-dimensional porous silica network with a sufficient reaction rate to prevent agglomeration across droplets. This was addressed by combining tetraethyl silicate (TES40) as network building compound with phenyltrimethoxysilane (PTMS) and [3-(2-aminoethylamino)propyl]trimethoxysilane (AAMS). Phenyltrimethoxysilane enhances the droplet stability through the hydrophobic organo-functionalization. The aminosilane is added to auto-catalyze the sol-gel reaction by providing a basic pH inside the precursor droplet, since the molecule is simultaneously anchored in the siloxane network. The dissolution of non silane based acids and bases in water is the reason why they are insufficient for such kind of emulsion synthesis. An ideal solvent for the precursor solution is aniline, since it combines a low solubility in water and it

has a beneficial effect on the reaction rate due to the distinctive basicity with a pK_b value of 9.4.

The application of such precursor solutions containing the three different silanes and a triblock copolymer solved in aniline results in around 90% yield of calcined silica spheres.

3.3.2 Effect of the surfactant on the physical and chemical properties of the spheres

All silica spheres presented in this paper are prepared using a continuously operated reactor column. Compared to a stirred tank reactor, this allows a highly reproducible synthesis and a narrow size distribution of the macroscopic silica spheres (Figure 3.3). The diameter of the spheres is significantly decreased after calcination due to removal of the solvent, surfactant and organic groups

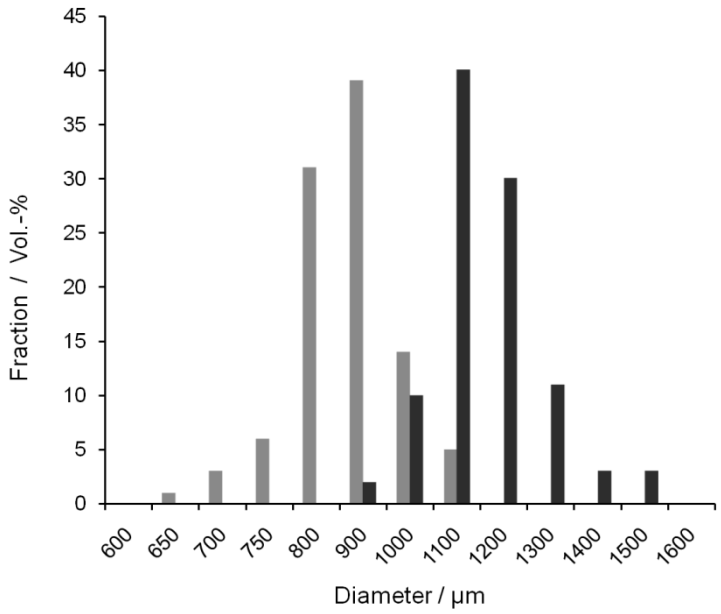

Figure 3.3. Particle size distribution of calcined (light gray) and uncalcined (dark gray) spheres made with Pluronic® RPE1740.

The total weight loss during calcination is approximately 40 - 70% depending on the surfactant and is divided into three steps: evaporation of water (up to 200°C), decomposition of the surfactant (200 - 500°C) and removal of the organic groups bound to the silanes and

residual carbonaceous matrix (500 - 700°C). The temperature of surfactant decomposition is slightly shifted to higher temperatures compared to the decomposition of Pluronic® P123 in SBA-15.[13] Although the last fractions of weight loss in a TGA experiment were observed above 600°C, careful calcination at 600°C, i.e., a heating rate of 1 K/min and the 3 hour duration led to a carbon content below the detection limit in the materials synthesized.

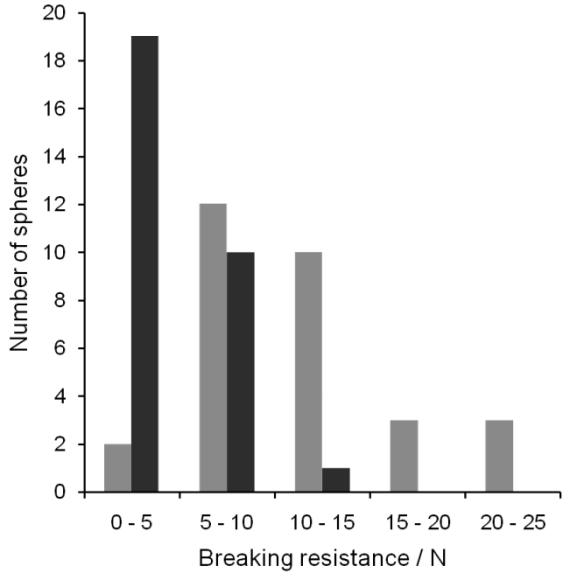

Figure 3.4. Mechanical stability of calcined (light gray) and uncalcined (dark gray) spheres made with Pluronic® RPE1740.

In addition to the decrease in size, the calcination leads to a hardening of the spheres (Figure 3.4). The most likely reason for the higher mechanical stability of calcined spheres is the removal of the soft organic matter, which can be clearly seen by comparing SEM images of the cross-section of as-synthesized and calcined silica spheres (Figure 3.5). Also, it is obvious that further crosslinking of silanol groups leads to shrinkage and, thus, to a stabilization of the siloxane network. The shrinkage of the siloxane network and the associated loss of material volume during drying and calcination is typical for silica gels.[14] In the case of the macroscopic silica spheres the volume loss reaches approximately 20%. The slightly higher temperature of the surfactant decomposition compared to SBA-15 is speculated to be caused by the macroscopic shape of the material in contrast to a powdered sample or due to the absence of the ordered mesopores.

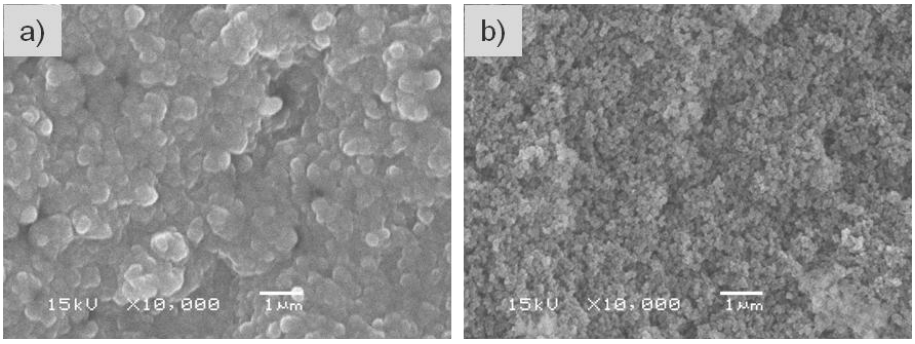

Figure 3.5. SEM images showing the difference between the core of as-synthesized (a) and calcined (b) silica spheres.

We successfully synthesized macroscopic silica spheres with a high specific surface area, mesopore volume and variable pore sizes (Table 3.2). The specific surface area was increased to around 700 m²/g using Pluronic® 25R4, which is the most hydrophilic triblock copolymer. Interestingly, the specific surface area as well as the mesopore diameter are not directly dependent on the molecular weight, but on the hydrophobicity of the surfactant molecules. Increasing hydrophobicity of the surfactants leads to an increasing median mesopore diameter from 9 to 22 nm and in addition to a decreasing BET surface area (Figure 3.7, Figure 3.8). The mesopore volumes of the materials were between 0.3 and 0.6 cm³/g.

Table 3.2. Results of BET analysis and mesopore characterization using the BJH calculation obtained from the measured N_2 adsorption/desorption isotherm. The samples are listed with increasing molecular mass of the surfactant.

surfactant	BET surface area m²/g	Mesopore volume cm³/g	Mesopore diameter nm
Pluronic®PE6100	506	0.38	18.1
Pluronic®RPE1720	477	0.64	17.3
Pluronic®RPE1740	564	0.51	10.0
Pluronic®RPE2520	438	0.50	18.2
Pluronic®RPE3110	342	0.35	21.7
Pluronic®25R4	692	0.56	9.5

The pore size calculated according to the BJH method agrees perfectly with the results obtained by mercury intrusion. Both measurements do not show significant difference between the analysis of the whole spheres and the powdered materials. This demonstrated the unhindered diffusion of nitrogen and mercury inside the sphere. However, the pore size distribution of meso- and macropores reveals again a dependence on the hydrophobicity of the surfactant. The more hydrophobic the surfactant is, the broader the observed pore size distribution (Figure 3.6). Only the most hydrophilic surfactants Pluronic® RPE1740 and 25R4 offer a narrow pore size distribution and relatively small pores.

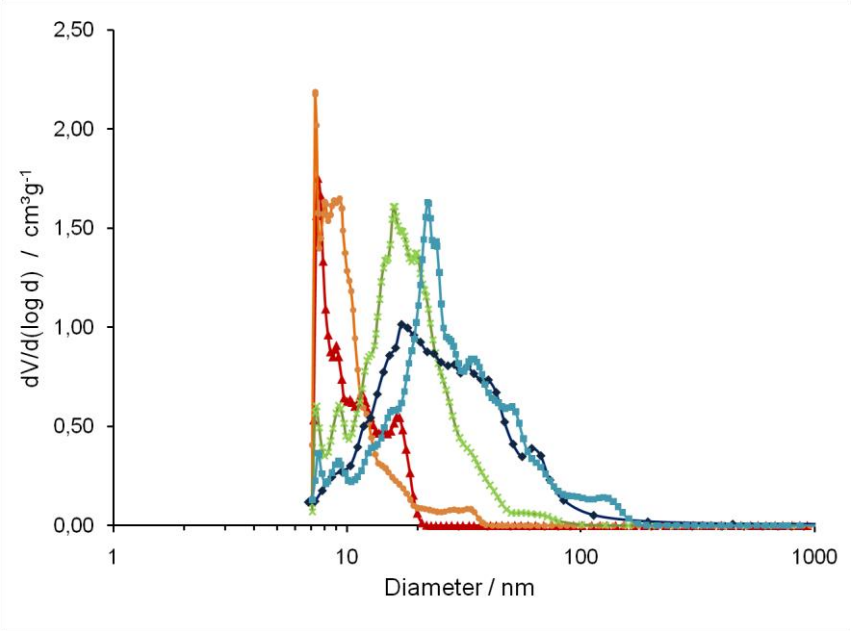

Figure 3.6. Mercury porosimetry of calcined silica spheres made with Pluronic RPE1740 (▲), Pluronic 25R4 (●), Pluronic RPE1720 (x), Pluronic RPE2520 (◆) and Pluronic RPE 3110 (■).

It is proposed that the observed correlation between the mesopore diameter and the hydrophobicity of the surfactant is based on the self-assembled aggregation of the triblock copolymers. Note that several examples in literature for self-assembling or even for the formation of a lyotropic liquid crystal phase using such triblock copolymers have been reported.[8, 15-17] The presence of silanes enforces a cooperative self-assembling via hydrogen bonds between the hydrophilic ethylene oxide and silanol groups.[8, 17] The successive condensation of the silanes results in siloxane embedded copolymer aggregates, which represents the porous structure after calcination or extraction of the surfactant. Zhao et al.[8] observed an increasing mesopore diameter by increasing the synthesis temperature of SBA-15. This is caused by temperature-dependent decrease of the hydrophilicity of the EO-block

which results in less interaction between the triblock copolymer and the siloxane network. Hence, the increase of the mesopore diameter with increasing M(PO)/M(EO) ratio, which corresponds to the hydrophobicity of the triblock copolymer is probably implicated due to less interaction between the copolymer and the silanes and siloxane network. Therefore, the copolymer can agglomerate to larger aggregates by the formation of hydrophobic domains because of the high propylene oxide content.

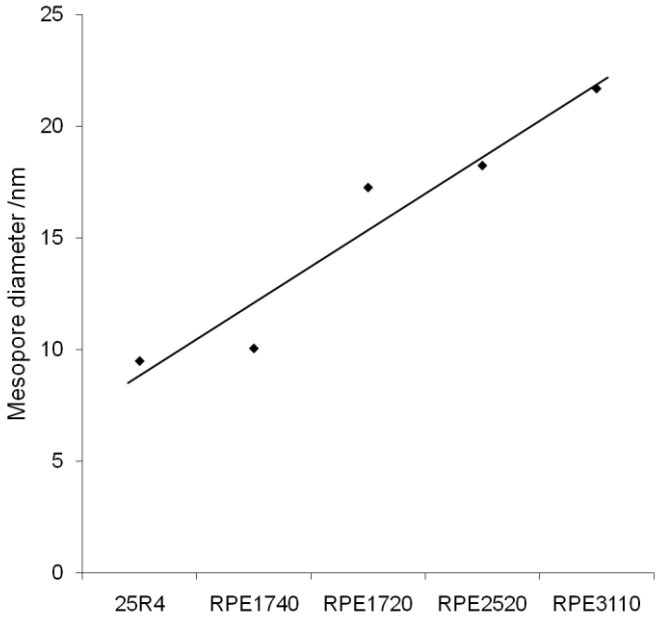

Figure 3.7. BJH median mesopore diameter of the calcined silica spheres made with different Pluronic® surfactants listed with increasing hydrophobicity.

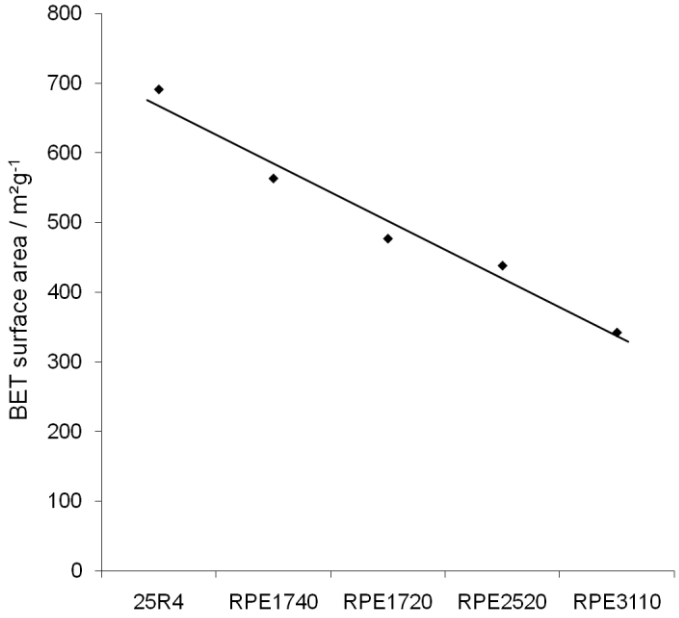

Figure 3.8. BET surface area of the calcined silica spheres made with different Pluronic® surfactants listed with increasing hydrophobicity.

In addition to the porosity, also the morphology of the spheres is influenced by the surfactants. The materials made with Pluronic® RPE1740 and 25R4 have a foam-like surface layer with macropores in the range of 0.6 – 4.0 µm. In contrast, the more hydrophobic surfactants led to a quite dense surface structure of the spheres. This tendency is more distinctive the more hydrophobic the surfactant is (Figure 3.9).

The changing surface structure with changing hydrophobicity of the surfactant suggests that the surfactant molecules are specifically arranged at the oil/water interface via their interaction with the hydrophobic precursor solution and the water phase. Thus, the question arises how these interactions and the ordering at the interface lead to the complex structure.

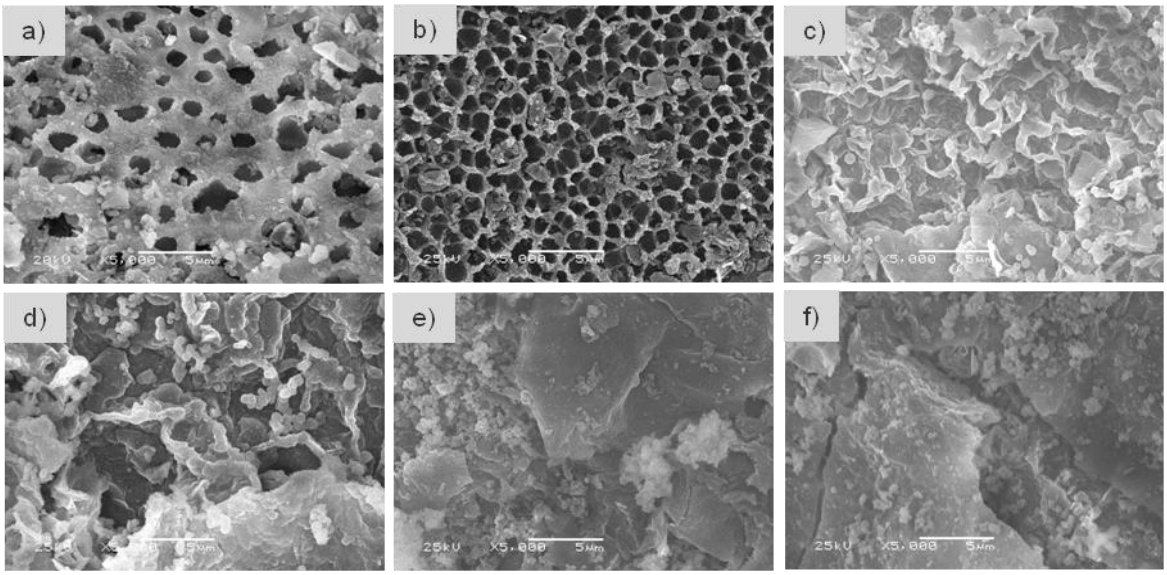

Figure 3.9. SEM images showing the dependency of the surface structure of calcined spheres on the hydrophobicity of the surfactant. (a) Pluronic 25R4. (b) Pluronic RPE 1740. (c) Pluronic RPE 1720. (d) Pluronic RPE 2520. (e) Pluronic RPE 3110. (f) Pluronic PE 6100.

3.3.3 Model for the formation of hierarchically structured silica spheres

Based on the structural data we are able to suggest a model for the formation process of macroscopic silica spheres, which are prepared via emulsion based sol-gel processing. The analytical evaluation of surface morphology and the inner texture of the spheres using different microscopic techniques revealed basically four different layered structures. The growth direction of the inorganic composite material from the oil-in-water interface into the organic phase was followed with high-speed real-time microscopy. The detailed information about the process of the formation of the particular structures of the spheres during the sol-gel process was obtained by using a variation of different surfactants. Overall, the conversion of dispersed droplets into solid silica spheres proceeds in four steps along the condensation sequence from the shell to the core.

The first step is the formation of a thin silica composite gel layer, which is clearly visible on SEM images especially of as-synthesized silica spheres (Figure 3.10). This layer is directly formed after dropping the precursor solution into water. As described by Schacht et al.,[3] the surfactant molecules are enriched at the oil-in-water interface and stabilize the dispersed droplet. The stabilization arises from the alignment of the surfactant molecules along the phase boundary according to their amphiphilic properties.[3, 9] The bridging hydrophilic

poly(ethylene oxide) block is bent so that the terminal hydrophobic poly(propylene oxide) chains are inside the droplets. This optimized interaction of the block co-polymer with the two phases results in a tight surfactant shell (Figure 3.10). The advantage of reverse triblock copolymers is obvious by visualizing the corresponding surfactant layer for PEO-PPO-PEO polymers. In this case the terminal poly(ethylene oxide) blocks interact with the continuous aqueous phase causing a lower stabilization effect. The formation of a stable layer with this type of polymer can only be realized with very short ethylene oxide chains such as found in Pluronic® PE 6100. The stabilizing effect of the surfactant is verified due to the fact that it is not possible to synthesize stable and uniform silica spheres without any suitable surfactant in the precursor solution.

The contact of the precursor droplet with water induces not only the alignment of the surfactant molecules, but also the base catalyzed hydrolysis and condensation of the silanes. This has the effect that the silica composite layer is directly formed at the oil-water interface. In contrast to the emulsion based synthesis of hollow silica particles reported by Schacht et al.[3] the growth of the inorganic material occurs from the aqueous into the organic phase. This is explained by the fact that the precursor solution contains all compounds including surfactant, catalyst and silanes, while in ref.[3] the surfactant and the catalyst are dissolved in the continuous aqueous phase.

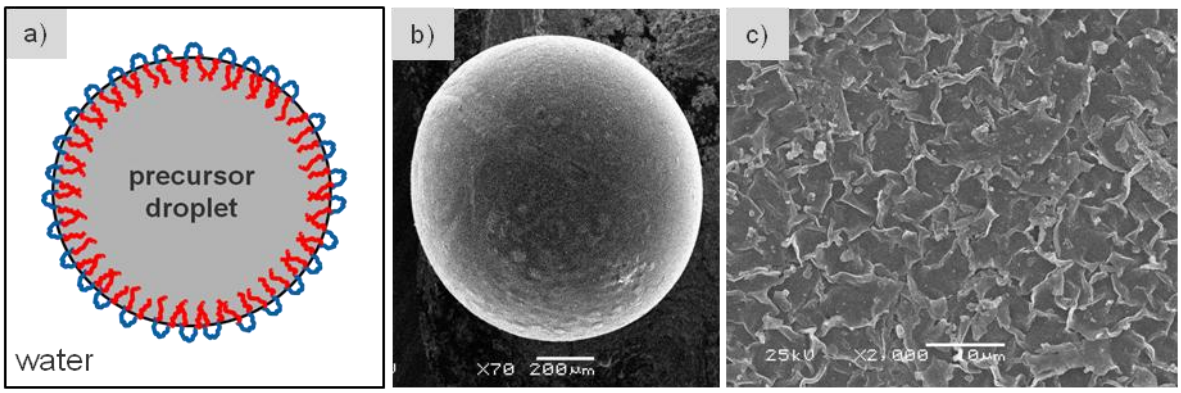

Figure 3.10. Resulting morphology of the first step of sphere formation and a schematic drawing of the stabilizing surfactant layer. (a) The contact of the precursor droplet with water causes a self assembly of the surfactant molecules (PEO in blue, PPO in red) at the oil-water interface and the formation of a silica composite gel layer. (b) SEM image of a sphere. (c) SEM image of the surface of an as-prepared silica sphere with the clearly visible silica composite gel layer.

As it can be seen in Figure 3.11a, there are also some surface areas where the primarily formed thin composite layer is partially removed. It seems that such open fractions originate from the evaporation of alcohol and water during drying of the silica spheres. The SEM analysis of the surface of calcined silica spheres shows that hardly any composite layer remains after calcination, which is attributed to the decomposition of organic matter (Figure 3.11b). The second layer is uncovered showing a foam-like structure including large macropores in the range of 0.6 – 4.0 µm. These macropores are separated by ca 0.6 µm thick siloxane walls and are arranged in a 0.6 – 5.8 µm thick layer. It should be noted that the foam-like layer is especially observed for the spheres made with the surfactants Pluronic® 25R4 and RPE 1740. Both polymers have a distinct hydrophilic character and share the ability to absorb high amounts of water by the formation of water containing inverse micelles (Figure 3.2).

In contrast to the synthesis of other macroporous hierarchical materials such as time-consuming natural creaming of an oil-in-water emulsion,[5] complex double-templating[18] or freezing of the oil phase of a micro-emulsion,[19] the macroporous layer of the silica spheres is straightforwardly generated by diffusion of water inside the precursor droplet through the thin and highly permeable silica composite gel layer. Presumably, the high permeability of the surface layer enables the diffusion of large amounts of water, which is promoted by the formation of a water-in-oil micro-emulsion. The small water droplets are probably stabilized by surfactant molecules resulting in water-filled micelles, which can act as water transport vesicles (Figure 3.11d). A sufficient hydrophilicity of the surfactant molecules, which is given for example by the high ethylene oxide content of Pluronic® 25R4 and RPE 1740 facilitates the arrangement of such water-filled micelles. However, the diffusion of the water transport vesicles inside the precursor droplet is interrupted by condensation of silanes due to the contact with water. The highly reactive auto-catalyzed silane mixture converts directly at the water-in-oil interface to a solid siloxane network, which fills the interstitial spaces between the inverse micelles.[20] Thus, the water droplets are embedded in the silica matrix. After the removal of water during drying and calcination the cavities are remaining and appear as foam-like macropores.

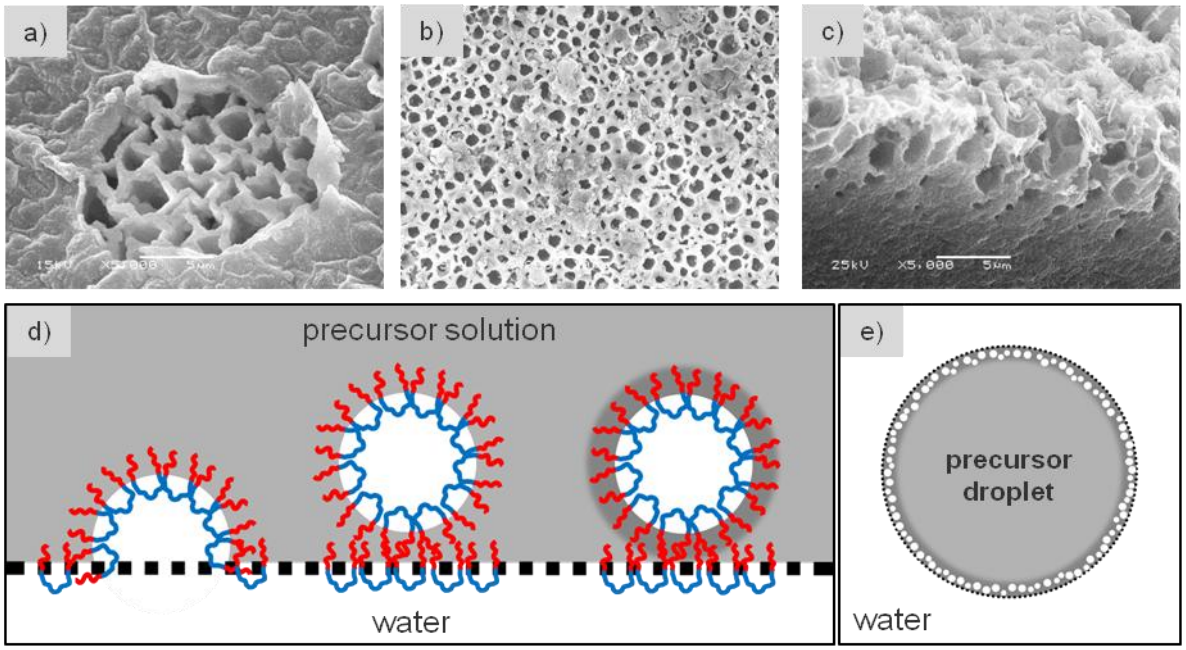

Figure 3.11. Morphology caused in the second step of sphere formation and the schematic drawing of this formation step. (a) SEM image of the surface of a dried sphere with partially removed silica composite layer. (b) SEM image of the surface of a calcined silica sphere showing the foam-like macroporous structure. (c) Cross-section of a calcined sphere with the foam like layer. (d) Schematic drawing of macropore formation divided in water diffusion through the composite layer, stabilization by surfactant molecules and condensation at the interface. (e) Sketch of the cross-section with the composite and the foam-like layer.

The investigations on the polished cross section of the silica spheres using photography and optical microscopy show a clear differentiation between the shell and the core. Note that the two outer layers, described above, are too thin to be analyzed with optical methods. The photographs of the polished cross-section of two samples, which are shown in Figure 3.12 demonstrate that the structural differences between the shell and the core are visible to the bare eye. The shell seems translucent with slightly bluish color whereas the core is opaque and white. Comparing the images recorded with reflected and transmitted light the slightly bluish shell of the spheres made with Pluronic® RPE 1740 appears transparent and the core changes from a white to yellow or reddish brown. In contrast, the spheres prepared with Pluronic® RPE 2520 exhibit a yellow or orange shell and a black core in transmitting light.

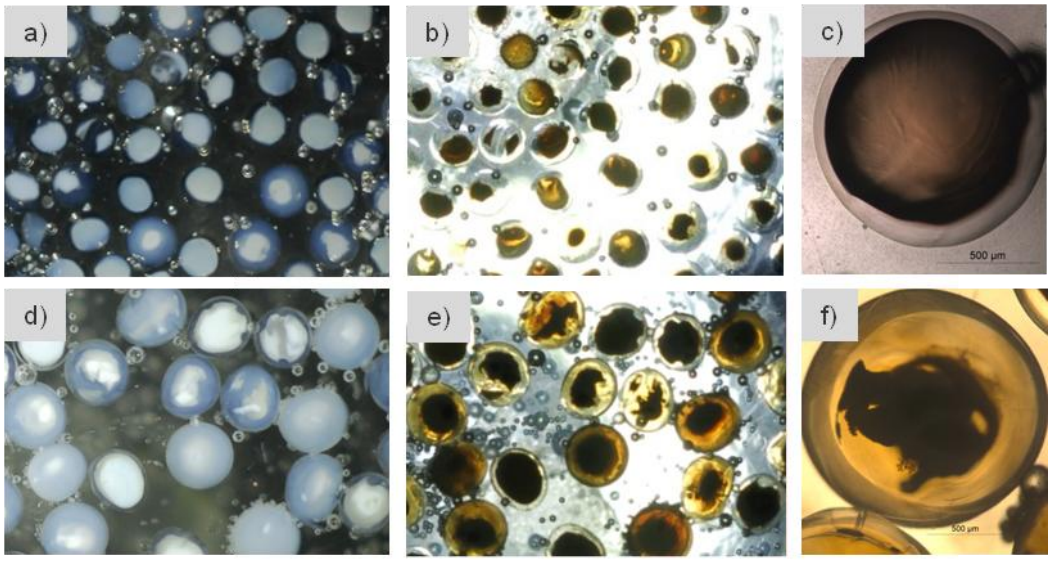

Figure 3.12. Photographs and optical microscopy images of the polished cross-section of spheres made with Pluronic RPE1740 (a – c) and Pluronic RPE2520 (d – f). (a, d) Photographs made with reflected light showing the transparent and opaque parts of the spheres. (b, e) Photographs made with transmitted light showing the coloring originating from differences in light scattering. (c, f) Microscopy images in transmitting light mode.

Since the analyzed spheres are calcined the organic matter is completely removed and only silicon dioxide is remaining. Therefore, some structural aspects have to be the reason for the changing appearance. In order to explain the different optical properties and to provide a deeper insight into the microstructure optical as well as scanning electron microscopy was used for analysis. The image of the polished cross-section obtained via bright field optical microscopy suggests a dense shell and a porous core (Figure 3.13a). The SEM analysis represents a particulate structure for both, the shell and the core of the sphere, but there are clear differences concerning the packing density of the primary silica particles (Figure 3.13b, c). The shell offers a relatively dense structure with hardly distinguishable particles, which are located in a well-defined layer. The thickness of this layer depends on the hydrophilicity of the surfactant. Hydrophilic surfactants like Pluronic® RPE 1740 induce a thin layer of around 45 – 120 µm, whereas the thickness is increased to 120 – 270 µm with increasing hydrophobicity of the surfactant.

In contrast, the core reveals a fine-grained structure of less interconnected primary particles. The diameter of the primary silica particles lies between 150 and 230 nm, while the particles inside the shell are slightly smaller with an estimated size of 80 to 150 nm. Note that the average size of the primary particles decreases with increasing hydrophilicity of the surfactant.

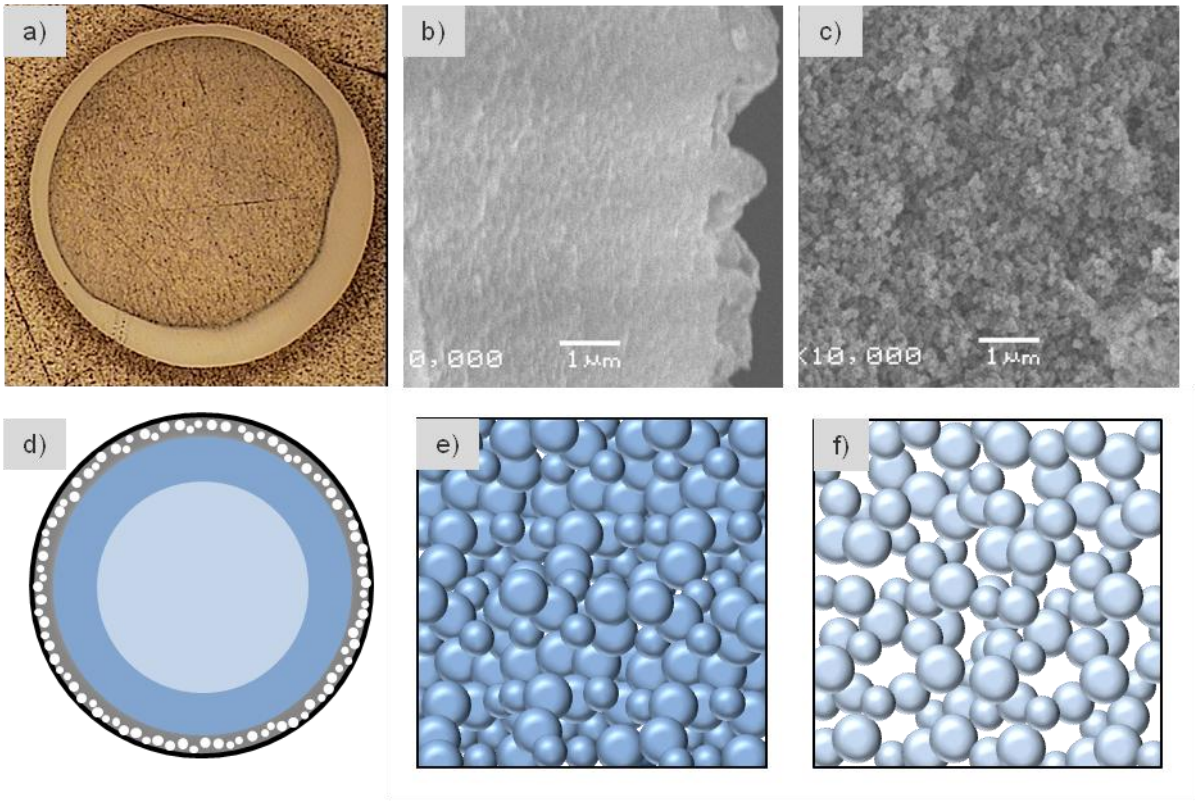

Figure 3.13. Morphology of the inner part of the sphere. (a) Bright field optical microscopy image of the polished cross-section. (b, c) SEM images of the edge and the core of a sphere. (d-e) Schematic drawings of the hierarchically layered structure of the sphere with a detailed sketch of the inner shell structure and the core structure.

Apparently, the structural differences result from changing condensation behavior between the edge and the core of the sphere. It seems most likely, that the silica composite surface layer molded during the first two steps determines not only the final size, shape and morphology of the material, but also acts as a barrier reducing the water diffusion inside the droplet. However, the presence of water is crucial to hydrolyze the silanes and initiate the condensation and it is known that the concentration of water strongly influences the structure of sol-gel based materials.[14]

The limitation of the water diffusion through the solid surface layer leads to a lower condensation rate and to a homogeneous distribution of the molecularly diffusing water. These reaction conditions are comparable to the base catalyzed preparation of silica gel using excess of water, which results in highly interconnected primary silica particles. The particulate structure of silica is typical for a base catalyzed sol-gel process originating from the highly branched siloxane network.[21]

The consumption of water by the silanes and the proceeding condensation inside the shell causes strongly hindered water diffusion to the center of the sphere. This induces a diluted reaction medium consisting of the silane mixture, surfactant and water in aniline and alcohol. Part of the water and the alcohol are products of the sol-gel process. The concentration of water is sufficiently high to provide complete condensation, but the reaction rate is considerably lower resulting in larger and more separated primary silica particles. The cavities, which are enclosed between the primary silica particles, determine the inhomogeneous appearance of the core using bright field optical microscopy.

The varied optical appearance, which is shown in Figure 3.12, is caused by interaction of light waves with the material. The glassy-like appearance of the shell, which is caused by transmission of light, is in good agreement with the observed structurally homogeneous layer of dense packed primary silica particles. In contrast, the grain boundaries and cavities between the less interconnected primary silica particles of the core can act as scattering centers. Since the size of the primary particles is definitely smaller than the wavelength of visible light we observe wavelength dependent scattering. Therefore the emerging color varies from white to orange by changing the illumination from reflectance to transmittance mode. This shows that the observed color is a consequence of the better transmittance of longer wavelengths through the sample.

The differences of the optical properties of the spheres made with Pluronic® RPE 1740 and RPE 2520 results from the slightly increasing size of the primary particles with increasing hydrophobicity of the surfactant. Thus, less light can pass through the spheres because of the more pronounced light scattering. This finally leads to the black appearance of the core due to completely inhibited light transmission.

3.4 Conclusion

Hierarchically structured macroscopic silica spheres have been synthesized by combining silanes, surfactant and solvent with emulsion-based sol-gel processing. This allows the simultaneous control of the micro- and macroscopic structure as well as the physical and chemical properties.

The morphology and porosity of the macroscopic silica spheres is determined by the hydrophobicity of the surfactant in relation to the water diffusion inside the precursor droplet. Therefore, the crucial feature of the synthesis of macroscopic silica spheres is the balance

between the stabilization of the oil-water interface and the efficiency of water diffusion inside the precursor droplet, which can be controlled by the type of surfactant. Additionally, the porosity of the materials is controlled via the formation of aggregates and micelles of the surfactant molecules and the interaction with the silanes, which depends on the ratio of the hydrophilic ethylene oxide block to the hydrophobic propylene oxide block of the surfactant molecule. Increasing hydrophobicity of the surfactant results in larger mesopores. In contrast, specific hydrophilicity of the surfactant leads to a macroporous foam-like surface layer of the spheres and to a reduction of the mesopore diameter. All silica spheres provide a considerably high specific surface area, which can be adjusted by variation of the surfactant. Remarkably, the high mechanical stability of the spheres is not negatively affected by the high porosity.

The combination of the interfacial interaction, partitioning of the surfactant into micelles and the sol-gel transition of the silanes allows a highly variable synthesis of narrow sized macroscopic silica spheres. The simultaneous control of the morphology and porosity of the spheres has distinguished this method for the preparation of tailor-made materials as catalyst support or sorption material.

3.5 Acknowledgement

Financial support by Wacker Chemie AG and fruitful discussions within the Wacker-Institut für Siliciumchemie and the framework of the network of excellence IDECAT is gratefully acknowledged. The authors also thank Dipl.-Ing. Martin Neukamm and Hans Bongard for SEM analysis, Dipl.-Ing. Xaver Hecht and Dipl.-Ing. Matthias Lesti for BET analysis and Hg-porosimetry, Dr. Günter Grundmann for optical microscopy measurements, Georgeta Krutsch and Aleksandra Jonovic for NMR and TGA measurements, Helmut Krause for MALDI-TOF analysis as well as Dipl.-Ing. Oliver Gobin and Dr. Yongzhong Zhu for many helpful discussions and for recording the highly resolved photographs.

3.6 References

[1] B. Alonso, A. Douy, E. Veron, J. Perez, M. N. Rager, D. Massiot, *Journal of Materials Chemistry* **2004**, *14*, 2006.

[2] C. Oh, S. C. Chung, S. I. Shin, Y. C. Kim, S. S. Im, S. G. Oh, *Journal of Colloid and Interface Science* **2002**, *254*, 79.

[3] S. Schacht, Q. Huo, I. G. Voigt-Martin, G. D. Stucky, F. Schüth, *Science* **1996**, *273*, 768.

[4] K. Suzuki, K. Ikari, H. Imai, *Journal of Materials Chemistry* **2003**, *13*, 1812.

[5] T. Sen, G. J. T. Tiddy, J. L. Cascic, M. W. Anderson, *Chemical Communications* **2003**, 2182.

[6] T. Sen, G. J. T. Tiddy, J. L. Casci, M. W. Anderson, *Microporous and Mesoporous Materials* **2005**, *78*, 255.

[7] J. S. Beck, J. C. Vartuli, W. J. Roth, M. E. Leonowicz, C. T. Kresge, K. D. Schmitt, C. T. W. Chu, D. H. Olson, E. W. Sheppard, S. B. Mccullen, J. B. Higgins, J. L. Schlenker, *Journal of the American Chemical Society* **1992**, *114*, 10834.

[8] D. Y. Zhao, Q. S. Huo, J. L. Feng, B. F. Chmelka, G. D. Stucky, *Journal of the American Chemical Society* **1998**, *120*, 6024.

[9] R. Schiller, C. K. Weiss, J. Geserick, N. Hüsing, K. Landfester, *Chemistry of Materials* **2009**, *21*, 5088.

[10] M. Grün, I. Lauer, K. K. Unger, *Advanced Materials* **1997**, *9*, 254.

[11] Q. S. Huo, J. L. Feng, F. Schüth, G. D. Stucky, *Chemistry of Materials* **1997**, *9*, 14.

[12] H. Witossek, E. Bratz, *Chemical Engineering & Technology* **1997**, *20*, 429.

[13] F. Kleitz, W. Schmidt, F. Schüth, *Microporous and Mesoporous Materials* **2003**, *65*, 1.

[14] R. K. Iler, *The Chemistry of Silica*, John Wiley & Sons, New York, **1979**.

[15] Y. Wan, D. Y. Zhao, *Chemical Reviews* **2007**, *107*, 2821.

[16] M. Svensson, P. Alexandridis, P. Linse, *Macromolecules* **1999**, *32*, 637.

[17] G. J. D. Soler-illia, C. Sanchez, B. Lebeau, J. Patarin, *Chemical Reviews* **2002**, *102*, 4093.

[18] J. H. Smatt, S. Schunk, M. Linden, *Chemistry of Materials* **2003**, *15*, 2354.

[19] S. D. Sims, D. Walsh, S. Mann, *Advanced Materials* **2005**, *10*, 151.

[20] S. Mann, S. L. Burkett, S. A. Davis, C. E. Fowler, N. H. Mendelson, S. D. Sims, D. Walsh, N. T. Whilton, *Chemistry of Materials* **1997**, *9*, 2300.

[21] W. Stöber, A. Fink, E. Bohn, *Journal of Colloid and Interface Science* **1968**, *26*, 62.

Chapter 4

Controlling properties of macroscopic silica spheres

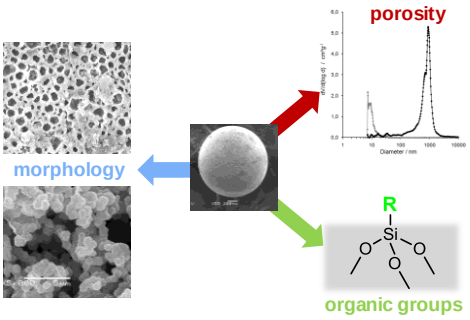

Tailored hierarchically structured macroscopic silica spheres are prepared using an emulsion based sol-gel approach. Surfactants, solvents and silanes are used to direct morphology and porosity. The silica spheres provide specific surface areas up to 900 m²/g and tailored porosity in the meso- and macroporous region. The texture includes particulate structures with controllable size of primary silica particles and a macroporous foam-like shell of the spheres with different densities. The high variability of this preparation method and simultaneous control of the macroscopic shape as well as the microscopic structure including the morphology and porosity allow the design of tailor-made materials as catalyst supports or sorption material.

4.1 Introduction

Mesoporous materials with tunable properties are of great interest in many fields of application like catalyst supports or chromatographic adsorbents. In addition to the pore size, it is an important issue to adjust the morphology and shape of the materials in terms of mass transport optimization. The simultaneous control of both, macroscopic and microscopic properties of porous materials is challenging, but it is the key for designing new functional materials. It is promising for technical applications, since this method allows a less time-consuming and highly reproducible synthesis. For preparation of spherical mesoporous particles different preparation pathways have been proposed. The three most typical ones are based on a biphasic emulsion system[1], controlled hydrolysis by combination of the Stöber synthesis with mesophase formation[2, 3] and spray-drying of sol droplets.[4] The disadvantages of these procedures are usually small particle sizes in the nano- and micrometer range, relatively broad particle size distributions and the formation of agglomerates. The first uniform macroscopic silica spheres with a controllable diameter from 0.1 - 2 mm and pore size between 1 and 5 nm were prepared from Stucky et al.[5] The marble like spheres were synthesized using an oil-in-water emulsion by addition of tetrabutyl orthosilicate (TBOS) to a solution of the cationic surfactant CTAB in water and NaOH and stirring of this mixture for 15 – 30 h.

This work about the emulsion based control of shape and porosity on two different length scales led to intensive studies on biphasic and multiple phase systems. Most of these studies are focused on the synthesis of larger mesopores and especially on the preparation of hierarchical mesoporous-macroporous materials [6]. Meso- and macro-cellular silica foams were synthesized by an acid catalyzed gelation of a TEOS - mesitylene mixture which was slowly added to an aqueous CTAB solution.[7] A macroporous silica monolith with vermicular-type mesostructure could be prepared by a time-consuming emulsion-based addition of dodecane to an acidic sol of tetraethyl orthosilicate (TEOS) and tetradecyltrimethylammonium bromide (TTAB).[8] Another possibility to synthesize hierarchically structured silica materials is a double templating route and a multiple emulsion system ($O_1/W/O_2$) with different surfactants like Tween 20, Span 80, polyethylene glycol or hydroxypropyl cellulose and organic solvents like n-hexane and *n*-decyl alcohol.[9] This complex system allows the synthesis of spherical nanoparticles. Since an emulsion is a metastable system it is still challenging to prepare hierarchically macroporous-mesoporous materials which exhibit a macroscopic shape.

In this paper we describe the preparation of millimeter sized hierarchically structured silica composite spheres using an oil-in-water emulsion system. The hydrophobic phase contains different silanes and a surfactant, which are dissolved in *n*-butanol or aniline. The hydrolysis and condensation of the silicon alkoxides, which leads to the formation of solid material is known as mild and exceptionally variable reaction system. We investigated the influence of surfactant, solvent and silanes on the structure and properties of macroscopic silica spheres to design tailor-made materials as catalyst supports or sorption materials. Furthermore the removal of the surfactant by extraction as well as calcination was examined. The monodisperse silica spheres were characterized regarding their morphology and textural composition.

4.2 Experimental

4.2.1 Materials

Tetraethyl silicate (TES40), Geniosil® GF92, Geniosil® XL973, Geniosil® XL926, Geniosil® XL924 from Wacker Chemie AG; [3-(2-aminoethylamino)propyl]trimethoxysilane (AAMS, 97%), phenyltrimethoxysilane (PTMS, 97%), aniline (99%), 1-butanol (99.9%) from Sigma Aldrich, ethanol from Merck and the surfactants Pluronic® 25R4, Pluronic® RPE1740, Pluronic® RPE1720 and Pluronic® RPE3110 from BASF were used in the described synthesis. All chemicals were used without further purification. The reactions were carried out with deionized water.

4.2.2 Synthesis of silica spheres

Silica composite spheres were prepared by injection of the precursor solution in a water filled reactor column. The copolymer (14.0 g) was dissolved in 15 ml aniline under stirring. The silanes TES40 (15.50 g), PTMS (11.16 g) and AAMS (8.63 g) were mixed and added to the copolymer solution. This solution was injected via a syringe pump with 15 ml/h into the recycling water flow of the reactor column which was heated to 65°C. The product was recovered by decantation, washed three times with water and dried under ambient conditions. The samples were calcined in air at 600°C for 3h with a heating rate of 1°C/min to remove the surfactant and organic moieties. The used surfactants are Pluronic® 25R4, Pluronic® RPE1740, Pluronic® RPE1720 and Pluronic® RPE3110. The variation of the surfactant

concentration was carried out with Pluronic® 25R4 changing the silane to surfactant weight ratios from 2.2 to 30.4. The precursor solution with 1-butanol to investigate the influence of the solvent contains 6.0 ml (5.6g) TES40, 2.48 ml AAMS, 3.16 ml PTMS and 5.6 g Pluronic® 25R4 solved in 8.0 ml 1-butanol. The influence of the silane mixture was studied with precursor solutions containing 3.0 ml TES40, 1.24 ml AAMS, x ml Geniosil® silane and 2.8 g Pluronic® 25R4 solved in 3.0 ml aniline. The applied Geniosil® silanes are N-cyclohexyl-3-aminopropyltrimethoxysilane (Geniosil® GF92, x = 2.21 ml), N-phenylaminomethyl-trimethoxysilane (Geniosil® XL973, x = 1.76 ml), N-cyclohexylaminomethyltriethoxysilane (Geniosil® XL926, x = 2.46 ml) and N-cyclohexylaminomethylmethyldiethoxysilane (Geniosil® XL924, x = 2.23 ml).

The silica composite spheres which were used for the solvent extraction were prepared according to the described method with TES40, AAMS, PTMS, Pluronic® RPE1740 and aniline. After drying at ambient conditions 1.07 g of the silica composite spheres were extracted with 300 ml boiling ethanol for 24 h using a Soxhlet apparatus.

4.2.3 Characterization

The thermogravimetric analyses of the samples were performed using a Netzsch STA 409PC Luxx instrument or TGA Q5000 V3.10 Build 258 instrument. The measurements were carried out under synthetic air with a heating rate of 5°C/min for as-synthesized samples. The morphology was investigated with scanning electron microscopy (SEM) (JEOL JSM-5900LV). SEM images of the Au-sputtered samples (whole spheres and cross-section) were taken at acceleration voltages between 10 and 25 kV. The porosity of the products was investigated using nitrogen physisorption (Thermo Finnigan, Sorptomatic 1990 series) and mercury porosimetry (PMI Europe, Porous Materials Inc.). Prior to the measurements the samples were degassed at 250°C for 2 h. The specific surface area was calculated according to the BET method, the mesopores were analyzed according to the BJH and the micropores via the t-plot method.

4.3 Results and discussion

The focus of this work is to investigate the influence of type and concentration of surfactant, solvent and silanes on the morphology and properties of macroscopic silica spheres. The preparation of silica spheres is carried out in a continuously operated reactor column with a recycling heated water flow.[10, 11] This system provides high reproducibility of the synthesis, narrow size distribution of the silica spheres and an easy scale-up. The hydrolysis and condensation of the silanes is initiated by injection of the precursor solution into the reactor column. This leads to a surfactant stabilized oil-in-water emulsion which results in mechanically stable silica spheres by solidification of each droplet. The advantage compared to other silicon alkoxide emulsion systems is that the precursor solution contains all relevant chemicals and that the continuous phase consists only of water.[5, 9] This allows a cost-saving and environmentally friendly synthesis.

In the next sections we discuss the role of the different precursor components and their influence on the properties of the resulting hierarchically structured silica spheres. The target of these investigations is the assembly of a tool box in order to facilitate the tailor-made preparation of macroscopic silica spheres for several potential applications, e.g. in catalysis or sorption techniques.

4.3.1 Variation of the surfactant concentration

It was observed that especially hydrophobic amphiphilic block copolymers such as the reverse Pluronic® polymers are able to stabilize an emulsion system of a precursor solution containing silanes, surfactant and solvent in water.[11] These polymers tend to form micelles and ordered mesophases, which makes them good candidates for the preparation of macroscopic porous silica spheres. The comparison of triblock co-polymers with varying ethylene oxide and propylene oxide chain length and molecular weights reveals the dependency of the morphology and porosity on the hydrophobicity of the surfactant.

It was observed that an increasing hydrophobicity of the surfactant molecule results in a decreasing specific surface area and an increasing mesopore volume. A high content of ethylene oxide in the reverse Pluronic® polymers ($PO_xEO_yPO_x$) leads to a distinctive hydrophilic character and induces the formation of a foam-like macroporous surface layer of

the spheres. Increasing hydrophobicity of the surfactant causes tight and quite dense surface layers (Figure 4.1).

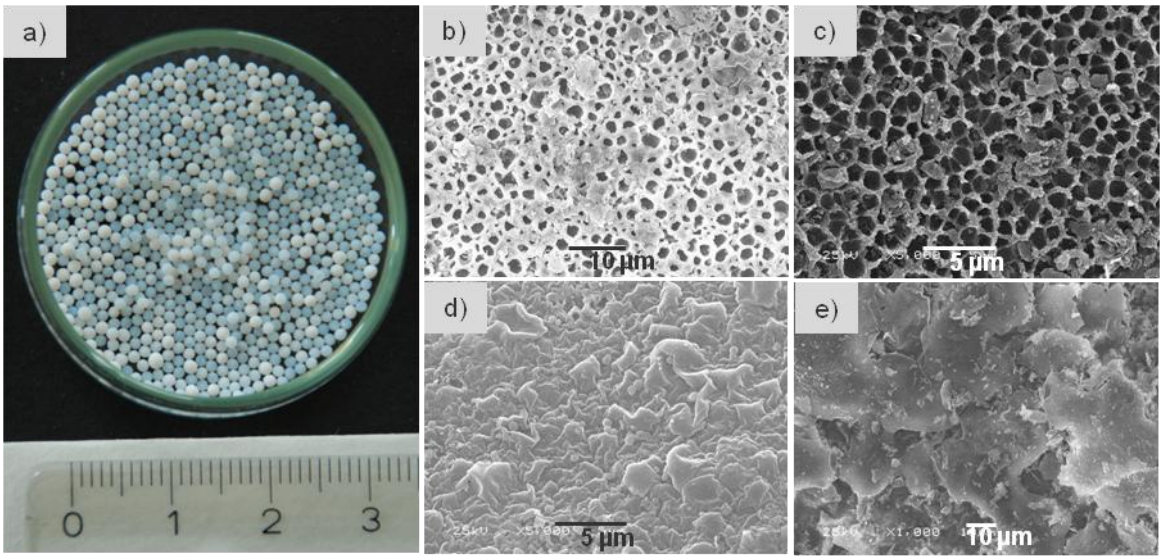

Figure 4.1. Morphology of calcined silica spheres made with different surfactants. Photograph of calcined silica spheres (a) and SEM images of the sphere surface with increasing hydrophobicity of the surfactant (b) $(PO)_{18}(EO)_{45}(PO)_{18}$ (Pluronic® 25R4), (c) $(PO)_{11}(EO)_{27}(PO)_{11}$ (Pluronic® RPE 1740), (d) $(PO)_{13}(EO)_{16}(PO)_{13}$ (Pluronic® RPE 1720) and (e) $(PO)_{27}(EO)_{6}(PO)_{27}$ (Pluronic® RPE 3110).

Besides the molecular composition the influence of the surfactant concentration was investigated by varying the content of Pluronic® 25R4 relatively to the amount of silanes. The silica spheres were synthesized with silane to surfactant weight ratios from 2.2 to 30.4. The produced silica spheres are mechanically stable and offer a translucent milky appearance. It was observed that the precursor droplets with the lowest surfactant concentration are less stabilized resulting in some egg-shaped spheres. The influence of the surfactant concentration on the surface structure of the spheres is clearly visible in Figure 4.2. High surfactant concentrations induce the formation of a well-structured macroporous surface with pore diameters from 1 to 4 µm. The reduction of the surfactant concentration causes a successive variation of the surface to less ordered structures. This is observed as less pronounced macropores covered by a compact silica layer and further inhomogeneous surface morphology consisting of dense and particulate parts.

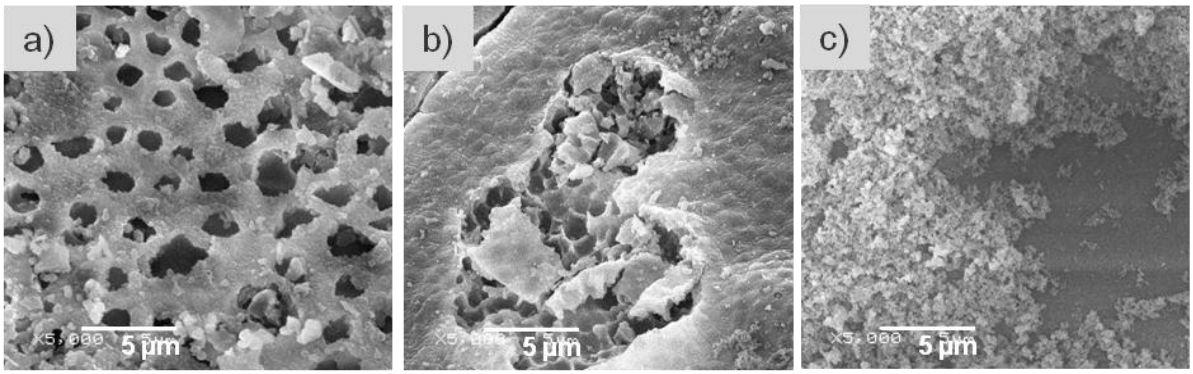

Figure 4.2. SEM images of the surface of silica spheres with silane to surfactant ratios of 2.2 (a), 15.3 (b) and 30.4 (c).

The change of surfactant concentration did not only influence the surface structure of the spheres, but also the inner structure. The analysis of N_2-adsorption using the BJH method shows that the mesopore diameter is decreasing with decreasing concentration of surfactant except for the sample with the highest surfactant concentration (Figure 4.3). This material reveals also a larger BET surface area than the other samples. Apart from that it seems that the BET surface area and the meso- and micropore volume are practically not affected by the concentration of the used surfactant (Table 4.1).

Table 4.1. Results of BET analysis, mesopore characterization (BJH calculation) and micropore analysis (t-plot) obtained from the measured N_2 adsorption/desorption isotherm for varying silane to surfactant ratios.

wt.-ratio silanes / surfactant*	BET surface area / m^2g^{-1}	Mesopore diameter / nm	Mesopore volume / cm^3g^{-1}	Micropore volume / cm^3g^{-1}
2.2	692	9.5	0.56	0.18
7.6	641	22.3	0.54	0.20
15.3	659	18.9	0.58	0.21
2.8	643	17.8	0.54	0.20
30.4	640	13.5	0.50	0.18

* Silane mixture contains TES40, AAMS and PTMS and the surfactant is Pluronic® 25R4.

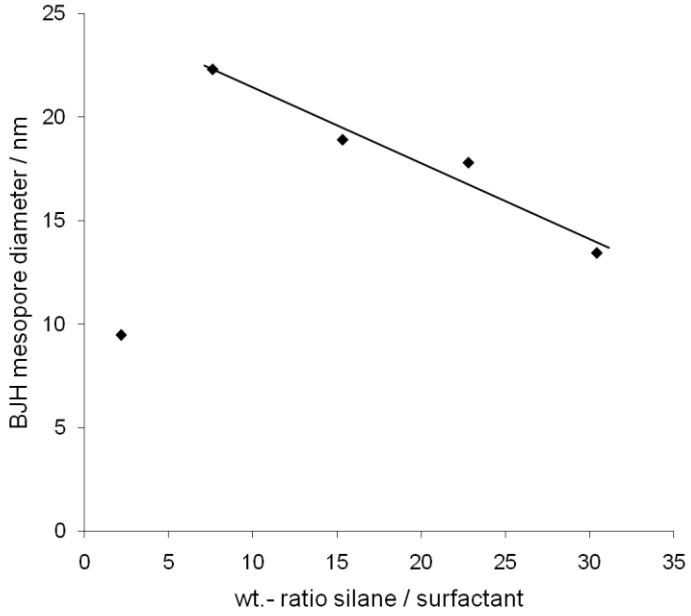

Figure 4.3. Dependence of the BJH mesopore diameter of calcined silica spheres on the silane to surfactant weight ratio.

The results show that the variation of the surfactant concentration has an effect on both, the morphology of the spheres and the mesopore diameter. The surface structure of the spheres is determined by the reaction behavior at the interface between the precursor droplet and the continuous water phase. The dependency on the surfactant concentration demonstrates an interaction of the surfactant molecules with the hydrophobic precursor phase as well as with the continuous water phase. It can be assumed that the triblock copolymer molecules are aligned along the interface according to their amphiphilic character. This surfactant layer stabilizes the precursor droplet.[12]

Presumably, the water diffusion inside the precursor droplet implicates the macroporous surface structure via some phase separation aspect. A feasible procedure for the water diffusion through the precursor-water interface is the formation of a micro-emulsion consisting of water-filled micelles in the precursor droplet. The highly reactive silane mixture hydrolyzes due to the contact with water resulting in encapsulated water droplets.[13] After drying and calcination only solid silica is remaining and the encapsulated water droplet appears as macropore. In consequence, this process can only occur if the surfactant has sufficient hydrophilicity and if the surfactant concentration is considerably higher than the critical micelle concentration (cmc). The first suggestion is proven by SEM analysis of the sphere surface using different surfactants, whereas the macroporous surface is only observed

for surfactants with distinct hydrophilicity (Figure 4.1). The second suggestion can be confirmed by SEM analysis of the spheres with reduced surfactant concentration. A reduction by 80% compared to the initial concentration of the surfactant results in less pronounced macropores and the sample containing only 10% of the initial concentration completely lacks surface macropores (Figure 4.2). This last sample having a low surfactant concentration already indicates a destabilization of the precursor droplet due to the occurrence of some egg-shaped silica particles.

The variation of the surfactant does not only concern the morphology of the spheres via the stabilization of the emulsion and the enhancement of the water diffusion, but also the mesopore formation. The self-assembly of surfactant molecules and silica species to micelles and ordered mesophases was extensively studied.[14-16] The mesopore diameter and structure can be controlled by the type and amount of surfactant. The behavior of surfactant molecules concerning micelle formation is strongly influenced by the temperature, pH value, interacting molecules and the solvent. The precursor solution and the reaction procedure used in this work is in contrast to the typical standard procedure, e.g., for the preparation of SBA-15 regarding almost all synthesis parameters.[17] The macroscopic silica spheres presented in this paper were prepared using a biphasic system under basic conditions with organosilanes and an organic solvent.

Additionally, the crucial point of high interfacial systems such as foams or emulsions is the overlap of interfacial interaction and microphase separation of amphiphilic polymers. Thus, the accessible fraction of surfactant molecules in the bulk phase is lowered by interfacial alignment. Notably, the mesopore diameter decreases, however, in linear correlation with decreasing surfactant concentration. This suggests that for all described samples approximately the same absolute amount of surfactant molecules is involved in interfacial interactions. This is in agreement with the observations during the preparation of thin silica films with varying concentrations of Brij-76.[18] But the sample containing the highest amount of the triblock copolymer does not fit this correlation (Figure 4.3). The reason could be that the extremely high interfacial surface of the water-in-oil microemulsion induces a large number of surface macropores. Consequently, the surfactant concentration in the bulk phase, i.e., inside the precursor droplet is markedly reduced resulting in smaller mesopores. Increasing hydrophobicity of the surfactant results in larger mesopores, which is speculated to be caused by larger hydrophobic self-assemblies.

4.3.2 Influence of the solvent

The predominant role of the solvent is the stabilization of the o/w emulsion by providing a rather low miscibility with water. To investigate the influence of the solvent on the morphology and porosity of the silica spheres two different solvents were used – 1-butanol and aniline. 1-Butanol was selected because alcohols are typically used as solvents to control the hydrolysis and condensation during the sol-gel process. In contrast to the Stöber process[3], methanol, ethanol or propanol are not suitable due to their complete miscibility with water. In addition, aniline was chosen as solvent, because it combines basicity and low miscibility with water. Both precursor solutions result in stable droplets and macroscopic silica spheres, whereas the butanol containing droplets turn to opaque white spheres and the ones with aniline have a transparent milky appearance.

This difference is attributed to variations in the mesoscopic morphology of the spheres, which was analyzed by scanning electron microscopy (Figure 4.4). The surface of the spheres made with the butanol mixture is rougher and consists of strongly interconnected silica particles. The structure changes from the edge to the core of the spheres to less interconnected silica particles with clear spherical shape. In contrast the calcined aniline based silica spheres have a macroporous foam-like surface layer, a relatively dense inner shell with hardly distinguishable particles and a fine grained core structure. It should be noticed that the inner part of both samples include particulate structures, whereas the primary silica nanoparticles originating from the butanol mixture are approximately 10–times larger than the ones of the spheres made with aniline as solvent.

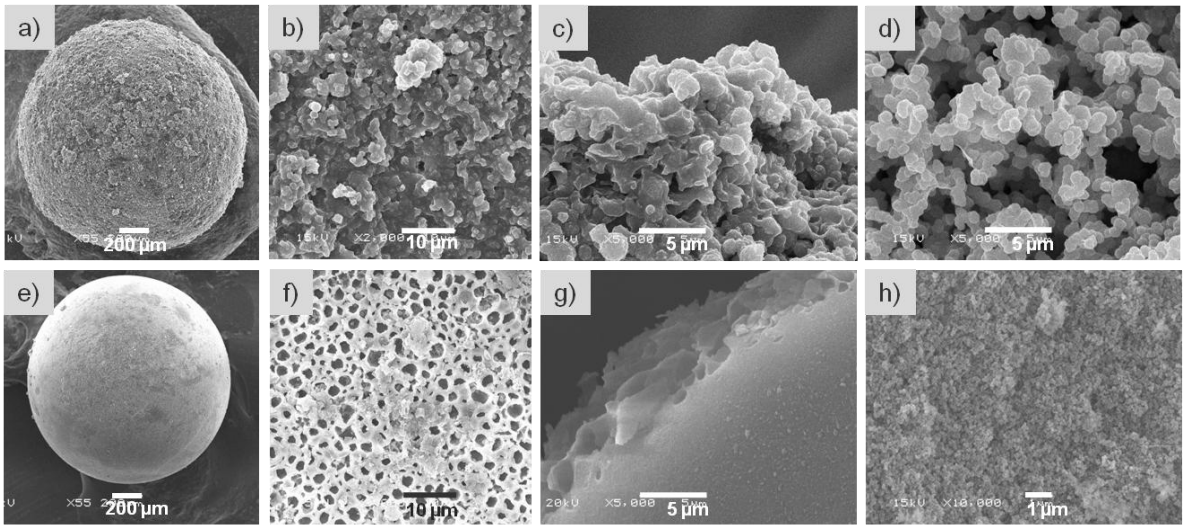

Figure 4.4. SEM images showing the differences between silica spheres made with 1-butanol (a-d) or aniline (e-h) as solvent. (a, e) whole sphere, (b, f) surface of the sphere, (c, g) edge of the cross-section, (d, h) center of cross-section.

Besides the obvious differences in the morphology of these two samples also the pore size distribution is completely different. The butanol based silica spheres show a high macropore content with a maximum at ~ 1 µm. This value would fit to the cavities between the primary silica particles inside the silica spheres. In comparison the aniline based silica spheres provide no macropores, but only mesopores which are two orders of magnitude smaller (Figure 4.5). The calculated mesopore volume (BJH) is nearly four times higher than for the macroporous sample. Furthermore the preparation mixture with aniline offers a slightly higher BET surface area and mesopore diameter (Table 4.2).

Table 4.2. Results of BET analysis, mesopore characterization (BJH calculation) and micropore analysis (t-plot) obtained from the measured N_2 adsorption/desorption isotherm.

	Precursor solution with aniline	Precursor solution with 1-butanol
Surface area / m^2g^{-1}	692	601
Mesopore diameter / nm	9.5	7.1
Mesopore volume / cm^3g^{-1}	0.56	0.15
Micropore volume / cm^3g^{-1}	0.18	0.25

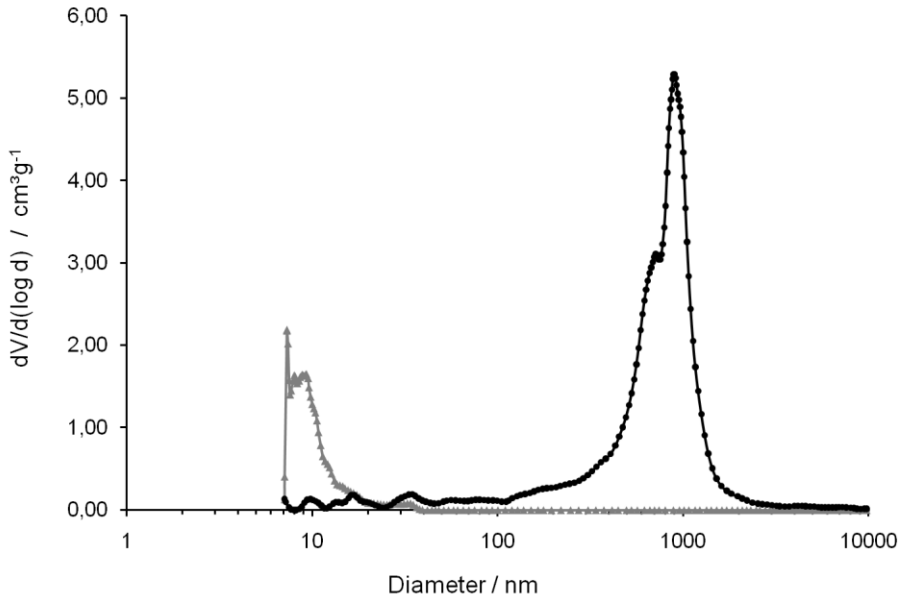

Figure 4.5. Mercury porosimetry of calcined silica spheres made with aniline (grey line) and 1-butanol (black line) as solvent of the precursor solution.

The thermogravimetric analysis represented in Figure 4.6 shows that the decomposition of the surfactant appears at lower temperature (180°C) for the spheres made with butanol than of the ones made with aniline (200°C). Additionally the weight loss by surfactant decomposition of the butanol based spheres occurs rapidly (180 – 200°C) and is with 13% less than the half compared to the sample made with aniline. The further decomposition of the organic matter of the two samples runs nearly parallel. The weight loss up to 500°C includes the removal of residual carbonaceous species and of the aminosilane and the last step between 500 and 700°C is assigned to the decomposition of phenyltrimethoxysilane.[19] The total weight loss is 53% for the butanol and 61% for the aniline based spheres, which is similar to mesostructured materials like MCM-41 or SBA-15.[19]

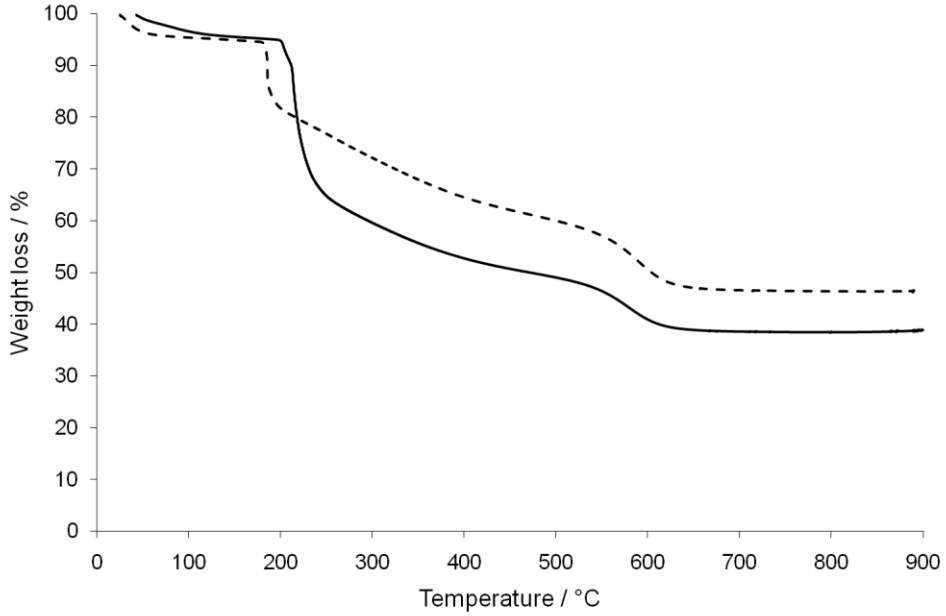

Figure 4.6. TGA measurement performed on as-made silica composite spheres made with 1-butanol (dashed line) and aniline (solid line).

Thus, two totally differently structured materials concerning the morphology and porosity of the spheres have been prepared by only changing the solvent of the precursor solution. The main difference between the solvents is the basicity of aniline with a pK_b value of 9.4. Therefore, aniline contributes to the basic catalysis of the hydrolysis and condensation of the silanes. Primarily the [3-(2-aminoethylamino)propyl]trimethoxysilane acts as autocatalyst for the hydrolysis and condensation of the silanes due to the strong basic reaction in aqueous medium. Thus, the particulate structure inside the macroscopic silica spheres originates from the high pH value during the condensation reaction. The fact that an alkaline catalyzed sol-gel process of silicon alkoxides results in a highly branched siloxane network with particulate structure, whereas under acidic conditions linear polysiloxanes are formed is frequently applied to produce defined silica materials.[3, 17, 20]

The higher reaction rate through the use of aniline as solvent encourages the formation of a large number of primary silica nanoparticles and suppresses the growth of the single particles. The sol-gel process of butanol containing precursor droplets, however, is only catalyzed by the basicity of the aminosilane. In addition, the hydrolysis rate of the silanes is decreased by catalytic alkoxy exchange reactions. Thus, the differences in the morphology are the direct consequence of a lower hydrolysis rate using butanol as solvent. The lower hydrolysis rate in the presence of butanol results in a smaller initial number of primary silica nanoparticles,

which subsequently grow due to reaction with residual silanes. Additionally, the lower reaction rate for the butanol mixture induces a phase separation into a solvent-rich phase and an organosilica-surfactant phase.[21, 22] The emerging cavities between the loosely packed large primary silica particles are detected as macropores by mercury intrusion. The significant lower mesopore volume of the spheres made with butanol is mirrored in the results of thermogravimetric and elementary analysis. Both methods confirm a reduced concentration of the surfactant in the as-made silica spheres.

The loss of surfactant is attributed to the better solubility of butanol in water. With 90 g/l it shows more than twice the solubility of aniline. Therefore, a significant amount of the surfactant, which is solved in butanol, will transfer to the water phase.

Another reason for the lower mesoporosity is the described phase separation due to the low reaction rate for the butanol mixture. Note that the concentration of surfactant which is solved in the separated butanol phase is not available for mesopore formation.

Apparently, the porosity of the spheres is not only determined by microphase separation due to self-assembly of surfactant molecules, but also by polymerization-induced phase separation, which can be controlled by the reaction rate.[21, 22] These processes allow mesoporous and macroscopic ordering, respectively or a combination of both.

4.3.3 Variation of the silane mixture

The silanes which were selected for the precursor solution to prepare macroscopic silica spheres combine three different functions. Tetraethyl orthosilicate is the network building compound to provide stable silica spheres by a three dimensional connectivity of SiO_4 tetrahedra. The hydrolysis and condensation of the silanes is auto-catalyzed by the basic [3-(2-aminoethylamino)propyl]trimethoxysilane to prevent the solubility of the base in the water phase by anchoring to the silica network. Phenyltrimethoxysilane was added to increase the hydrophobicity of the precursor solution for a better phase separation.

To investigate the influence of the silane composition on the structure and properties of the silica spheres phenyltrimethoxysilane was substituted by phenyl- or cyclohexylaminosilanes, whereas the other components like TES40, AAMS, Pluronic® 25R4 and aniline were kept constant. The variation of the silanes includes methoxy- and ethoxysilanes, additional basicity by secondary amines, steric demanding functional groups and branched silanes. All these

precursor mixtures allow the preparation of silica composite spheres by the formation of stable droplets and a sufficient reaction rate to prevent agglomeration of the silica spheres.

After calcination some of the spheres made with the ethoxysilanes Geniosil® XL926 and Geniosil® XL924 were cracked and the mechanical stability of these spheres is much lower than the other materials. The reason for this relative low mechanical stability of these samples is elucidated by determining the structure of the spheres via SEM (Figure 4.7). Right from the preparation of the cross-section the difference is obvious because the hemispheres of the two samples easily fragment into the shell and the core. The shell seems to be completely dense silica but a closer look reveals numerous macropores with a diameter of 80 – 540 nm especially for the sample made with Geniosil® XL926 (Figure 4.7). In contrast, the core consists of large and regular primary silica particles which are hardly connected. The size distribution of the primary silica particles is broader and slightly shifted to smaller particles for the spheres prepared with the monofunctional Geniosil® XL926 compared to the branched silane (Geniosil® XL924).

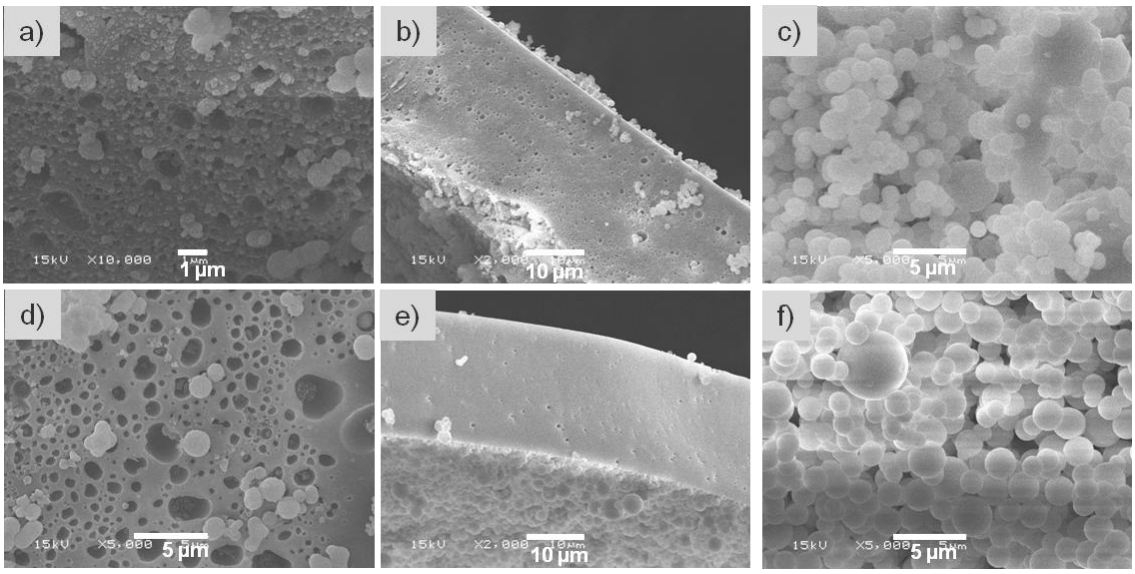

Figure 4.7. SEM images of calcined silica spheres made with Geniosil XL926 (a - c) and with Geniosil XL924 (d - f). (a, d) Surface of the spheres, (b, e) edge of the cross-section, (c, f) center of the cross-section.

The textural composition of the spheres made with methoxysilanes can also be divided in a core and shell, but these spheres do not break up due to the interconnection between the two parts. Even the primary particles in the core are perfectly grown together and for the material made with Geniosil® GF92 the diameter of the particles is one magnitude smaller compared to

the others (Figure 4.8c, f). The macropore containing shell exhibits a thickness between 20 and 26 µm for all samples except for the spheres prepared with Geniosil® GF92 (Figure 4.8b, e). In this case the macropores are only arranged in the surface layer and they are well-ordered providing a very narrow pore size distribution with a diameter of approximately 0.8 µm (Figure 4.10). The surface of the other materials is also macroporous, but with a more random distribution of size and arrangement.

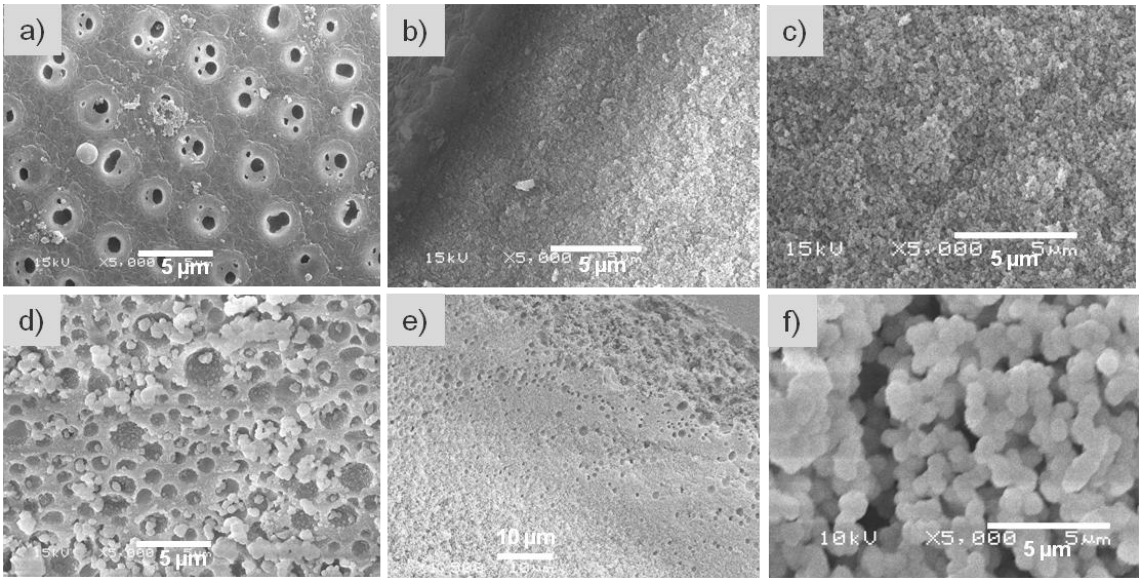

Figure 4.8. SEM images of calcined silica spheres made with Geniosil GF92 (a - c) and with Geniosil XL973 (d - f). (a, d) Surface of the spheres, (b, e) edge of the cross-section, (c, f) center of the cross-section.

According to thermogravimetric analysis the samples can also be classified into the spheres prepared with ethoxy- and methoxysilanes (Figure 4.9). The spheres made with the ethoxysilanes (Geniosil® XL924, XL926) loose around 10% water and alcohol. Also the decomposition of the surfactant occurs rapidly and at lower temperature (160°C) compared to the other samples with methoxy-Geniosil®, where the surfactant removal starts at 200°C. The material with the branched Geniosil®-silane is the only one with a distinct second decomposition step. It should be noticed that the decomposition step between 500 and 700°C which was observed for the sample containing phenyltrimethoxysilane is missing. This means that in principle a lower calcination temperature could be applied for the Geniosil® samples.

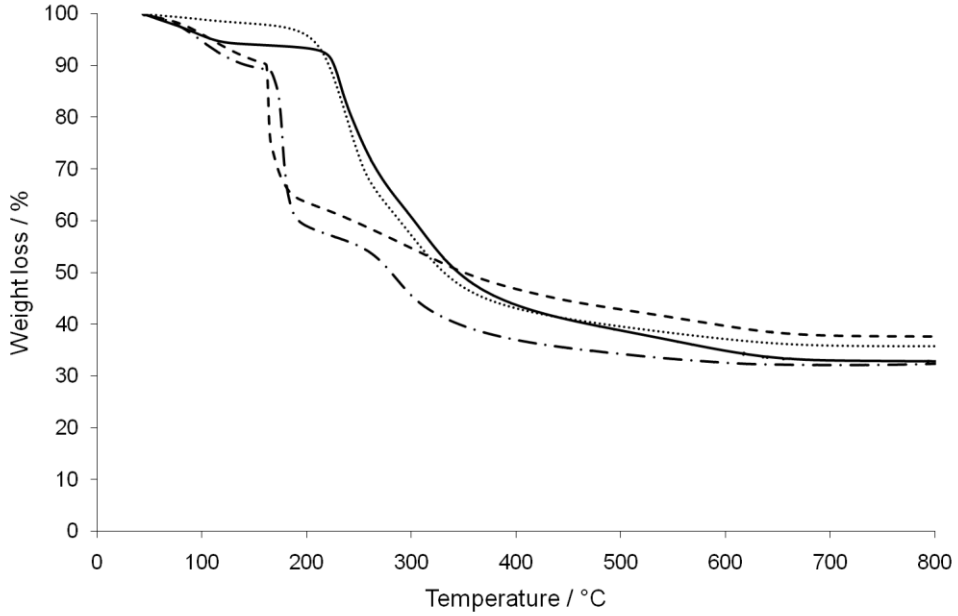

Figure 4.9. TGA measurement performed on as-synthesized silica composite spheres made with Geniosil® XL973 (dotted line), Geniosil® GF92 (solid line), Geniosil® XL926 (dashed line) and Geniosil® XL924 (dot-dash line).

Besides the morphology, the variation of the silane composition drastically changes the porosity of the spheres. The BET surface area could be increased to almost 900 m²/g and the median mesopore diameter can be controlled between 3.8 and 20.6 nm. The detailed values obtained from the N_2 adsorption/desorption isotherm are summarized in Table 4.3.

Table 4.3. Results of BET analysis, mesopore characterization (BJH calculation) and micropore analysis (t-plot) obtained from the measured N_2 adsorption/desorption isotherm showing the influence of silane variation.

Silanes *	BET surface area / m^2g^{-1}	Mesopore diameter / nm	Mesopore volume / cm^3g^{-1}	Micropore volume / cm^3g^{-1}
GF92	675	20.6	0.22	0.12
XL973	888	12.1	0.20	0.14
PTMS	692	9.5	0.56	0.18
XL926	713	3.8	0.06	0.14
XL924	636	3.8	0.03	0.10

* silane mixture contains TES40, AAMS and variable silane listed in the table

The comparison of the mesopore diameter shows an increase with increasing steric demand of the organic group which is bound at the trimethoxysilane. This effect is probably caused by interaction of the organic groups with the self-assembling surfactant molecules and, thus, the size of the aggregate is increased.

However, the properties of the materials made with the ethoxysilanes Geniosil® XL926 and XL924 do not fit to this trend. They offer both a very low mesopore diameter and volume. It can be assumed that the considerably low mesopore volume is induced by phase separation. The correlation between sol-gel transition and phase separation is the crucial point for the final morphology of the material, whereas both processes behave competitive to each other.[22] Since the hydrolysis rate of ethoxysilanes is definitely lower than the one of methoxysilanes, the phase separation in a silane- and a solvent-rich phase is favored. The dissolution of the surfactant in the separated solvent phase is preferred, if the interaction between the surfactant and the silanes is low, e.g. through bulky organic functionalities. The final morphology of the material is determined by the reaction rate, which is not only influenced by the reactivity of the silane, but also by the availability of water. Therefore, differences between the shell and the core of the spheres are most likely to form.

The hindered water diffusion inside the precursor droplet causes controlled hydrolysis resulting in particulate structures, whereas the diameter of the primary silica particles increases for decreasing reaction rate.[3] In contrast, the reaction rate in the shell of the spheres is higher due to the direct contact with water at the interface of the precursor droplet and the continuous phase. The water diffusion inside the precursor droplet is enhanced by the formation of water filled micelles. This results in a shell structure consisting of highly condensed silica with numerous macropores, which are supposed to originate from the embedded water filled micelles.[11] At a certain thickness of the macroporous solid shell (which depends on the precursor solution) the water diffusion is strongly hindered inducing the sharp boundary between shell and core. It seems, however, that the thickness of the shell decreases with increasing reactivity of the precursor solution. Remarkably, Geniosil® GF92 which exhibits the longest organic chain as functional group provides a macroporous layer only restricted to the surface. Despite of the steric hindrance this silane is more reactive than the other methoxysilane Geniosil® XL973 due to a distinct basicity (pH = 10 in water). Geniosil® XL973, however, reacts neutral since the secondary amino group is stabilized via the aromatic ring. Another outstanding feature of the spheres made with Geniosil® GF92 is the ordered arrangement of nearly regular sized macropores on the surface of the spheres

(Figure 4.10). Apparently the organic group of the Geniosil® silane interacts with the surfactant self-assemblies and enforces a regular distance between the macropores.

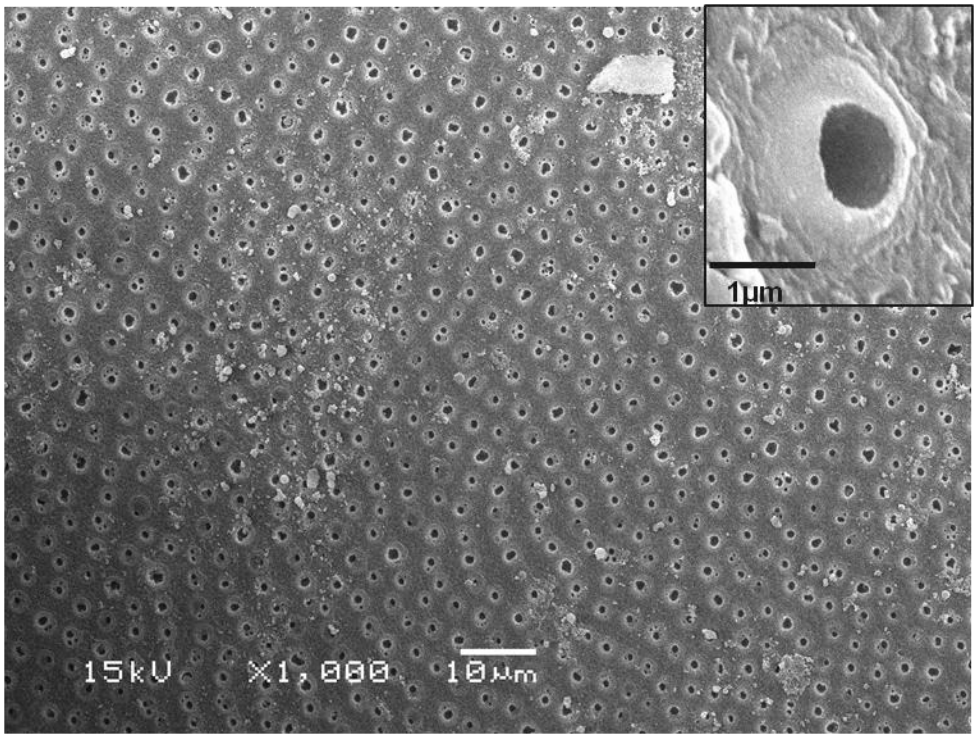

Figure 4.10. SEM image showing the ordered arrangement of the macropores on the surface of the calcined silica spheres made with Geniosil GF92 and the magnification of a single pore as inset.

The structural differences, especially the density of the synthesized spheres affects the decomposition of the organics. In consequence, the spheres with the lower packing density like the ones made with the Geniosil® ethoxysilanes allows a faster decomposition of the surfactant at lower temperature. The decomposition temperature is even lower than for the spheres prepared with 1-butanol.

The variation of the silanes shows therefore a wide variety of possibilities to tune the morphology as well as the porosity of the spheres. The only limitation in this case is a sufficient reaction rate, which can be controlled by the reactivity of the silanes, the addition of a catalyst or the water diffusion influenced by the type of surfactant.

4.3.4 Extraction of the surfactant

All samples mentioned before were dried and calcined after preparation. As reported in literature solvent extraction can be applied to remove the organic copolymer without decomposition.[17] Another advantage of this method (in addition to the recovery of the surfactant) is the possibility to obtain organofunctionalized silica since the organic groups, which are bound to the silica network are retained. The extraction was carried out with ethanol for 24 h and 48 h in a Soxhlet apparatus to prevent the breaking of the spheres due to magnetic stirring. During extraction of the surfactant neither the macroscopic shape nor the structure of the spheres changes significantly. The quality of the extraction can be estimated by elementary and thermogravimetric analysis. The amount of C, H and N of the as-prepared sample were determined to 40.51 wt.-%, 5.53 wt.-% and 3.09 wt.-%, respectively. After extraction this values are diminished to 29.51 wt.-% carbon, 3.75 wt.-% hydrogen and 3.75 wt.-% nitrogen. These values fit rather well to the calculated amounts for the total removal of the surfactant. But all measured amounts are slightly lower than the calculated values. This is probably related to the fact that the aminosilane AAMS is not completely bound into the silica network. Due to protonation of the amino group the water solubility is significantly increased. The thermogravimetric analysis indicates a small weight loss between 200 and 500°C which probably is a result of the decomposition of residual surfactant and the aminosilane (Figure 4.11). Compared to the as-synthesized silica spheres more than 70% of the surfactant could be extracted.

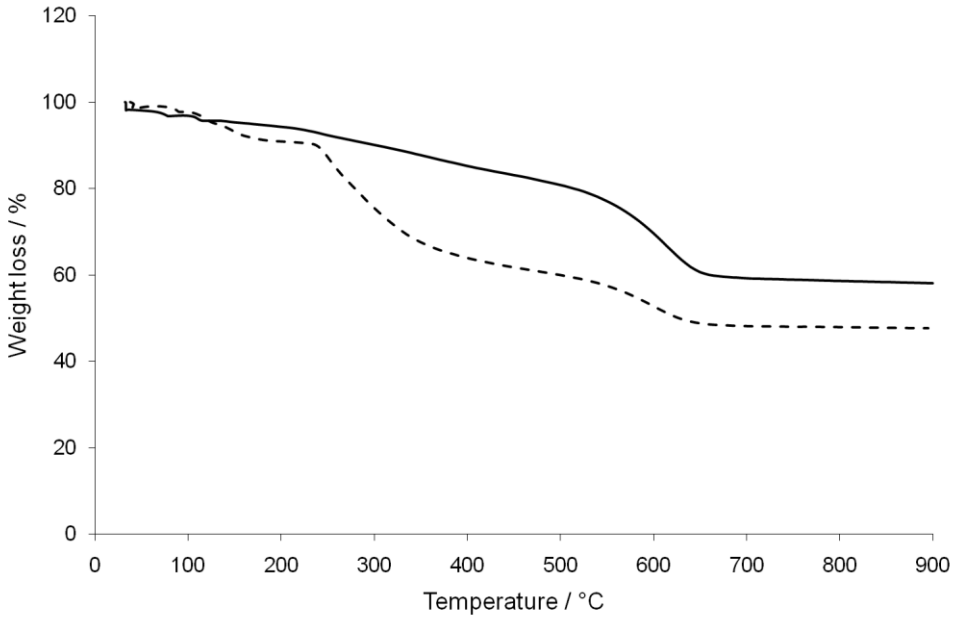

Figure 4.11. TGA measurement performed on as-synthesized silica composite spheres (dashed line) compared to extracted silica spheres (solid line) containing TES40, AAMS, PTMS, Pluronic® RPE1740 and aniline.

4.4 Conclusion

Well-tuned macroscopic (organo)silica spheres have been prepared in a one-step synthesis. The final morphology of the spheres is determined by the combination of phase separation and sol-gel transition. While it is important to know the influence of each precursor component, also the interaction between them control the structure and properties of the spheres.

The hierarchical structure of the spheres is mainly controlled by the reactivity of the precursor solution in combination with the water diffusion. The observed structural change during variation of the surfactant concentration confirms the suggested alignment of the surfactant molecules along the oil-water interface and the water diffusion inside the droplet by the formation of a water-in-oil microemulsion. The macroporous surface layer, which results from the microemulsion can only be detected for high surfactant concentrations. The comparison of the solvents reveals a great advantage of aniline as bifunctional compound providing hydrophobicity to stabilize the droplet and basicity to catalyze the sol-gel reaction resulting in mesoporous highly stable silica spheres. Reducing the reaction rate by changing the solvent or the silane mixture allows the preparation of macroporous silica spheres.

The mesopore diameter cannot only be adjusted by the variation of the surfactant but also by the differentiation of the organofunctionalized silanes. Increasing steric demand of the organic group increases the mesopore diameter. Additionally, the interaction of the large cyclohexylaminopropyl moiety with the self-assembling surfactant molecules allows the preparation of ordered macropores on the surface of the spheres.

The composition of the precursor solutions which were investigated during this work offers a high variability of the morphology and porosity of the prepared silica spheres including hierarchically structured materials with different ratios of micro-, meso- and macropores allowing subtle tailoring the final material.

4.5 Acknowledgement

Financial support by Wacker Chemie AG and fruitful discussions within the Wacker-Institut für Siliciumchemie and the framework of the network of excellence IDECAT is gratefully acknowledged. The authors thank Dipl.-Ing. Martin Neukamm for SEM analysis, Dipl.-Ing. Xaver Hecht for BET analysis and Hg-porosimetry, Georgeta Krutsch and Aleksandra

Jonovic for TGA measurements, Ulrike Ammari and co-workers from the microanalytical lab for elementary analysis and Dr. Yongzhong Zhu for helpful discussions.

4.6 References

[1] S. Schacht, Q. Huo, I. G. Voigt-Martin, G. D. Stucky, F. Schüth, *Science* **1996**, *273*, 768.

[2] M. Grün, I. Lauer, K. K. Unger, *Advanced Materials* **1997**, *9*, 254.

[3] W. Stöber, A. Fink, E. Bohn, *Journal of Colloid and Interface Science* **1968**, *26*, 62.

[4] B. Alonso, A. Douy, E. Veron, J. Perez, M. N. Rager, D. Massiot, *Journal of Materials Chemistry* **2004**, *14*, 2006.

[5] Q. S. Huo, J. L. Feng, F. Schüth, G. D. Stucky, *Chemistry of Materials* **1997**, *9*, 14.

[6] Z. Y. Yuan, B. L. Su, *Journal of Materials Chemistry* **2006**, *16*, 663.

[7] T. Sen, G. J. T. Tiddy, J. L. Cascic, M. W. Anderson, *Chemical Communications* **2003**, 2182.

[8] F. Carn, A. Colin, M. F. Achard, H. Deleuze, E. Sellier, M. Birot, R. Backov, *Journal of Materials Chemistry* **2004**, *14*, 1370.

[9] C. Oh, S. C. Chung, S. I. Shin, Y. C. Kim, S. S. Im, S. G. Oh, *Journal of Colloid and Interface Science* **2002**, *254*, 79.

[10] H. Witossek, E. Bratz, *Chemical Engineering & Technology* **1997**, *20*, 429.

[11] S. Scholz, J. A. Lercher, *Journal of Materials Chemistry* **2010**, submitted.

[12] K. Landfester, *Annual Review of Materials Research* **2006**, *36*, 231.

[13] S. Mann, S. L. Burkett, S. A. Davis, C. E. Fowler, N. H. Mendelson, S. D. Sims, D. Walsh, N. T. Whilton, *Chemistry of Materials* **1997**, *9*, 2300.

[14] D. Y. Zhao, Q. S. Huo, J. L. Feng, B. F. Chmelka, G. D. Stucky, *Journal of the American Chemical Society* **1998**, *120*, 6024.

[15] J. S. Beck, J. C. Vartuli, W. J. Roth, M. E. Leonowicz, C. T. Kresge, K. D. Schmitt, C. T. W. Chu, D. H. Olson, E. W. Sheppard, S. B. Mccullen, J. B. Higgins, J. L. Schlenker, *Journal of the American Chemical Society* **1992**, *114*, 10834.

[16] Q. S. Huo, D. I. Margolese, U. Ciesla, P. Y. Feng, T. E. Gier, P. Sieger, R. Leon, P. M. Petroff, F. Schüth, G. D. Stucky, *Nature* **1994**, *368*, 317.

[17] D. Y. Zhao, J. L. Feng, Q. S. Huo, N. Melosh, G. H. Fredrickson, B. F. Chmelka, G. D. Stucky, *Science* **1998**, *279*, 548.

[18] S. B. Jung, H. H. Park, *Thin Solid Films* **2006**, *494*, 320.

[19] F. Kleitz, W. Schmidt, F. Schüth, *Microporous and Mesoporous Materials* **2003**, *65*, 1.

[20] R. K. Iler, *The Chemistry of Silica*, John Wiley & Sons, New York, **1979**.

[21] R. Schiller, C. K. Weiss, J. Geserick, N. Hüsing, K. Landfester, *Chemistry of Materials* **2009**, *21*, 5088.

[22] K. Nakanishi, *Journal of Porous Materials* **1997**, *4*, 67.

Chapter 5

Controlled synthesis of platinum loaded hierarchic silica spheres

Hierarchically structured macroscopic Pt-silica spheres were prepared in a one-step procedure using emulsion based sol-gel processing. The composition of the precursor solution was varied in order to study the influence of the Pt compound, the surfactant and the preparation method on the Pt particle size and concentration. Platinum was immobilized by coordination with an aminosilane and the nanoparticles were stabilized using different PPO-PEO-PPO copolymers. For removal of the surfactant, calcination as well as solvent extraction was used and the co-condensed samples were compared with silica spheres functionalized by ion-exchange. The activity of different catalysts was investigated via the methylcyclopentane ring opening reaction, which revealed a beneficial effect of the macroscopic shape and hierarchical structure of the support material. The simultaneous structural control over several scales of dimension from the macroscopic shape of the support to the nanometer size of the Pt nanoparticles allows the easy and highly reproducible synthesis of tailor-made catalysts.

5.1 Introduction

The design of tailor-made materials in materials science and catalysis ideally bridges length scales from macroscopic to molecular level. Conceptually, it allows an easier transfer from simple model catalysts to more complex ones adapted for a particular process and is helping to predict the catalytic performance of new materials.[1, 2]

In recent years, mesoporous oxide supported catalysts attract more and more interest of industry and fundamental research, since these materials offer high surface areas and are suitable for the catalytic conversion of bulky molecules avoiding mass transfer limitations.[3] So far, different preparation methods have been developed to attach noble metal nanoparticles such as platinum or palladium on mesoporous oxides, but most of the procedures are time-consuming involving several synthesis steps. The most prominent methods are incipient wetness impregnation,[4] impregnation with preformed metal particles[5] or ion-exchange inside the mesoporous channels using metal salts.[6] Highly dispersed metal particles can be achieved via complexation of metal atoms at functionalized silica pore walls.[7] The opposite method to the above-mentioned impregnation is the encapsulation of stabilized platinum particles by mesoporous silica or by core-shell particles consisting of a platinum metal core coated with a mesoporous silica shell.[1, 8, 9] However, the one-step preparation of hierarchically structured materials with a macroscopic shape and supported metal particles, which is required for the technical application of such materials, was hardly considered. Recently, hierarchically structured Pt containing membranes were prepared by slip-casting of a silica sol containing acidic hydrolyzed tetraethoxysilane (TEOS), a triblock co-polymer as mesopore template, a platinum salt, ethylene glycol and polystyrene spheres as macrotemplate on macroporous alumina support.[10]

In this paper we investigate the simultaneous control of the platinum nanoparticle diameter and size distribution as well as of the macro- and microstructure of the silica support. The final material possess a hierarchical structure, which can be controlled on different length scales from the millimeter sized shape of the support over the macro-, meso- and microporous structure to the nanometer sized Pt particles. The materials were synthesized by the combination of a recently developed preparation of macroscopic hierarchically structured silica spheres[11, 12] with the concomitant immobilization of platinum. The multidimensional control was achieved by the combination of oil-in-water emulsion with a templated sol-gel reaction and the stabilization of platinum via complexation with aminosilanes or block co-

polymers. The influence of the platinum compound, the surfactant (triblock copolymer) and the preparation method on the diameter and size distribution of the Pt nanoparticles as well as on the effectiveness of the Pt immobilization will be addressed. The catalytic activity of the materials was investigated in methylcyclopentane ring opening reaction.

5.2 Experimental

5.2.1 Materials

Tetraethylsilicate (TES40) from Wacker Chemie AG; N-[3-(trimethoxysilyl)propyl]-ethylenediamine (AAMS, 97%), phenyltrimethoxysilane (PTMS, 97%), aniline (99%), platinum chloride (98%), platinum tetraammine hydroxide and methylcyclopentane (97%) from Sigma Aldrich, the surfactants Pluronic® 25R4 ($PO_{18}EO_{45}PO_{18}$, M_w = 4074), Pluronic® RPE2520 ($PO_{18}EO_{14}PO_{18}$, M_w = 2699) and Pluronic® RPE1740 ($PO_{11}EO_{27}PO_{11}$, M_w = 2503) from BASF and platinum acetylacetonate (50% Pt) and ethanol from Merck were used in the described synthesis. All chemicals were used without further purification. The reactions were carried out with deionized water.

5.2.2 Synthesis of Pt functionalized silica spheres

The platinum silica composite spheres were prepared by injection of the precursor solution in a water filled reactor column according to the procedure published in ref.[11] The precursor solution contains the silanes TES40, AAMS and PTMS in the molar ratio 5:2:3, a platinum compound, 2.4 g surfactant and 2.3 ml aniline, the total volume of the solution being approx. 10 ml. The amount of platinum compound is calculated in order to achieve 1 wt. % Pt in the final material. The preparation of the precursor solution was performed according to three different procedures: Mix A: Stirring the Pt compound with AAMS for 24 h followed by the addition of TES40, PTMS and the surfactant dissolved in aniline. Mix B: The mixture of the platinum compound, surfactant and aniline was treated 30 – 60 min in the ultrasonic bath, then stirred for 24 h and mixed with TES40, AAMS and PTMS. Mix C: This procedure represents the combination of mix A and mix B, by stirring the platinum compound, AAMS and the surfactant in aniline for 24 h prior to the addition of TES40 and PTMS. The variation of the platinum compound with $PtCl_2$, $Pt(acac)_2$ and $Pt(NH_3)_4(OH)_2$ was investigated according to the procedure “mix A”, the variation of the surfactant with Pluronic® 25R4,

Pluronic® RPE2520 and Pluronic® RPE1740 according to the procedure "mix B". The macroscopic Pt-silica composite spheres were prepared by injection of the precursor solution via a syringe pump (15 mL/h) into the recycling water flow of the reactor column, which was heated to 65°C. The product was recovered by decantation, washed three times with water and dried under ambient conditions. The samples were calcined in air at 600°C for 3h with a heating rate of 1 K/min to remove the surfactant and organic moieties followed by H_2-treatment for 2 h at 200°C with a heating rate of 2°C/min.

5.2.3 Ion exchange post-functionalization of silica spheres with Pt

1.0 g of calcined silica spheres, which were prepared with TES40, AAMS, PTMS, Pluronic® RPE1740 and aniline were added to a solution of 0.0152 g $Pt(NH_3)_4(OH)_2$ in 200 ml water at pH = 8. The pH was adjusted with aqueous NH_3 solution prior to the addition of the silica spheres. The mixture was shaked for 3 h. The product was recovered by decantation, washed three times with water and dried under vacuum for 17 h. The spheres were treated in synthetic air at 150°C for 2 h and in H_2 at 200°C for 2 h.

5.2.4 Soxhlet extraction

1.0 g of as-prepared Pt-silica composite spheres containing $PtCl_2$, the silanes AAMS, TES40 and PTMS, the surfactant Pluronic® 25R4 and aniline was extracted with 300 ml boiling ethanol for 24 h using a Soxhlet apparatus. The spheres were recovered by decantation, dried at 80°C for 15 h and treated with H_2 at 200°C for 2 h.

5.2.5 Methylcyclopentane ring opening as probe reaction

Methylcyclopentane (MCP) ring opening experiments were conducted at atmospheric pressure in a fixed-bed, continuous flow stainless-steel reactor with an internal diameter of 4 mm. The reactant flow at 20 cm^3/min contained hydrogen and methylcyclopentane in the molar ratio of 40 without any balance gas. Typically, the reactor is filled with 0.02 - 0.04 g catalyst, which is diluted with acid-washed quartz. The sieve fraction of each catalyst is listed in Table 5.1. Before each run, the catalyst was treated in situ in a 20 ml/min flow of H_2 at 350°C for 2 h. The reaction products were on-line analyzed using Agilent MicroGC 3000A,

equipped with a TC detector (TCD) and an 8-m OV-1 column, to allow a short sampling interval of 3.7 min.

All reactions were carried out under differential conditions, i.e. conversion < 5% and the activities of all catalysts were compared using reaction rates measured at 270^{o}C. The reproducibility of the catalytic behavior was checked for all catalysts.

5.2.6 Characterization

The block copolymers were characterized via ^{1}H-NMR spectroscopy (Bruker, Advance DPX 400) and MALDI-TOF measurements (Bruker Daltonics Ultraflex TOF/TOF) to determine the molecular composition and the molecular weight. The Pt particle size was determined with x-ray diffraction (XRD) using a Philips/PANalytical's X'Pert PRO System. The XRD patterns were measured with Cu Kα radiation from 5 to 70° 2θ using a scan speed of 0.019 °/s. The average metal particle size is calculated from the half width of the [111], [200] and [220] reflections by the Debye-Scherrer equation; the peaks were approximated by a Gaussian function. The average particle size of the Pt-silica spheres prepared by ion-exchange and of the sample obtained after Soxhlet extraction was determined by TEM, since the particles are too small to generate diffraction signals. Also, the particle size distribution was analyzed with transmission electron microscopy (JEOL JEM-2010) at 120 kV. The samples were grinded, suspended in ethanol and ultrasonically dispersed. One drop of this suspension was placed on a copper grid with holey carbon film. The platinum concentration was determined by atomic absorption spectroscopy (AAS) using a UNICAM Solaar M5 spectrometer (GF95 graphite furnace). Typically, 60 - 100 mg of the sample was mixed with 2.0 ml hydrofluoric acid (10%), 0.1 ml hydrochloric acid and 0.1 ml nitric acid and boiled until the solution is clear. The morphology of the spheres was investigated with scanning electron microscopy (SEM) (JEOL JSM-5900LV) of the Au-sputtered samples (whole spheres and cross-section) at acceleration voltages between 10 and 25 kV.

5.3 Results and Discussion

The platinum containing silica spheres were synthesized via an emulsion based sol-gel process by immersing well-controlled droplets of the hydrophobic precursor solution in water using a continuously operated reactor column with a recycling heated water flow.[11] This system provides a high reproducibility of the synthesis, narrow size distribution of the silica spheres and an easy scale-up.

The applied precursor solutions consist basically of three different silanes, a platinum compound, a triblock copolymer as surfactant and template as well as the solvent aniline. The silane mixture accounts for the stability of the prepared silica spheres, whereas tetraethylsilicate (TES40) acts as network building compound, N-[3-(trimethoxysilyl)propyl]-ethylenediamine (AAMS) as autocatalyst providing a basic pH inside the precursor droplet and phenyltrimethoxysilane (PTMS) enhances the stability of the droplet due to its hydrophobicity. According to Schubert et al.,[13, 14] the aminosilane is simultaneously used as ligand for the in situ coordination of platinum. $Pt(AAMS)_2$ is formed in analogy to the composition of ethylenediamine complexes, but this complex can be tethered to the siloxane network via Si-O-Si linkages (Scheme 5.1). Besides the aminosilane also the triblock copolymer may interact with platinum via the ether group as electron donor. Additionally, the triblock copolymers of the type $(PO)_x(EO)_y(PO)_x$ are able to template mesopores by forming micelles and ordered mesophases.

In order to investigate the influencing factors on the platinum particle size and the effectiveness of coordination, the synthesis mixtures were varied concerning the Pt compound, the type of surfactant and the preparation method by changing the reaction time and composition of the complexation mixture.

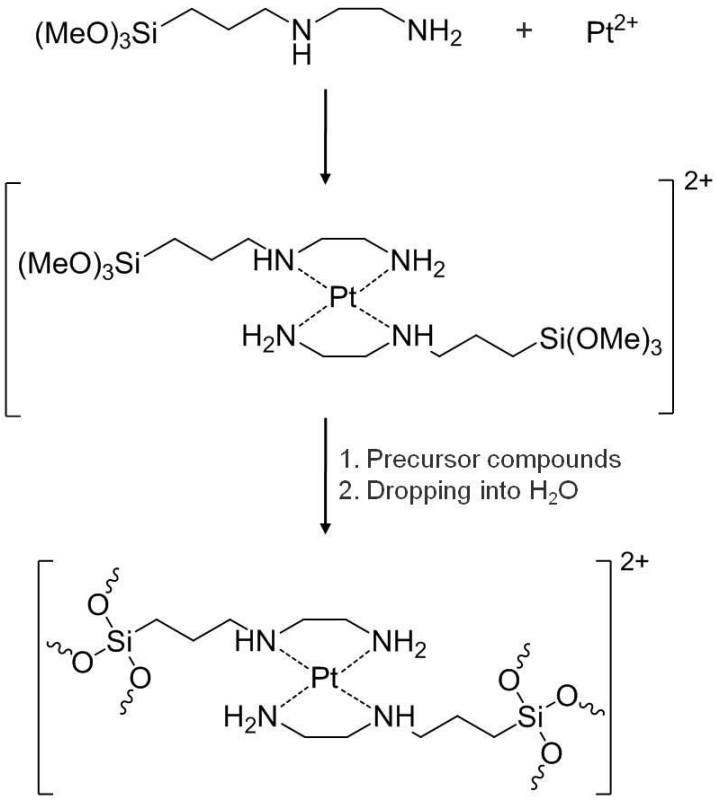

Scheme 5.1. Formation of the $Pt(AAMS)_2$ complex and immobilization in the siloxane network via sol-gel reaction.

5.3.1 Variation of the platinum compound

It is known that the platinum compound as well as the type of aminosilane strongly influence the Pt particle size.[15] Here, the silane composition was kept constant, because the properties of the parent silica spheres made with the precursor solution containing different silanes, a surfactant and solvent were studied in detail previously.[11, 12] This allows the structural control of the final macroscopic spheres and the sole analysis on the interaction between precursor and platinum compounds. The precursor solutions contain the silanes TES40, AAMS and PTMS, the surfactant Pluronic® RPE1740 and the solvent aniline. The added Pt compound was selected from $PtCl_2$, $Pt(acac)_2$ and $Pt(NH_3)_4(OH)_2$, which was mixed primarily with the aminosilane AAMS for 24h prior to addition of the other precursor compounds and the injection into water. The silane with the ethylenediamine type functional group was employed, because it coordinates with Pt^{2+} very effectively due to the nitrogen donor groups.[15] The complexation is indicated by the changing of color from pale yellow to red for $Pt(acac)_2$ and to bright yellow for $PtCl_2$. Only the mixture with $Pt(NH_3)_4(OH)_2$ remains a white suspension.

The differences in the solubility and complexation behavior are reflected in the measured Pt concentration. The spheres made with $Pt(NH_3)_4(OH)_2$ contain only 0.35 wt. % platinum instead of the intended 1 wt. %. The measured Pt concentration is more than doubled using other Pt precursors, with 0.85 wt. % for the $Pt(acac)_2$ and 0.77 wt. % for the $PtCl_2$ derived spheres. Remarkably, the smallest Pt particles were not observed in the material with the lowest Pt concentration, but in the Pt-silica spheres made with $PtCl_2$. In comparison, the other Pt compounds show a broader particle size distribution and a drastically increased average Pt diameter especially for $Pt(acac)_2$ (Figure 5.3). It should be noticed that in all cases the particle diameter determined by XRD (Figure 5.2) using the Scherrer equation is larger than the average particle size determined by TEM (Figure 5.1) through measuring of at least 100 particles, but the trends are the same for both analytical methods. This is most likely caused due to the more distinguished contribution of large Pt particles to the diffraction signal than that of smaller particles.

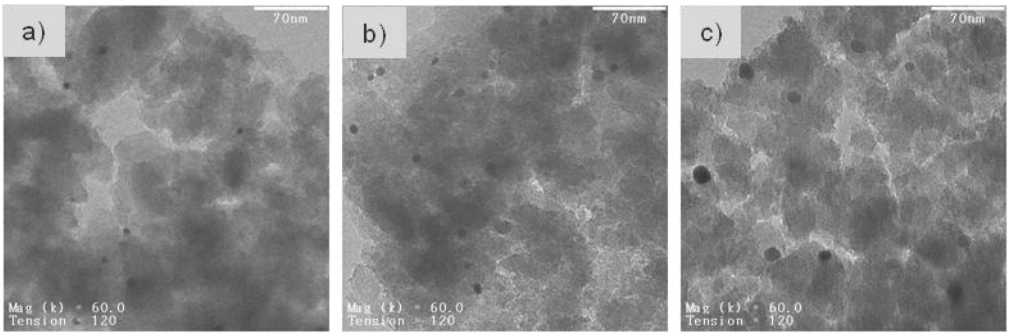

Figure 5.1. TEM images (scale bar = 70 nm) of Pt-silica spheres prepared with different Pt compounds: (a) $PtCl_2$, (b) $Pt(NH_3)_4(OH)_2$ and (c) $Pt(acac)_2$.

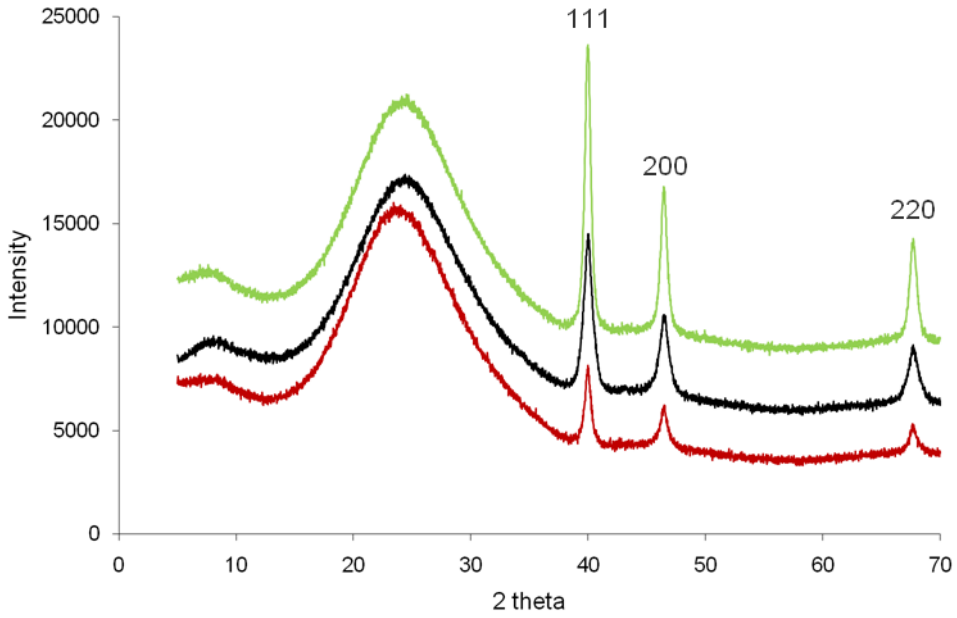

Figure 5.2. XRD pattern of the Pt-silica spheres prepared with $Pt(NH_3)_4(OH)_2$ (red line), $PtCl_2$ (black line) and $Pt(acac)_2$ (green line). The broad peak around 23° is assigned to amorphous silica and the other reflections belong to elemental platinum.

The huge discrepancy in the Pt concentration and Pt particle size among various materials reveals a great influence of the Pt compound on the complex formation with AAMS and the resulting particle size. The synthesis of Pt-silica spheres determines the coordination of the aminosilane ligand by the Pt^{2+} ion as a crucial point for obtaining good dispersion of platinum over the whole material. Only Pt complexes with at least one AAMS ligand can anchor to the siloxane network via Si-O-Si linkages (Scheme 5.1). Therefore, the dissociation of the applied Pt compound and the ligand exchange reaction is decisive.

The Pt-Cl bond dissociates easily and even more so in the presence of nitrogen donor ligands, since the remarkable increase of the ligand field splitting energy encourages the square planar low spin coordination of Pt^{2+}. Therefore the complex formation using $PtCl_2$ is most favored due to the high energy and stability gain for replacing chlorine by the ethylenediamine group. In the case of the $Pt(NH_3)_4(OH)_2$ derived Pt-silica spheres, the driving force to exchange NH_3 against ethylenediamine is low due to the similar position in the spectrochemical series, i.e., both ligands provide a similar splitting of the ligand field. The large Pt particles of the material made with $Pt(acac)_2$ are probably caused by the hindered ligand exchange of acetylacetonate with the aminosilane due to higher bond strength and entropic reasons, since both molecules are chelate ligands. The average size of the Pt nanoparticles and the larger particles with $Pt(acac)_2$ compared to $PtCl_2$ are in good agreement with the results of

Lembacher and Schubert[15] obtained by the impregnation of silica pellets with a sol containing in situ prepared Pt-aminosilane complex.

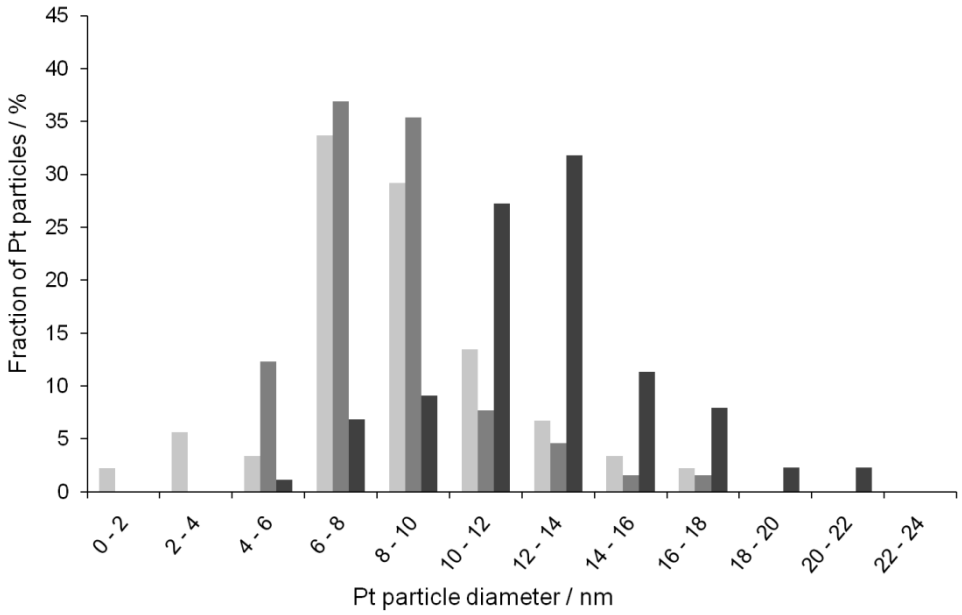

Figure 5.3. Platinum size distribution for Pt-silica spheres made with $Pt(NH_3)_4(OH)_2$ (light gray), $PtCl_2$ (gray) and $Pt(acac)_2$ (dark gray).

Overall, the platinum loading of the silica spheres depends on the complexation of the Pt as well as on the solubility of the Pt compound. In contrast to the mixture of $PtCl_2$ or $Pt(acac)_2$ with AAMS, which exhibits typical colors for Pt-amino complexes,[16, 17] $Pt(NH_3)_4(OH)_2$ is only suspended in AAMS, but soluble in water. Since the Pt-silica spheres are prepared using emulsion based sol-gel processing of precursor droplets dispersed in the continuous water phase, the water solubility of Pt compounds is disadvantageous. This explains the considerably low Pt concentration of $Pt(NH_3)_4(OH)_2$ derived Pt-silica spheres, which is less than half of the other two materials due to the loss of water dissolved platinum molecules.

5.3.2 Variation of the surfactant

Besides the interaction of the aminosilane with the platinum compound the Pt particle diameter and the size distribution can also be controlled by the type of surfactant. Therefore, the silane mixture (TES40, PTMS, AAMS), the platinum compound and the solvent were kept constant, whereas $PtCl_2$ was chosen since it gave the silica spheres with the highest Pt dispersion. In order to analyze the influence of the surfactant, the triblock copolymers Pluronic® RPE1740 ($PO_{11}EO_{27}PO_{11}$), RPE2520 ($PO_{18}EO_{14}PO_{18}$) and 25R4 ($PO_{18}EO_{45}PO_{18}$) were selected, which differ in the molecular weight and in the hydrophobicity represented by the M(PO)/M(EO) ratio. During the preparation, the mixture of $PtCl_2$, surfactant and aniline were stirred 24 h for equilibration prior to addition of the silanes. In each case the interaction was visually obvious through the brownish-red color of the solution. The Pt particle size shows a clear trend of an increasing diameter with increasing molecular weight of the polymer (Figure 5.4), whereas the Pt concentration decreases.

Increasing metal particle size with increasing molecular weight of the polymer was also observed for Rh and Pt nanoparticles which were stabilized by the commonly used polymer poly(vinylpyrrolidone) (PVP).[1, 18, 19] Borodko et al.[20, 21] indentified the stabilizing effect of PVP as charge transfer interaction between platinum and the carbonyl group as electron donor. Accordingly, also the ether group of the Pluronic® triblock copolymer can act as electron donor, although the interaction is weaker since carbonyl oxygen is more nucleophilic. Apparently, both, the ethylene oxide and the propylene oxide chains interact with platinum since the particle size increases with increasing molecular weight and not with increasing EO block length. The influence of the EO and PO blocks on the average particle size is in agreement with the observations of Sakai and Alexandridis,[22] who used different PEO-PPO-PEO polymers to stabilize and reduce Au particles. In contrast, PEO homopolymers are not suitable to efficiently stabilize metal nanoparticles, since they lead to larger particles[23] or in the case of colloidal Rh particles to the formation of agglomerates[19].

For the prepared Pt-silica spheres, the growth of the Pt particles happens during the calcination step as it is proven by Soxhlet extraction instead of calcination (see below). Thus, it can be assumed that longer polymer chains cause an easier sintering of platinum than shorter interacting polymer chains. The reason therefore can be a higher local heat or differences in the degradation and diffusion of the polymer chains during the calcination process.

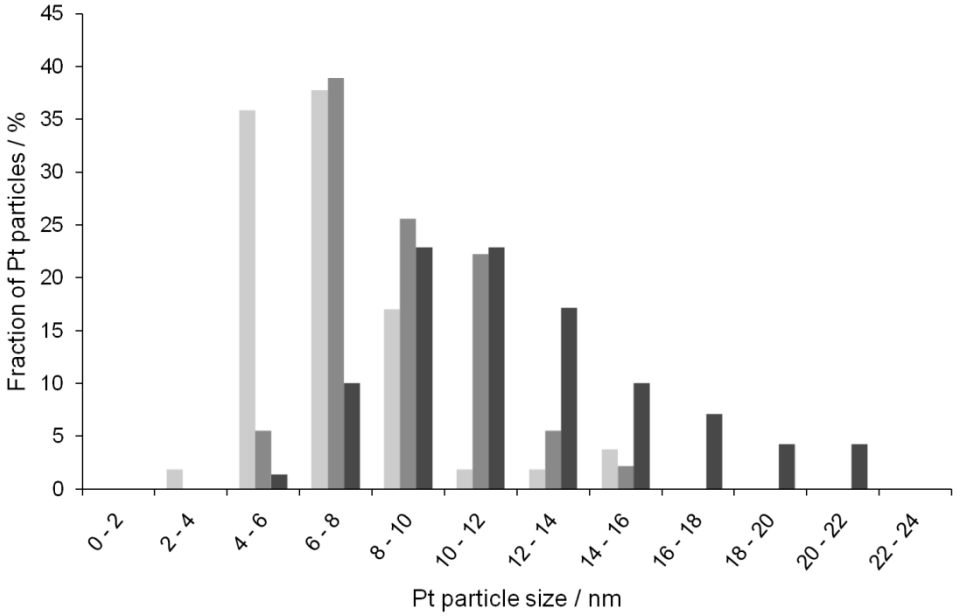

Figure 5.4. Platinum size distribution for Pt-silica spheres made with the surfactants Pluronic® RPE1740 (light gray), Pluronic® RPE2520 (gray) and Pluronic® 25R4 (dark gray).

5.3.3 Variation of the preparation method

Additionally to the kind of Pt compound and surfactant, also the preparation method may impact the properties of the Pt particles. Obviously, the preparation of the precursor solution was changed by mixing the Pt compound with AAMS (mix A) or by dissolving $PtCl_2$ in the aniline-surfactant solution (mix B) for 24 h in order to study the influence of Pt compound and surfactant, respectively. These two preparation methods were compared with the combination of them, i.e., Pt-silica spheres based on the mixture of $PtCl_2$, AAMS, Pluronic® RPE1740 and aniline, which was stirred for 24 h (mix C). $PtCl_2$ and Pluronic® RPE1740 were selected for these experiments, since they resulted in products with the highest Pt dispersion. It should be noted that each of these three samples contains exactly the same components (TES40, AAMS, PTMS, $PtCl_2$, Pluronic® RPE1740 and aniline), but they vary in the chronological order of the compound addition. The difference in the resulting Pt particle size is negligible when comparing mix A and mix B, but it is increased by around 30% for the Pt-silica spheres prepared according to mix C (Figure 5.5). The Pt concentration, however, shows a gradual increase with the complexity of the preparation mixture (Table 5.1).

The reason therefore is probably related to the better solubility and complexation through the addition of the solvent, because the amino group of aniline can also interact with platinum.

The larger particles obtained for mix C might result from the concurrent interaction of AAMS and the surfactant.

According to the results of Lembacher and Schubert[15] the complete complexation of Pt by aminosilanes usually needs several days except for a large excess of aminosilane. They obtained that a high concentration of aminosilane shortens the time for complexation to approximately one day, but also leads to larger Pt nanoparticles. Concerning the preparation of macroscopic Pt-silica spheres the aminosilane concentration is not only determined by the complexation of the Pt compound but also by the function as base auto-catalyst for the sol-gel reaction. Therefore, the excess of AAMS accounts to 64 equivalents per Pt, which should be enough for complete complexation in between 24 h.[15] However, the prolongation of the complexation time to 5 days instead of 1 day led to a slight increase of the Pt concentration from 0.77 to 0.84 wt. %, which indicates that in this case the equilibrium was not totally achieved after 24 h stirring.

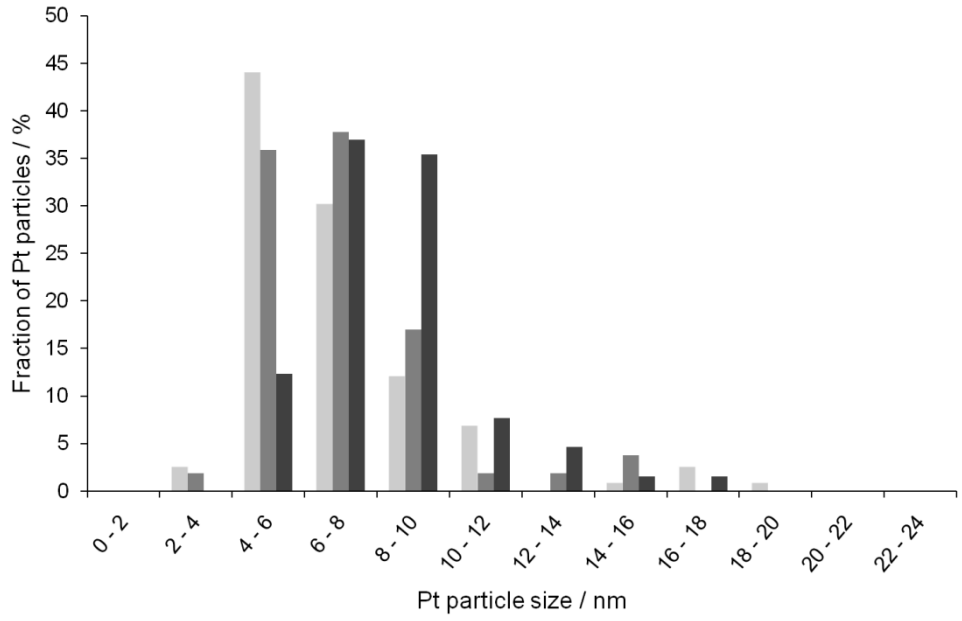

Figure 5.5. Platinum size distribution for Pt-silica spheres made with different pre-precursor mixtures. Mix C: $PtCl_2$, AAMS, Pluronic® RPE1740 and aniline (light gray); mix B: $PtCl_2$, Pluronic® RPE1740 and aniline (gray); mix A: $PtCl_2$ and AAMS (dark gray).

5.3.4 Ion-exchange functionalization of macroscopic silica spheres

In order to compare the one-step preparation procedure to a more conventional one, Pt-silica spheres were prepared via ion-exchange of parent macroscopic silica spheres. We selected calcined silica spheres, which were prepared with Pluronic® RPE1740 as support and used the ion-exchange method with $Pt(NH_3)_4(OH)_2$ under basic conditions. The Pt concentration of the sample was determined to 0.78 wt. % and the average particle size was 2 nm. As can be seen in Figure 5.6, the comparison of the cross-section of Pt-silica spheres prepared via co-condensation and ion-exchange reveals a clear difference. The Pt distribution of the post-functionalized silica spheres is inhomogeneous in terms of a concentration gradient from the edge to the center of the spheres. Instead, the cross-section of the spheres prepared with co-condensation method represents an allover grey color, which indicates a homogeneous distribution of platinum. Another advantage of this method is the shorter reaction time due to the one-step procedure, whereas the ion-exchange method requires the preparation of the support including drying, calcination and subsequently the functionalization with platinum.

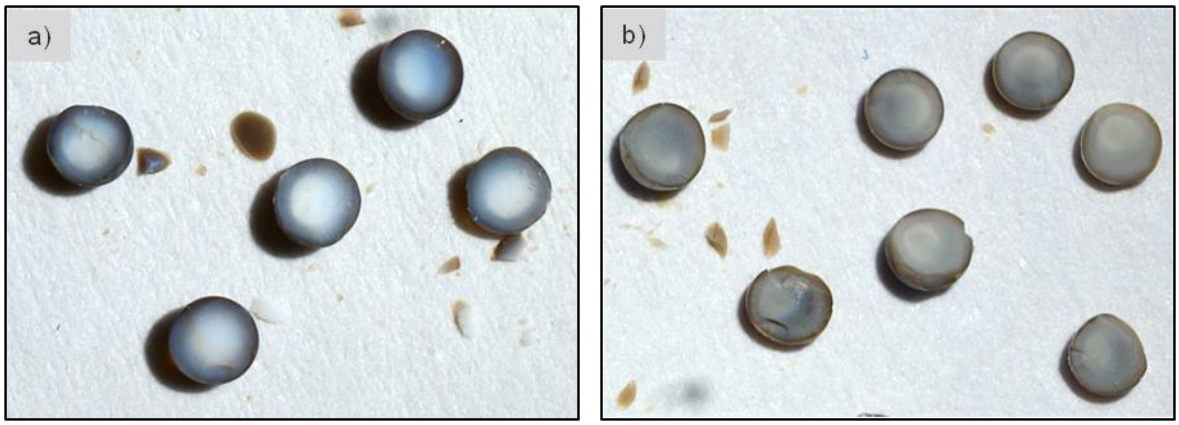

Figure 5.6. Photograph of the cross-section of Pt-silica spheres prepared via ion-exchange (a) and co-condensation (b).

5.3.5 Post-treatment of Pt-silica spheres: calcination vs. Soxhlet extraction

Due to the relatively large Pt nanoparticles of the co-condensed samples, the question arises, if the particle growth is a consequence of the emulsion based preparation or of the high calcination temperature. The high temperature is necessary to decompose the surfactant and the functional groups of the organosilanes. Thus, the preparation procedure was alternatively completed by removing the surfactant by extraction with ethanol. The silica spheres, which

were used for Soxhlet extraction were prepared according the "mix A" procedure, i.e., mixing of $PtCl_2$ together with AAMS in order to form the $Pt(AAMS)_2$ complex. Remarkably, the Pt concentration of the extracted Pt-silica spheres is only reduced by 10% compared to the calcined Pt-silica spheres and the TEM analysis reveals considerably small Pt particles with an average size of 1 - 2 nm (Figure 5.7). This Pt particle diameter corresponds approximately to the particle size of supported platinum prepared by the ion-exchange method.

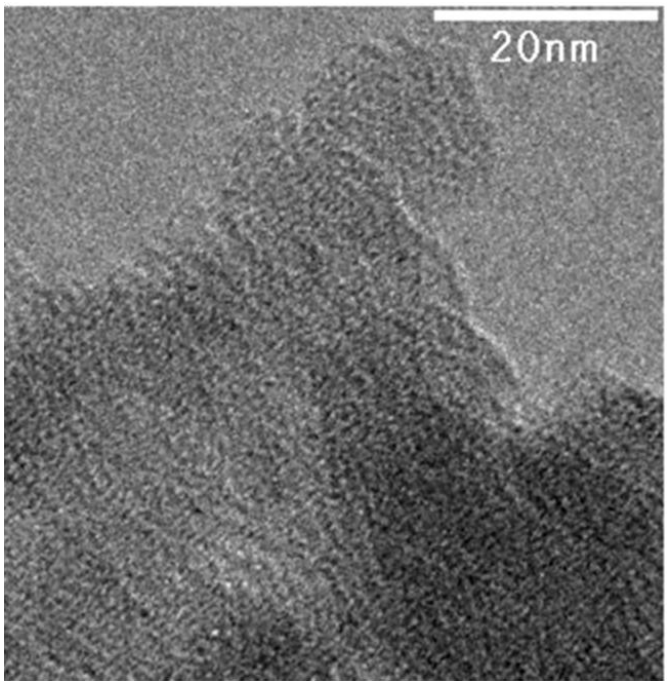

Figure 5.7. TEM image of Pt-silica spheres prepared with $PtCl_2$, AAMS, TES40, PTMS, Pluronic® 25R4 and aniline after Soxhlet extraction with ethanol and H_2 treatment.

The low Pt leaching during the solvent extraction demonstrates, together with the color change of the $PtCl_2$ – AAMS mixture that platinum is anchored in the silica network via aminosilane coordination. If platinum would be solely stabilized by the surfactant molecules, a distinct loss of Pt during extraction would be expected due to the removal of Pt together with the surfactant. The small Pt particles, additionally, indicate highly dispersed platinum ions and particles during preparation, which confirms the anchored $Pt(AAMS)_2$ complexes. It can be concluded that the particles grow during the calcination of the Pt-silica spheres at 600°C due to sintering and not formed in the preparation of the composite spheres. Thus, extraction method represents a much better alternative to preserve high mass specific active Pt surface compared to high temperature decomposition of the surfactant.

5.3.6 Catalytic evaluation in methylcyclopentane ring opening reaction

Methylcyclopentane (MCP) ring opening was chosen as probe reaction to compare the activity of various spherical macroscopic Pt-silica catalysts with conventional prepared silica-supported Pt catalysts. The materials were applied in their as-synthesized macroscopic shape usually with the sphere diameter of the most frequently occupied sieve fraction. The absence of diffusion limitations were verified by using different sieve fractions and by changing space velocity. This confirms also the primary nature of all ring opened C6-alkanes since their selectivities did not vary with changing conversion.

As it can be seen in Figure 5.8, the TOF decreases significantly, if the spheres are crushed or pulverized. It should be mentioned that the powder is afterwards pressed in the size range of 180 to 280 µm for the reason of reactor handling. The MCP ring opening reaction is known as structure sensitive reaction to distinguish between very small and large supported Pt particles resulting in statistical and non-statistical product distribution, respectively.[24] The statistical product distribution between 2-methylpentane (2-MP), 3-methylpentane (3-MP) and n-hexane was observed for the Pt-silica spheres functionalized via ion-exchange, which reveal by far also the highest reaction rate. All the other catalysts show the formation of 2-MP and 3-MP at the expense of n-hexane. Concerning the TOF, however, it can be assumed that the MCP ring opening reaction is essentially structure insensitive, since the TOF does not change much by varying the Pt dispersion.[25] There is, for example, no distinct difference between the sample prepared via ion-exchange compared to the co-condensed samples, despite of the more than five times smaller Pt particles. A similar behavior was observed for Pt supported on Aerosil. If the Pt particle size is increased by nearly one order of magnitude from 1.4 to 13 nm, the TOF decreases only by a factor of three from 1.5 to 0.5 min^{-1}. Also, the Pt-silica spheres synthesized by co-condensation reveal no clear trend between the activity of the different catalysts and the Pt particle size or concentration. The material made with $Pt(acac)_2$, for example, provides the largest particle size, but also a considerable high activity. Instead, the material prepared according to the preparation method mix C offers the highest Pt concentration, but the activity is rather low.

Table 5.1. Average Pt particle size and Pt concentration of the synthesized materials and their catalytic performance in the MCP ring opening reaction.

	Catalyst characterization		**MCP ring opening reaction**		
catalyst	XRD particle size [nm]	Pt concentration [wt. %]	Pt-silica sphere fraction [mm]	Rate (mol MCP / mol Pt) [min^{-1}]	TOF [min^{-1}]
Variation of the Pt compound					
$PtCl_2$	10.5	0.77	0.71-1.00	0,26	2.7
$Pt(acac)_2$	18.4	0.85	1.12-1.25	0,21	3.9
$Pt(NH_3)_4(OH)_2$	14.6	0.35	1.12-1.25	0,06	0.9
Variation of the Pluronic® surfactant					
RPE 1740	10.4	0.82	1.40-1.60	0,24	2.5
RPE 2520	11.9	0.70	1.40-1.60	0,19	2.2
25R4	16.7	0.57	1.40-1.60	0,10	1.7
Variation of the preparation method					
Mix A	10.5	0.77	0.71-1.00	0,26	2.7
Mix B	10.4	0.82	1.40-1.60	0,24	2.5
Mix C	15.2	0.91	1.00-1.12	0,08	1.3
Variation of the macroscopic shape					
Spheres	10.5	0.77	0.71-1.00	0,26	2.7
Crushed spheres	10.5	0.77	0.50-0.71	0,18	1.9
Powdered spheres	10.5	0.77	0.18-0.28	0,08	0.8
Post-functionalization of silica spheres					
Ion-exchange	2.0	0.78	1.12-1.25	0,97	1.9

All these observations suggest that the reactivity of these catalysts is more influenced by the properties of the support material than by the size and concentration of the Pt particles. Therefore, the differences between the various materials are mainly based on the accessibility of the supported Pt particles by methylcyclopentane. Apparently, the fragmentation of the macroscopic structure via crushing or grinding Pt-silica spheres with the same chemical composition exhibits a stepwise decreasing TOF (Table 5.1). The explanation therefore could be that the macroscopic sphere act like a stirred tank microreactor inside the plug flow reactor, which leads to an extended contact time of the reactant with the catalyst. This would enhance the number of MCP molecules, which can access and react over the platinum surface.

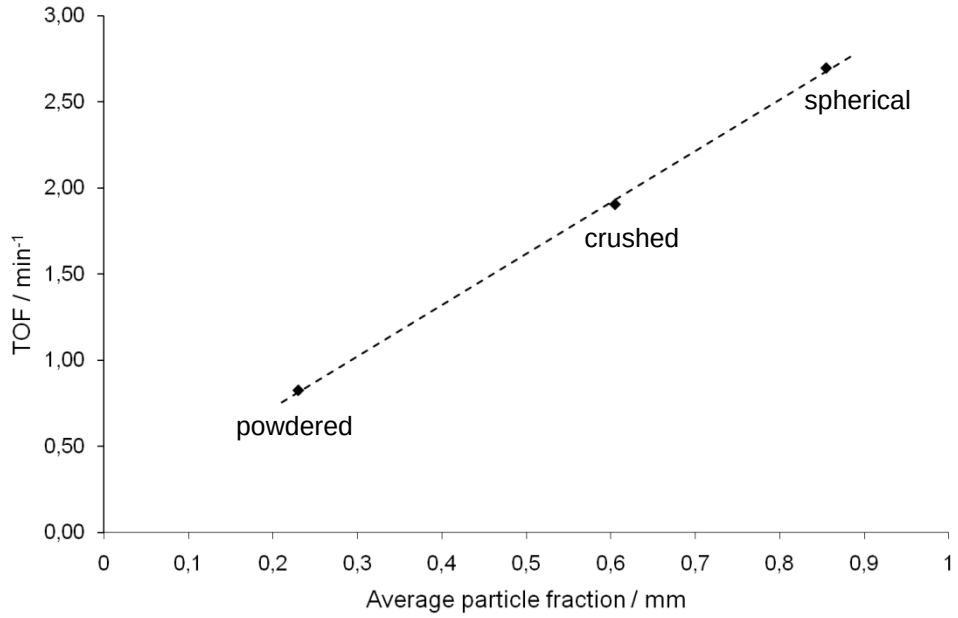

Figure 5.8. Turnover frequency of methylcyclopentane for different shapes of a Pt-silica catalyst with the same chemical composition.

This assumption applies also to the Pt-silica spheres prepared with $Pt(NH_3)_4(OH)_2$, which provides a similar low TOF as the powdered sample. As it can be seen in Table 5.1 this catalyst provides a considerably low Pt loading, which is caused by the high water solubility of this Pt compound. Therefore, the Pt particles are most likely located inside the macropores of the silica support, which are formed through the competitive processes of phase separation and sol-gel transition during the emulsion based synthesis of the Pt-silica spheres.[12, 26] Therefore, the low TOF is caused by the fact that the residence time and reaction probability of a molecule inside a macropore is lower than in a 3-dimensional cross-linked mesopore system.

It is interesting to note that this suggestion would also explain the comparatively low TOF for the catalyst prepared via ion-exchange having a considerably higher Pt dispersion than the co-condensed Pt-silica spheres. The analysis of these materials shows that Pt in these ion-exchanged spheres is mainly located in the shell of the spheres leading again to a low contact time of MCP with platinum.

5.4 Conclusion

Macroscopic silica spheres functionalized with Pt nanoparticles have been prepared in a one-step synthesis via emulsion based sol-gel processing. The precursor solution is composed in order to fulfill two different functions: i) the complexation and stabilization of platinum, ii) the formation of a hierarchically structured silica support with a macroscopic shape.

The size and concentration of the supported Pt particles are controlled by the solubility and stability of the Pt compound, the coordination through the aminosilane and the interaction with the surfactant. The complexation of platinum was best realized with $PtCl_2$ and AAMS since the ligand exchange is energetically favored. In contrast, the driving force to exchange the chelate ligand of $Pt(acac)_2$ or an ammin ligand of $Pt(NH_3)_4(OH)_2$ is considerably lower. Thus, the critical point concerning the efficiency of the Pt immobilization is the solubility and coordination ability of the Pt compound, whereas $Pt(NH_3)_4(OH)_2$ is not suitable for this preparation method.

Another possibility to control the Pt particle size is the stabilization with polymers, which prevent agglomeration of the particles via capping the particle surface. The different PPO-PEO-PPO block co-polymers led to an increasing particle diameter with increasing molecular weight due to differences during the calcination procedure. Simultaneously, the Pluronic® triblock co-polymers are applied as pore forming template and as surfactant to stabilize the emulsion. Organo-functionalized Pt-silica spheres with considerably small Pt particles with an average diameter of 1 - 2 nm were prepared by Soxhlet extraction of as-synthesized materials. The advantage of this method is a small particle size, but also, in contrast to the impregnated samples, a homogeneous metal distribution over the whole sphere.

Comparing the activity of the different materials in methylcyclopentane ring opening reaction reveals a great influence of the support properties, since the TOF decreases drastically due to crushing or grinding the macroscopic spheres. Thus, we suppose that the hierarchically structured, mechanically stable spheres act as microreactors inside the plug flow reactor, which enhance the contact time of the reactant with the supported platinum particles.

The one-step preparation of mechanically stable macroscopic Pt-silica spheres, which was investigated during this work offers a highly variable method (also for the immobilization of other metals) to simultaneous control the properties of the support, including the morphology, texture and porosity and of the metal particles.

5.5 Acknowledgement

Financial support by Wacker Chemie AG and fruitful discussions within the Wacker-Institut für Siliciumchemie and the framework of the network of excellence IDECAT is gratefully acknowledged. The authors thank Dipl.-Ing. Martin Neukamm for AAS measurements, Dipl.-Ing. Oliver Gobin for the highly resolved photographs and Dipl.-Chem. Sonja Wyrzgol for helpful discussions.

5.6 References

[1] H. Song, R. M. Rioux, J. D. Hoefelmeyer, R. Komor, K. Niesz, M. Grass, P. Yang, G. A. Somorjai, *Journal of the American Chemical Society* **2006**, *128*, 3027.

[2] R. Schlögl, S. B. Abd Hamid, *Angewandte Chemie-International Edition* **2004**, *43*, 1628.

[3] A. Taguchi, F. Schüth, *Microporous and Mesoporous Materials* **2005**, *77*, 1.

[4] U. Junges, W. Jacobs, I. Voigtmartin, B. Krutzsch, F. Schüth, *Journal of the Chemical Society-Chemical Communications* **1995**, 2283.

[5] R. M. Rioux, H. Song, J. D. Hoefelmeyer, P. Yang, G. A. Somorjai, *The Journal of Physical Chemistry B* **2004**, *109*, 2192.

[6] R. Ryoo, C. H. Ko, J. M. Kim, R. Howe, *Catalysis Letters* **1996**, *37*, 29.

[7] T. Huang, W. Tu, *Applied Surface Science* **2009**, *255*, 7672.

[8] A. Chen, W. Zhang, X. Li, D. Tan, X. Han, X. Bao, *Catalysis Letters* **2007**, *119*, 6.

[9] S. H. Joo, J. Y. Park, C.-K. Tsung, Y. Yamada, P. Yang, G. A. Somorjai, *Nat Mater* **2009**, *8*, 126.

[10] C. Yacou, A. Ayral, A. Giroir-Fendler, M. L. Fontaine, A. Julbe, *Microporous and Mesoporous Materials* **2009**, *126*, 222.

[11] S. Scholz, J. A. Lercher, *Journal of Materials Chemistry* **2010**, submitted.

[12] S. Scholz, J. A. Lercher, *Chemistry of Materials* **2010**, submitted.

[13] M. Malenovska, S. Martinez, M. A. Neouze, U. Schubert, *European Journal of Inorganic Chemistry* **2007**, 2609.

[14] U. Schubert, *Polymer International* **2009**, *58*, 317.

[15] C. Lembacher, U. Schubert, *New Journal of Chemistry* **1998**, *22*, 721.

[16] F. Basolo, J. C. Bailar, B. R. Tarr, *Journal of the American Chemical Society* **1950**, *72*, 2433.

[17] L. Kumar, N. R. Kandasamy, T. S. Srivastava, *Inorganica Chimica Acta-Bioinorganic Chemistry* **1982**, *67*, 139.

[18] D. G. Duff, P. P. Edwards, B. F. G. Johnson, *Journal of Physical Chemistry* **1995**, *99*, 15934.

[19] G. W. Busser, J. G. van Ommen, J. A. Lercher, *Journal of Physical Chemistry B* **1999**, *103*, 1651.

[20] Y. Borodko, S. M. Humphrey, T. D. Tilley, H. Frei, G. A. Somorjai, *Journal of Physical Chemistry C* **2007**, *111*, 6288.

[21] Y. Borodko, S. E. Habas, M. Koebel, P. D. Yang, H. Frei, G. A. Somorjai, *Journal of Physical Chemistry B* **2006**, *110*, 23052.

[22] T. Sakai, P. Alexandridis, *Langmuir* **2004**, *20*, 8426.

[23] L. Longenberger, G. Mills, *Journal of Physical Chemistry* **1995**, *99*, 475.

[24] H. Du, C. Fairbridge, H. Yang, Z. Ring, *Applied Catalysis A: General* **2005**, *294*, 1.

[25] M. Che, C. O. Bennett, *Advances in Catalysis* **1989**, *36*, 55.

[26] K. Nakanishi, *Journal of Porous Materials* **1997**, *4*, 67.

Chapter 6

Summary and Outlook

6.1 Summary

In recent years the focus of material research was shifted more and more towards the synthesis of complex architectures including hybrid and composite materials as well as hierarchical structured porous solids which are tailor-made for special applications. The driving force for these developments is on the one hand the requirements of industry for highly efficient and economic production and on the other hand environmental reasons, e.g. the enhancement of separation techniques to minimize the pollution. The challenge in catalysis is preferentially given by the shortage of natural resources and thus, an increasing complexity of the feedstock. The multidimensional control of porosity and morphology, e.g. the application of mesoporous zeolites is a substantial progress to avoid mass transport limitations and to improve the activity.

The target of this thesis was to develop a one-step synthesis for macroscopic silica spheres, which allows the controlled implementation of hierarchical pore structure, organic functionalization and catalytically active sites. The preparation method is based on the combination of the sol-gel process with emulsion chemistry and was carried out in a continuously operated reactor column. This allows the generation of narrow sized silica spheres with an average diameter of 1 mm. The size distribution of the spheres and the required reaction time can be controlled via the injection rate of the precursor solution and the water flow inside the reactor column. The reaction of the precursor solution consisting of different silanes, a block co-polymer and a solvent results in stable and crack-free silica composite spheres. During calcination the mechanical strength increases, which is accompanied by weight loss and shrinkage due to the removal of the organic template and further crosslinking of silanol groups.

The crucial point for the synthesis of macroscopic silica spheres via emulsion-based sol-gel processing is the balance between the stabilization of the oil-water interface and the efficiency of water diffusion inside the precursor droplet. This discrepancy was bridged by the usage of amphiphilic triblock copolymers with hydrophilic ethylene oxide and hydrophobic propylene oxide chains. Thus, these surfactants are able to stabilize the precursor droplet by alignment along the oil-water interface and to enhance the water diffusion inside the droplet by the formation of polymer micelles as water transport vesicles. The interfacial interaction was confirmed by the structural change of the surface morphology through variation of the surfactant concentration. Also, it was found out that ‘reverse’ Pluronic® block copolymers

with the composition $(PO)_x(EO)_y(PO)_x$ are most suitable for the combination of template-based sol-gel processes and emulsion chemistry. The advantage compared to triblock copolymers with terminal EO chains is the arrangement in a more stable and shielded surfactant layer along the o/w-interface through the bended EO chain.

The investigations with different triblock copolymers, which vary in the molecular weight and in the hydrophobicity, represent the control of porosity and hierarchical structure of the silica spheres. Surfactants with relatively high ethylene oxide content, i.e. with specific hydrophilicity, such as Pluronic® 25R4 and RPE1740 favor the development of a foam-like macroporous surface layer, since they are able to stabilize small water droplets inside the hydrophobic precursor solution. Also, the mesopore diameter and the pore size distribution are determined by the relative amount of propylene to ethylene oxide monomers in the surfactant molecule. Increasing hydrophobicity encourages the enlargement of the mesopores from 9 to 22 nm due to the formation of larger surfactant aggregates. Consequentially, this effect is accompanied with a decreasing specific surface area, which is reduced by half based on the maximum value of almost 700 m^2/g obtained with Pluronic® 25R4. Despite of the large internal surface, the high mesopore volume up to 0.64 cm^3/g and intraparticle porosity of 50% the mechanical stability of the spheres is not negatively affected.

However, the morphology and porosity of the silica spheres is not only influenced by the type of surfactant, but also by the combination of silanes and solvent in the precursor solution. During the solidification of the precursor droplet the hierarchical core-shell structure and the texture of silica originates mainly from the competitive process of micro-phase separation and sol-gel transition. Therefore, the rate of condensation, i.e. the reactivity of the silanes in combination with the water diffusion and catalyst is decisive. The typically applied precursor solution contained – besides the surfactant and solvent – the silanes tetraethyl silicate (TES) as network building compound, phenyltrimethoxysilane (PTMS) to increase the hydrophobicity of the droplet and [3-(2-aminoethylamino)propyl]trimethoxysilane (AAMS) as base auto-catalyst. The replacement of PTMS by trimethoxysilanes with more steric demanding organic groups resulted in an increasing mesopore diameter and a specific surface area up to nearly 900 m^2/g. Remarkably, the precursor mixture with the bulky N-cyclohexyl-3-aminopropyltrimethoxysilane offers exceptionally ordered macropores on the surface of the silica spheres. These results prove the interaction of organic functional groups with the self-assembling surfactant molecules.

In contrast, organofunctionalized triethoxysilanes drastically lowered the condensation rate and thus, the phase separation process was encouraged. Hence, the cross-section of these spheres revealed a clearly separated core and shell structure, whereas the core consists of hardly connected, relatively large silica particles. Also, the mesopore diameter as well as the mesopore volume was remarkably decreased.

A similar effect in the correlation of condensation rate and morphology was observed by the variation of the solvent. Silica spheres, which were prepared with n-butanol represent a macroporous material providing a coarse texture composed of interconnected primary silica particles. Instead, the solvent aniline in combination with TES, PTMS, AAMS and Pluronic® 25R4 results in a fine grained silica structure exhibiting solely micro- and mesopores. This is caused mainly by the basicity of aniline, which additionally catalyzes the condensation of the silicon alkoxides. Furthermore, the increased hydrophobicity of aniline compared to n-butanol has a beneficial effect on the stability of the precursor droplet.

In addition to the purely siliceous macroscopic spheres, which were obtained after removal of the surfactant and the organic groups by thermal treatment with synthetic air the porous spheres can also be retained with organic functionalization. This was achieved by Soxhlet extraction of the triblock copolymer with ethanol.

Another possibility to produce functionalized silica spheres is the introduction of platinum as catalytically active metal. The immobilization of platinum during the sol-gel process was realized by the addition of Pt compounds, such as $PtCl_2$ or $Pt(acac)_2$ to the precursor solution in order to induce in situ chelating coordination with the ethylene diamine functionalized silane AAMS. This allowed the anchoring of Pt complexes in the silica network and a homogeneous distribution of platinum over the whole sphere. In contrast, post-functionalization of purely siliceous macroscopic spheres via ion-exchange with $Pt(NH_3)_4(OH)_2$ reveals a distinct concentration gradient from the shell to core of the sphere.

During calcination the tethered complexes and the surfactant decompose and the nanoparticle diameter increases to more than 10 nm, whereas the diameter is increasing with increasing molecular weight of the surfactant. However, the serious particle growth was avoided by removal of the surfactant via Soxhlet extraction resulting in organo-functionalized silica spheres with nanoparticles in the region of 1 – 2 nm.

Finally, the combination of the hierarchical pore structure and the high specific surface area with the homogenous distributed Pt nanoparticles reveals a beneficial catalytic behavior in

methylcyclopentane ring opening. This is confirmed by the increased activity of the spheres compared to material obtained after crushing and grinding, which is explained by the function of the hierarchically structured macroscopic spheres as micro-reactors inside the plug flow reactor.

6.2 Outlook

The one-step synthesis for macroscopic and mechanically stable silica spheres with various properties including the hierarchical structure, different ratios of micro-, meso- and macropores, organo-functionalization and tethered Pt-complexes provides a highly variable method to tailor-made materials. Potential applications are in the field of catalysis, separation or adsorption processes.

As it was demonstrated by the preparation of Pt-functionalized silica spheres, metal complexes can be easily and effectively tethered in the siloxane network. Of course, this method can be directly transferred to other metals like palladium or cobalt, which opens the field for many different catalytic reactions, such as hydrogenation or oxidation.

Also, catalytically active materials with macroscopic spherical shape might be accessible by the addition of other metal alkoxides to the siliceous precursor solution. Ideally, the mixture results in homogenous mixed oxide spheres, whereas this reaction requires detailed planning due to the different condensation behavior of the precursor compounds. Nevertheless, the promising combination of titania or zirconia precursors with Si-alkoxides would allow the formation of defined acid sites. Thus, the developed synthesis of controlled hierarchical structures by the variation of hydrophobicity and molecular weight of the surfactant might be advantageous for the accessibility of the acid sites by bulky reactant molecules.

Also, the very important zeolite structures in industrial catalytic processes exhibit extremely steric constraints due to the small micropores, which inhibit the conversion of bulky molecules. An alternative approach to the introduction of mesopores in the zeolite framework could be the embedding of zeolite nanocrystals in the macroscopic silica spheres by simple suspension in the precursor solution. This might enhance mass transfer to the catalytically active sites and the material is obtained in a macroscopic shape, which is required for almost all industrial processes. Furthermore, the combination of different templates or functional groups can be useful to adjust the micro-, meso- and macropore distribution.

However, not only catalysis should be addressed in the field of potential application, but also separation and adsorption processes as they are important for chromatographic applications. Therefore, especially the prepared organo-functional spheres might be of interest. As shown in Chapter 4 the tethered ethylene diamine group can effectively bind metal ions, which can also be inversely applied, e.g. for the separation of metal ions from products or waste water. Also, organo-functionalized inorganic materials are potential candidates for adsorption and storage of gas molecules.

In summary, hierarchically structured functionalized materials attract the interest of various fields of applications, but the simultaneous multidimensional control from the nanometer to the millimeter level is still challenging in material science.

Appendix

Reaction setup

The macroscopic silica spheres presented in this work were prepared in an emulsion based sol-gel process using a continuously operated reactor column with a recycling heated water flow (Figure A-1). The main parts of the reactor are the injection unit with the syringe pump, the heated reaction column and the product vessel. The precursor solution containing different silanes, a surfactant and a solvent is injected at the top of the column, whereas the droplet size is determined by the injection rate and the bypass flow (Figure A-2). The main flow and the increasing density of the spheres due to the formation of the siloxane network cause the transport of the solid spheres into the product vessel. The reaction time and the reaction rate can be adjusted by the length of the reaction column, the main flow, the temperature and the reaction mixture, respectively.

The applied reactor column, which is shown in Figure A-1 exhibits a relatively long reaction column of approx. 3.5 m as falling zone in order to allow the conversion of precursor solutions with highly variable reactivity into solid spheres. Typical preparation parameters are an injection rate of 10-40 ml/h into the recycling water flow (Figure A-3) with a temperature of 60-70°C and a flow rate of 0.002-0.03 m/s. Adjusting suitable reaction parameters allow the synthesis of millimeter-sized mechanically stable spheres with a narrow size distribution.

Alternatively the preparation can be carried out in a sealed stirred tank reactor, whereas the size distribution of the spheres is broader and depending on the reactivity of the precursor solution the spheres tend to agglomerate.

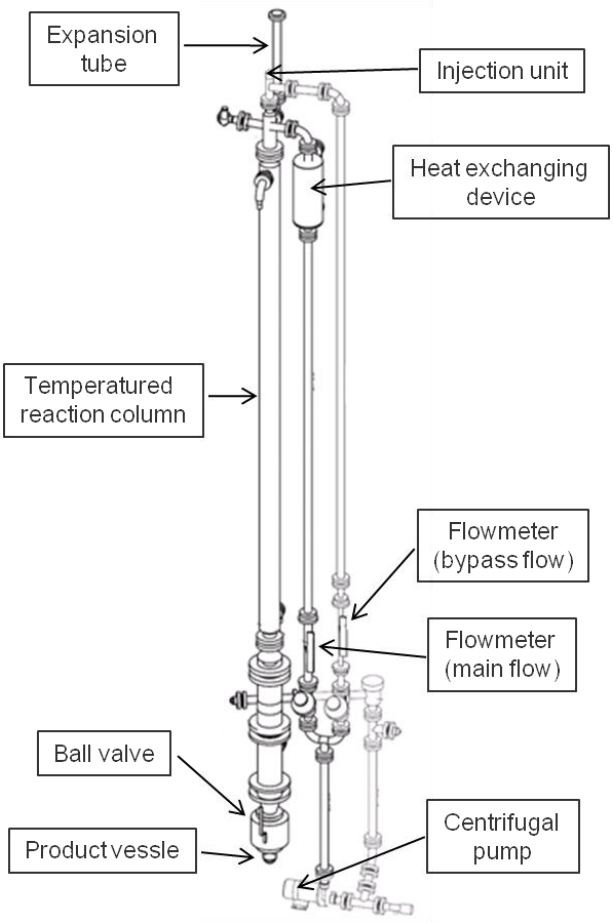

Figure A-1: Set-up of the reactor column.

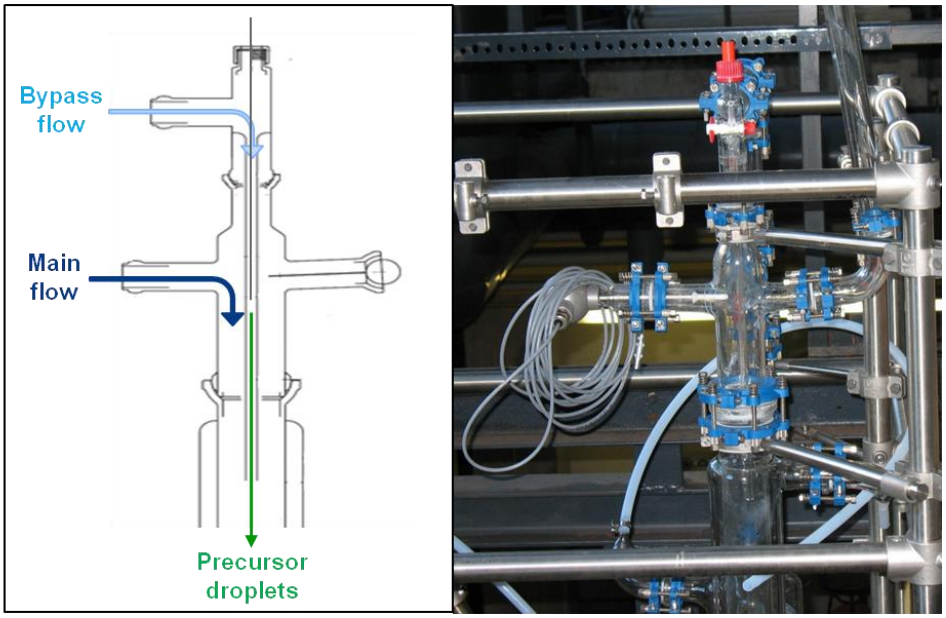

Figure A-2: Injection unit represented as drawing (left) to show the flow system and on a photograph (right).

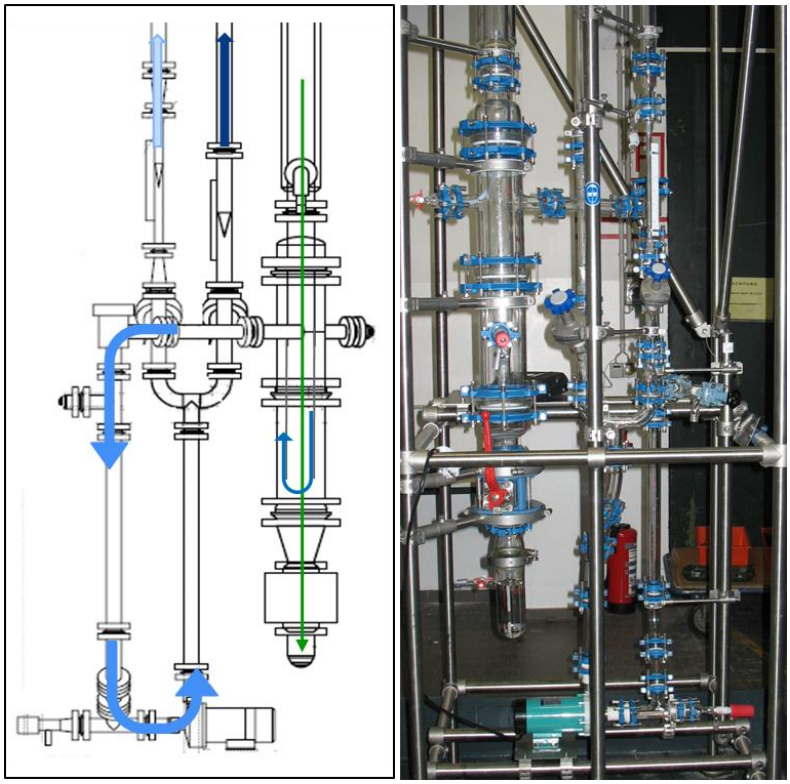

Figure A-3: Technical drawing (left) of the bottom part of the column with the product vessel and the schematic representation of the recycling water flow as well as a photograph of this unit (right).

List of Publications

Patent

S. Scholz, J. A. Lercher; Verfahren zur kontinuierlichen Herstellung Templat-basierter poröser Silicapartikel, Co10826 / P, **2009**.

Scientific Paper

S. Scholz, H. Shi, J. A. Lercher; Controlled synthesis of platinum loaded hierarchic silica spheres, in preparation.

S. Scholz, J. A. Lercher; Hierarchically structured millimeter sized (organo) silica spheres with a macroporous shell and a meso/microporous core, **2010**, *Chemistry of Materials*, accepted.

S. Scholz, S. Bare, S. Kelly, J. A. Lercher; Controlled synthesis of hierarchically structured macroscopic silica spheres, **2011**, *Microporous and Mesoporous Materials*, submitted.

T. Förster, S. Scholz, Y. Zhu, J. A. Lercher; One step synthesis of organofunctionalized transition metal containing meso- and macroporous silica spheres, **2011**, *Microporous and Mesoporous Materials*, doi: 10.1016/j.micromeso. 2010.12.032.

F. Eckstorff, Y. Zhu, R. Maurer, T. E. Müller, S. Scholz, J. A. Lercher; Materials with tuneable low-*k* dielectric constant derived from functionalized octahedral silsesquioxanes and spherosilicates, **2011**, *Polymer*, accepted.

List of Conference Contributions

S. Scholz, T. Förster, J. A. Lercher; Continuous preparation of functionalized porous silica spheres (Poster), 21. Deutsche Zeolith-Tagung, **2009**, Kiel, Germany.

S. Scholz, J. A. Lercher; Different properties of continuous prepared silica spheres (Poster), 5th European Silicon Days conference, **2009**, Wien, Austria.

S. Scholz, J. A. Lercher; New precursor solutions for the continuous preparation of macroscopic silica spheres (Poster), 22. Deutsche Zeolith-Tagung, **2010**, München, Germany.

S. Scholz, B. Blas Molinos, H. Shi, J. A. Lercher; Influence of surface modified mesoporous silica on the stability and reactivity of platinum nanoparticles (Poster), 43. Jahrestreffen Deutscher Katalytiker, **2010**, Weimar, Germany.

S. Scholz, J. A. Lercher; Surfactant templated functionalized silica spheres (Oral Presentation), 16th International Zeolite Conference and 7th International Mesostructured Materials Symposium, **2010**, Sorrento, Italy.